DISSERTATION

THE ROLE OF FATTY ACIDS ON ENDOPLASMIC RETICULUM PROTEOSTASIS IN NON-ALCOHOLIC FATTY LIVER DISEASE

Submitted by

Andrea Lee Estrada

Department of Food Science and Human Nutrition

In partial fulfillment of the requirements

For the Degree of Doctor of Philosophy

Colorado State University

Fort Collins, Colorado

Fall 2017

Doctoral Committee:

Advisor: Michael Pagliassotti

Benjamin Miller
Michelle Foster
Melinda Frye
Christopher Gentile

ABSTRACT

THE ROLE OF FATTY ACIDS ON ENDOPLASMIC RETICULUM PROTEOSTASIS IN NON-ALCOHOLIC FATTY LIVER DISEASE

Non-alcoholic fatty liver disease (NAFLD) is currently a significant health concern in both adults and children (*1-3*). NAFLD is a disease characterized by accumulation of fat in the liver (steatosis) in the absence of chronic alcohol consumption. In some individuals, steatosis progresses to non-alcoholic steatohepatitis (NASH), which is characterized by steatosis, inflammation, apoptosis and fibrosis, and can ultimately lead to end-stage liver disease (*4, 5*). The underlying causes of NAFLD are unclear, although recent evidence has implicated the endoplasmic reticulum (ER) in both the development of steatosis and progression to NASH (*6-9*). Disruption of ER homeostasis or "ER stress" has been observed in the livers and adipose tissue of humans with NAFLD and/or obesity (*10-13*). Downstream signaling events that arise from ER stress include lipid biogenesis, insulin resistance, inflammation, fibrosis and apoptosis, all of which are hallmark features of NAFLD and NASH.

Elevated circulating free fatty acids are a characteristic feature of humans with NAFLD and are positively correlated with disease severity (*14*). Our laboratory has demonstrated that in rodents, selective elevation of circulating free fatty acids induces ER stress in liver and adipose tissue. In addition, ER stress is exacerbated when the composition of fatty acids includes levels of saturated fats comparable to what is encountered in the typical western diet (*11, 15*). We, and others, have also demonstrated that saturated fatty acids provoke ER stress in cultured hepatocytes, pancreatic beta cells, and various other cell types (*16-19*). These data have led to the hypothesis

that the composition of fatty acids presented to and stored within the liver is an important determinant of ER homeostasis.

ER stress is characterized by an accumulation of unfolded proteins within the lumen of the ER. Therefore, the presence of ER stress in NAFLD implies that there is an imbalance between the protein load presented to the ER, and the ability of the ER to process, degrade and/or remove these proteins. The overall aim of this thesis was to examine how saturated fatty acids disrupt ER homeostasis in the liver. We explored in vivo hepatic protein synthesis in response to acute dietary intervention, namely using diets high saturated fat and sucrose, which promote hepatic steatosis and insulin resistance in rats. We utilized the saturated fat, palmitate in controlled delivery to H4IIE liver hepatocytes in order to assess protein synthesis and components of protein degradation. Lastly, we examined the roles of calcium homeostasis and protein palmitoylation in response to palmitate treatment in H4IIE liver hepatocytes. We found that diets high in saturated fat did not affect hepatic protein synthesis in rats. In agreement with this observation, H4IIE hepatocyte treatment with palmitate did not selectively stimulate cellular protein synthesis. Provision of palmitate increased protein ubiquitination, this result was observed independent of proteasome activity or total cellular protein degradation. Lastly, we found that palmitate-induced ER stress was characterized by a reduction in sarcoendoplasmic reticulum ATPase (SERCA) activity. Our data suggest that saturated fatty acid-induced ER stress is mediated via reduced SERCA activity, and subsequent disruption in protein handling.

DEDICATION

For Mom and Max

TABLE OF CONTENTS

CHAPTER 1: Introduction

Non-alcoholic fatty liver disease (NAFLD)

Nonalcoholic fatty liver disease (NAFLD) is a chronic metabolic disorder characterized by hepatic fat accumulation (steatosis) in the absence of excessive alcohol consumption (*20*). The prevalence of NAFLD has nearly doubled since 1980, and current US estimates indicate that NAFLD may affect up to 25% of the general population and 80% of obese and diabetic individuals (*4, 21*). Clinically, NAFLD encompasses a broad spectrum of hepatic derangements ranging from unaccompanied steatosis to nonalcoholic steatohepatitis (NASH), which is characterized by hepatic fat accumulation coincident with inflammation, reduced liver function, and fibrosis (*22*). Progression to NASH occurs in approximately 10% of NAFLD patients, and 20% of these individuals, in turn, progress to cirrhosis within 10-14 years (*23*). Individuals with NAFLD are also at an increased risk of cardiovascular disease, type 2 diabetes and all-cause and obesity-related mortality (*24*).

Clinically, even the more advanced stages of NAFLD, can remain asymptomatic for decades. Therefore, NAFLD is thought to be highly under-reported and under-recognized for its potential severity. Given the increasing prevalence and clinical consequences of NAFLD, identifying the molecular mechanisms responsible for NAFLD development and progression remain critical for designing strategies to combat the disease.

Lipids and NAFLD

The initial stage of NAFLD, steatosis, involves accumulation of hepatic triglycerides due to a positive imbalance between lipid uptake and output. The liver encounters lipids derived from

the diet, hepatic de novo lipogenesis, and circulating fatty acids released from adipose tissue. Donnelly et al. found that the latter source, circulating fatty acids released from adipose tissue, accounts for approximately 60% of intrahepatic triglyceride accumulation over a four-day period in individuals with NAFLD (*25*), thus emphasizing the potential impact of circulating fatty acids in the development of NAFLD.

Accumulating data also suggest that fatty acids play an important role in the progression from NAFLD to NASH. Circulating free fatty acids are elevated in NASH patients and are positively correlated with disease severity (*14*). Experimental suppression of circulating fatty acids improves hepatic insulin sensitivity and reduces liver enzymes in healthy individuals (*26*). These data have led to the emerging concept that elevated fatty acids and products of fatty acid metabolism, rather than triglycerides, per se, mediate the toxic effects of hepatic lipids. Indeed, hepatic triglycerides are higher in patients with benign steatosis compared to those with NASH (*27*).

Recent evidence suggests that the composition of fats within the liver is an important determinant of NAFLD progression. Preliminary data from our laboratory identified a direct correlation between high saturated fat content in the livers of morbidly obese individuals and liver injury. When comparing total liver fat with the same liver injury parameters, no correlation was found. Numerous studies have indicated that saturated fatty acids are more toxic to hepatocytes and liver function than unsaturated fatty acids (*18, 28*). Wang et al., found that a high saturated fat diet in experimental animals resulted in significant liver injury, greater susceptibility to endotoxin, and a reduced liver proliferative capacity. Whereas, a high *un*saturated fat diet did not induce liver damage despite similar levels of total hepatic triglyceride accumulation (*11*). These observations have been recapitulated in multiple experimental models where the saturated fat, palmitate

provokes ER stress in various cell types, including liver hepatocytes (*16-18, 29*), while the unsaturated fat, oleate does not (*16, 18, 30*). These data are consistent with the notion that the composition of fatty acids delivered to and stored within the liver is an important determinant of liver cell integrity, and potentially an independent risk factor for the progression to NASH (*31*).

The Endoplasmic Reticulum

The mechanisms by which saturated fatty acids contribute to liver injury are not completely understood, although accumulating data implicate disruption of endoplasmic reticulum (ER) homeostasis as a proximal event. The ER, one of the largest cellular organelles, functions as a calcium reservoir, engages lipid biosynthesis, and plays a critical role in protein processing and modifications. Proteins destined for the ER undergo translation initiation in the cytosol. Specific sequences direct approximately one-third of all proteins to the ER where they are inserted into the ER lumen for processing and/or modification, these include membrane and secretory proteins (*32*). The lumen of the ER is distinct from the cytoplasm, the composition includes a redox environment which promotes disulfide bond formation, the presence of chaperones which mediate protein folding, and co-factors such as calcium are stored within the lumen. Additionally, the ER possesses the machinery to carry out post-translational modifications such as proteolytic cleavage, acetylation, glycosylation, and palmitoylation.

ER Proteostasis

Accurate protein folding is imperative to ER protein homeostasis, or ER proteostasis, however, it is prone to error due to factors such as that it occurs in a complex, highly crowded environment that has been estimated to reach concentrations of up to 300 mg/ml (*33*). When the demand for protein processing and modification exceeds ER protein folding capacity, unfolded

and aggregate proteins accumulate in the ER lumen, causing disruption of ER proteostasis, or ER stress. Due to the hazardous and potentially deleterious effects that unfolded and aggregate proteins pose to cell function, the ER has evolved a highly specialized quality control system, the unfolded protein response (UPR), that monitors the status of ER protein assembly and serves to restore ER proteostasis when necessary (*34*). The UPR monitors ER proteostasis via three transmembrane proteins, RNA-dependent protein kinase-like ER eukaryotic initiation factor-2α kinase (PERK), activating transcription factor 6 (ATF6) and inositol-requiring ER-to-nucleus signaling protein 1 (IRE1), that act as proximal sensors of ER homeostasis (*34*). When activated, these sensors initiate three distinct but inter-related signaling cascades that reduce unfolded proteins by attenuating global protein translation, enhancing ER protein folding capacity, and facilitating protein degradation. The fundamental goal of this response is to restore ER proteostasis (*31*). If ER proteostasis is not achieved, the UPR facilitates in preparation for apoptosis (Figure 1.1). Beyond its role in maintaining ER proteostasis, the UPR functions as a complex signaling network that is capable of activating various intracellular stress pathways that can culminate in liver damage and cell death. Activation of the UPR has been observed in the liver and adipose tissue of obese humans as well as those with NAFLD (*10-13*) suggesting that ER stress is present in these organs on a chronic basis. Additionally, the degree of UPR activation correlates with disease severity (*10, 12, 13*). Finally, elevated free fatty acids, and in particular saturated fatty acids, activate the UPR in hepatocytes (*15, 18, 35*).

Research Objectives

ER stress is classically defined as the accumulation of mis- or un-folded proteins in the ER lumen (*36*). This scenario predicts that activation of the UPR in NAFLD, and in response to saturated fatty acids, results from an imbalance in the protein load presented to the ER and the

ability of the ER to fold, degrade, and transport these proteins. The aims of this dissertation project were to determine the roles of protein synthesis, protein folding and post-translational modifications, and protein degradation in saturated fatty acid-induced ER stress (Figure 1.2).

Figures

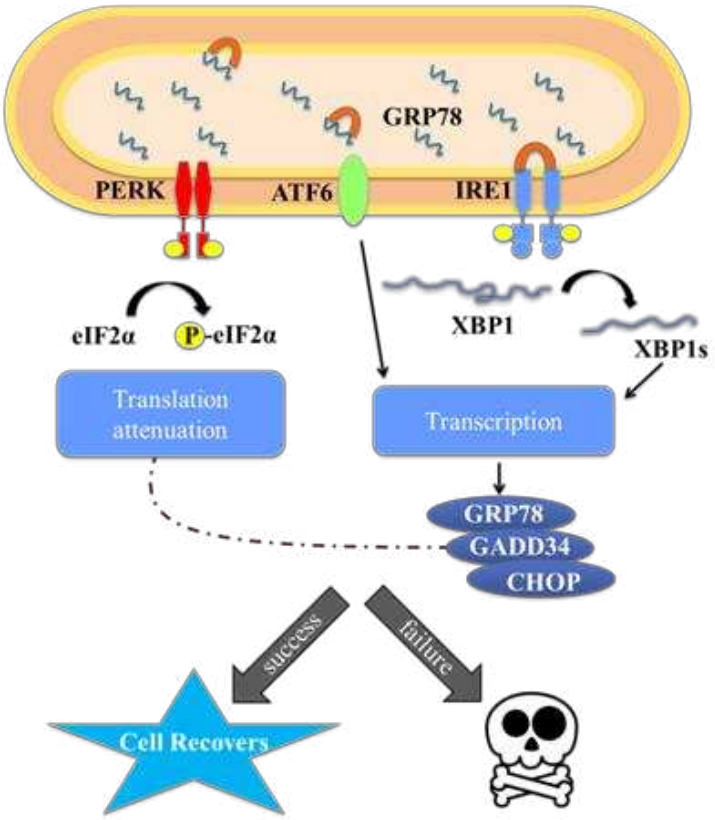

Figure 1.1: The unfolded protein response

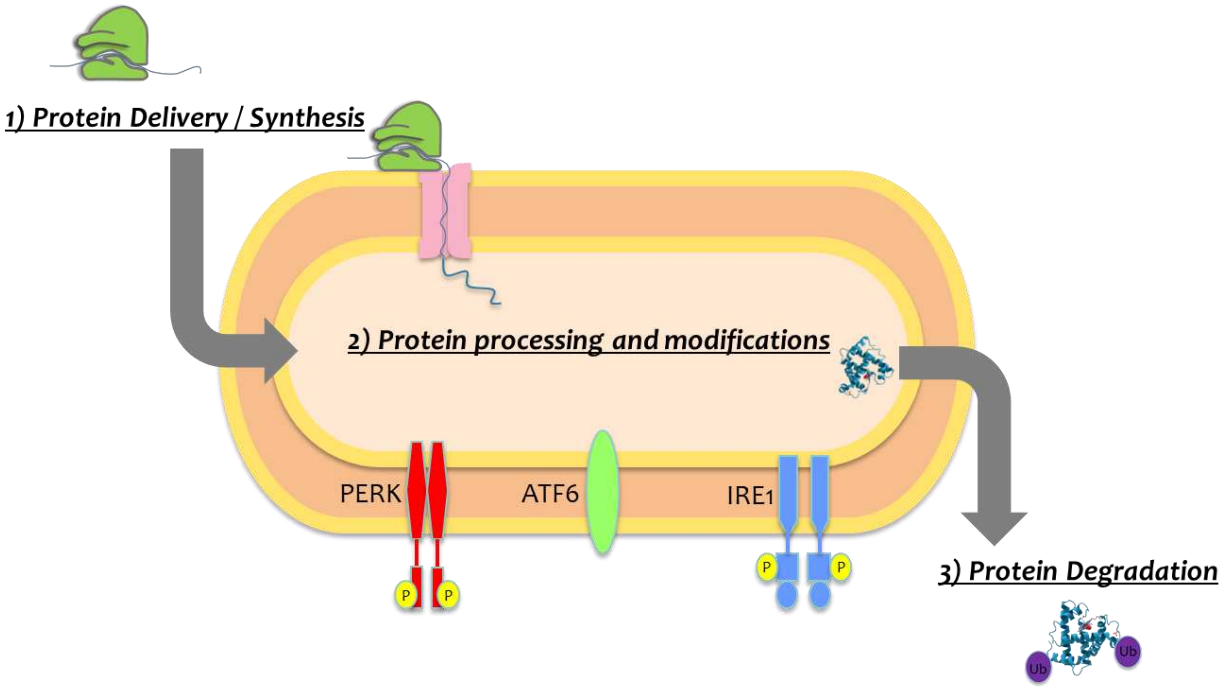

Figure 1.2: Determinants of ER proteostasis

Figure Legends

Figure 1.1: The unfolded protein response: The UPR is comprised of three ER-membrane localized proteins, inositol-requiring 1α (IRE1α), double-stranded RNA-dependent protein kinase-like ER kinase (PERK), and activating transcription factor-6α (ATF6α). UPR activation initiates a signaling cascade that includes transient attenuation of global protein synthesis, and upregulation of protein folding and degradation capacity. These responses, if successful, re-establish ER homeostasis. The inability to re-establish ER homeostasis can result in cell death.

Figure 1.2: Determinants of ER proteostasis: Disruption of ER proteostasis could be the result of 3 scenarios. The first scenario is increased protein synthesis which could overburden the processing and folding capacity of the ER. The second scenario is an inability of the ER to fold and process the client protein load, which could result in an accumulation of unfolded proteins. The last scenario is improper disposal of mis- or unfolded proteins, which would lead to accumulation of unfolded protein in the ER lumen.

CHAPTER 2: Short-term changes in diet composition do not affect in vivo hepatic protein synthesis in rats[1]

Summary

Protein synthesis is critical to protein homeostasis (proteostasis) and modifications in protein synthesis influence lifespan and the development of co-morbidities associated with obesity. In the present study, we examined the acute response of liver protein synthesis to either high fat or high sucrose diets in order to elucidate nutrient-mediated regulation of hepatic protein synthesis in the absence of body fat accumulation. Total and endoplasmic reticulum-associated protein synthesis were assessed by use of the stable isotope, deuterium oxide (^2H_2O), in rats provided a control diet or diets enriched in polyunsaturated fat, saturated fat, or sucrose for 2, 4, or 7 days. The three experimental diets increased hepatic triglycerides 46-91% on day 7 and fasting insulin levels 83-117% on day 7, but did not result in differences in body weight when compared to control (n=6/diet/time). The fraction of newly synthesized proteins in total liver lysates and microsomes was not significantly different among dietary groups (n=3/diet/time).

Footnote[1]

A modified version of this chapter is in press as Andrea Lee Estrada, William Max Hudson, Paul Y. Kim, Claire Marie Stewart, Frederick F. Peelor, Yuren Wei, Dong Wang, Karyn L. Hamilton, Benjamin F. Miller, Michael J. Pagliassotti, 2017. Short-term changes in diet composition do not affect in vivo hepatic protein synthesis in rats. *American Journal of Physiology Endocrinology and Metabolism,* ajpendo.00209.02017.

Table and figure numbers have been modified to reflect that they are specific to this chapter, e.g. Figure 1 is now Figure 2.1. This article is reproduced with permission, and only minimal modifications were made to meet formatting requirements. No other modifications were made, as per the licensing agreement.

To determine whether the experimental diets provoked a transcriptional response to enhance the capacity for protein synthesis we also measured a panel of genes linked to amino acid transport, synthesis and processing. There were no significant differences in any of the genes measured among groups. Therefore, dietary treatments that have been linked to impaired proteostasis, and that promote hepatic steatosis and insulin resistance, did not result in significant changes in total or ER-associated protein synthesis in the liver over a 7-day period.

Introduction

Protein homeostasis (proteostasis) is maintained by a network of cellular processes that broadly include protein synthesis, folding, and degradation (*37, 38*). Loss of, or impairments in proteostasis have been linked to aging and multiple metabolic diseases including obesity, diabetes, and non-alcoholic fatty liver disease (NAFLD) (*39-42*). Disruptions in proteostasis initiate adaptive responses including the heat shock response, mitochondrial unfolded protein response, and the endoplasmic reticulum unfolded protein response (ER UPR) (*37, 43*). Chronic activation of these responses, in particular the ER UPR, can lead to inflammation, impaired insulin signaling, and cell death, all of which are hallmark characteristics of obesity, diabetes, and NAFLD (*44, 45*).

Translation, or protein synthesis is the first process that can influence proteostasis (*46*). Increased protein synthesis that overburdens the processing and folding capacity of the cell can result in protein aggregates and cellular dysfunction (*47, 48*). Multiple studies have demonstrated that global reduction of translation, or modulation in the translation of specific genes can extend lifespan (*46, 49-53*). Genetic manipulation of the translation initiation factor Eukaryotic Initiation Factor-2α, that prevented its phosphorylation, resulted in improved glucose tolerance and reduced hepatic steatosis in mice (*8*). Metabolic diseases, such as obesity, also appear to modify protein synthesis in a time-dependent and tissue-specific manner. For example, high fat diet-induced

obesity over a 9 week period reduced meal-induced stimulation of muscle protein synthesis, however, did not affect basal muscle protein synthesis in mice (*54*). Muscle protein synthesis was increased in rats exposed to a high fat, high sucrose diet for 16 weeks. In contrast, muscle protein synthesis was reduced at 24 weeks on this same diet (*55*). Likewise, in a mouse model of genetic obesity, the liver was characterized by increased ER-associated protein synthesis at 2 months of age, but reduced protein synthesis at 3 and 6 months of age (*56*). These data suggest that protein synthesis can be modified by diet, aging and/or obesity, and that modifications in protein synthesis influence lifespan and co-morbidities associated with obesity. It is presently unclear whether diet composition can influence protein synthesis independently of changes in body composition.

Nutrient-mediated increases in protein synthesis that challenge the proteostasis network have been observed in pancreatic beta cells. Short-term (1-hour) exposure of pancreatic beta cells to high glucose concentrations increased insulin biosynthesis, whereas long-term (24-hours) exposure induced the ER UPR. The saturated fatty acid palmitate increased mRNA translation and the protein load to the ER, resulting in the activation of the ER UPR (*57, 58*). Islets isolated from mice fed a high fat diet for 7 days were characterized by increased polyribosome-associated RNA and activation of mammalian target of rapamycin (*58*). These data suggest that stimulation of protein synthesis may be a short-term response to changes in the amount or type of nutrient delivery in tissues and organs characterized by a high secretory capacity (e.g. pancreas, liver). The liver is particularly susceptible to short term changes in nutrient delivery and diet composition, however, the short-term protein synthetic response to dietary nutrients in the liver has not been characterized (*59-62*). Therefore, the present study examined protein synthesis in total liver lysates and microsomes in response to diets enriched in polyunsaturated fat, saturated fat, or sucrose at multiple time points over a 7-day period. These diets and timeframe were chosen because they can

provoke hepatic steatosis, hepatic insulin resistance and perturbations in hepatic proteostasis rapidly and prior to changes body composition in rodents (*11, 59, 60*).

Methods

Animals:

Male Wistar Crl(WI)BR rats (Charles River Laboratory, Wilmington, MA), age 6-8 weeks, were used in all experiments. Rats were housed individually in a temperature and humidity controlled environment with a 12-hour light:dark cycle. All procedures were reviewed and approved by the Colorado State University Institutional Animal Care Committee.

Dietary intervention:

Upon arrival all rats were placed on a control diet for 1 week (CON: 20% of kcal from protein, 67% of kcal from carbohydrate – corn starch, 13% kcal from fat; TD120001, Harlan Laboratories, Madison, WI). Following the 1-week acclimation period, rats were randomly assigned to CON or a high fat diet enriched in saturated fat (SAT: 20% kcal from protein, 35% kcal from carbohydrate, 45% kcal from fat – cocoa butter; TD120003, Harlan Laboratories), a high fat diet enriched in polyunsaturated fat (PUFA: 20% kcal from protein, 35% kcal from carbohydrate, 45% kcal from fat – corn and safflower oil; TD120002, Harlan Laboratories), or a low fat diet high in sucrose (SUC: 20% kcal from protein, 67% kcal from carbohydrate - sucrose, 13% kcal from fat; 140194, Harlan Laboratories) for 2, 4, or 7 days (n=6/diet/time). We have previously demonstrated that a 7-day feeding regimen of the SAT, PUFA or SUC diets induced hepatic steatosis and insulin resistance, but only SAT and SUC activated the ER UPR (*11*).

Study design for measurement of protein synthesis:

Following the 1-week acclimation period, a subset of rats (n=3/diet/time) received intraperitoneal injections of $^{2}H_2O$ over a 2-day period and were then randomly assigned to receive

one of the four diets (CON, SAT, PUFA, SUC) for 2, 4, or 7 days. Rats were provided supplemental ^2H_2O in their drinking water to achieve and maintain body water enrichment of ~5% (*52*). Protein synthesis was measured in total liver lysates and subcellular microsomal fractions, as well as skeletal and cardiac muscle using GC-MS. Body weight and food intake were monitored in all rats. At the time of sacrifice, rats (~ 6 hours fasted) were anesthetized with isoflourane, blood was collected by cardiac puncture, immediately centrifuged, and subsequently stored as plasma. A portion of the right lobe of the liver was dissected and frozen in liquid nitrogen. Gastrocnemius, soleus, and heart muscle were removed and immediately frozen in liquid nitrogen. Epididymal and retroperitoneal fat pads were dissected and weighed. All samples were stored at -80° C.

Subcellular fractionation:

Briefly, liver homogenates were suspended in 30mM Tris-HCl with 225mM mannitol, 75 mM sucrose, 0.5% BSA, 0.5mM EGTA pH 7.4, and washed in a series of centrifugation steps at 740 x g at 4°C for 5 minutes. Following washing, the supernatant was centrifuged at 9,000 x g for 10 minutes at 4° C. The resulting supernatant was centrifuged at 20,000 x g for 30 minutes at 4° C. The final supernatant was then centrifuged at 100,000 x g for 1 hour to yield the ER microsome fraction (*63*).

Plasma and liver biochemical analyses:

Glucose was measured using a kit (Sigma-Aldrich Chemical Company, St. Louis, MO). Insulin was analyzed by ELISA (Linco Research, St. Charles, MO). Free fatty acids were analyzed using the HR series NEFA kit (Wako Pure Chemical Industries, Osaka, Japan). Liver triglycerides were extracted using the methods described by Bligh and Dyer (*64*), and were measured using a kit (Sigma-Aldrich).

RNA isolation and analysis:

Total RNA was extracted from liver tissue using TRIzol reagent as per the manufacturer's protocol (Invitrogen, Carlsbad, CA). For Real Time PCR, reverse transcription was performed using 0.5 µg of DNase-treated RNA, Superscript II RnaseH- and random hexamers. PCR reactions were performed in 96-well plates using transcribed cDNA and IQ-SYBR green master mix (Bio Rad Laboratories, Hercules, CA). Primer sets are provided in Table 2.1. PCR efficiency was between 90% and 105% for all primer and probe sets and linear over 5 orders of magnitude. The specificity of products generated for each set of primers was examined for each amplicon using a melting curve and gel electrophoresis. Reactions were run in triplicate and data calculated as the change in cycle threshold (ΔCT) for the target gene relative to the ΔCT for β_2-microglobulin (reference gene) according to the procedures of Muller et al. (*65*).

Preparation of liver tissue and microsomes for gas chromatography - mass spectrometric (GC-MS) analysis:

Liver, skeletal and cardiac tissue homogenates, and isolated microsomes were solubilized in 1M sodium hydroxide and agitated at 56°C for 15 minutes. Cellular proteins were hydrolyzed with 6 M hydrochloric acid at 120°C for 24 hrs. Cation exchange was accomplished using a Dowex column (AG 50W–X8 resin, Bio-Rad Laboratories). Cation charged samples were eluted using 4 N ammonium hydroxide. Following vacuum drying, samples were reconstituted in 1 mL of molecular grade water. A portion (500 µL) of the reconstituted samples were then derivatized with 500 µl of acetonitrile (Mallinkrodt, Hazelwood, MO), 50 µL of 1 M potassium phosphate mono basic (ThermoFisher Scientific, Waltham, MA), 20 µL of pentafluorobenzyl bromide (Sigma-Aldrich), and heating at 100°C for 1-hour. Dried derivatives were reconstituted in 700 µL ethyl acetate for subsequent GC-MS analysis (*52, 66, 67*).

GC-MS analysis of derivatized amino acids:

Using negative chemical ionization (NCI), derivatized amino acids were analyzed on a DB5MS gas chromatograph column (Agilent, Santa Clara, CA). The starting temperature was 100°C, increasing 10°C per minute to reach a maximum of 220°C. For mass spectrometry, NCI with helium was used as the gas carrier and methane as the reagent gas. Mass-to-charge ratios of 448, 449, and 450 were monitored for the pentafluorobenzyl-*N*-*N*-di(pentafluorobenzyl) alanine derivative. Alanine standards (Fluka Analytical, St. Louis, MO) ranging from 7.8125 – 2000 µg/ml were used. All samples were run in duplicate. Run time was ~25 minutes, and peak elution occurred at ~17.8 minutes (*52, 67*).

Analysis of deuterated water enrichment:

Deuterated water was extracted from plasma samples using heat evaporation overnight. Acetone proton exchange was accomplished by adding 20 µL acetone and allowed to sit overnight at room temperature. Acetone extraction was accomplished by the addition of 200 µL hexane, and collection of the organic phase using anhydrous sodium sulfate for GC-MS analysis (*52, 67*).

GC-MS analysis of deuterated water enrichment:

Using electron ionization, deuterium labeled acetone was analyzed on a DB17MS gas chromatograph column (Agilent). The starting temperature was 60°C, increasing 20°C per minute to reach 100°C, followed by a second temperature ramp increasing 50°C per minute to reach a maximum of 220°C. For mass spectrometry, helium was used as the carrier gas. Mass-to-charge ratios of 58 and 60 were monitored for 2-pentanone, 4-hydroxy-4-methyl; 4-hydroxy-2-keto-4-methylpentane (diacetone alcohol). Deuterated water standards ranging from 0-20% enrichment were used. All samples were run in duplicate. Run time was ~5.4 minutes and peak elution occurred at ~2.9 minutes (*52, 67*).

Data analysis:

Protein synthesis was measured via deuterium incorporation into alanine. The fraction of newly synthesized proteins was calculated by dividing protein bound alanine enrichment by the true precursor enrichment. The true precursor enrichment used plasma deuterium enrichment, which was adjusted to free alanine enrichment using mass isotopomer distribution analysis (MIDA) (*52, 66, 68, 69*). The fraction of new protein synthesis was determined at 2, 4, or 7 days (*52, 66*).

Statistical analysis:

Two-way analysis of variance was used to examine the effects of diet and time. When appropriate, post-hoc analyses were conducted using a Tukey post-hoc test. Statistical significance was set at $P < 0.05$. All values are reported as mean ± SD.

Results

General animal characteristics:

Body weight, fat pad weight, plasma glucose, and plasma NEFA concentrations were not significantly different among dietary groups (Table 2.2). Total food intake was significantly increased in SAT compared to CON on day 7 only (Table 2.2). Plasma insulin concentration was significantly increased in SAT, PUFA and SUC compared to CON following 4 and 7 days of dietary treatment (Table 2.2). Hepatic triglyceride concentration was significantly increased in PUFA and SUC compared to CON following 4 and 7 days of dietary treatment (Table 2.2). The SAT diet tended to result in increased hepatic triglyceride concentrations (24% increase compared to CON at 4 days, and 32% compared to CON at 7 days), but this did not reach statistical significance.

Protein synthesis in response to dietary treatments:

Protein synthesis in total liver lysates and microsomes was not significantly different among dietary groups at 2, 4, or 7 days (Figure 2.1). Protein synthesis in skeletal muscle and heart were also not significantly different among dietary groups at 7 days (Figure 2.2). Note that protein synthesis was not assessed at 2 or 4 days in skeletal muscle and heart due to low levels of enrichment at these time points.

Gene expression in response to dietary treatments:

A number of genes that encode proteins involved in amino acid transport (Snat2, Snat3, Slc7a1, Slc7a5), protein translation (Eprs, Sars), ER import and translocation (Sec23a, Sec31a, Sec61a1, Srpr, Copa, Kdelr1), and ER quality control and degradation (Sil1, Hyou1, Serp1, Stt3a, Carl, Canx, Edem2, Derl3,) were analyzed. Two previous studies have observed changes in this gene network in response to perturbations that promoted protein remodeling and changes in protein synthesis in HEK 293 cells, Min6 cells and pancreatic islets (*70, 71*). In the present study, there was no consistent pattern of change in any of these genes in response to dietary treatments or days on the diet (Figures 2.3-2.6). The only significant changes involved Slc7a1 mRNA in SAT compared to CON at day 4 (Figure 2.3), Srpr mRNA in SUC compared to CON at day 4 (Figure 2.5), Copa mRNA in SUC compared to CON at day 4 (Figure 2.5), and Carl mRNA in SAT compared to CON at day 4 (Figure 2.6).

In contrast, several genes linked to the activation of the ER UPR were increased in response to dietary treatments. CHOP, GADD34, and spliced variant of X-box binding protein-1 (splXBP-1) mRNA were significantly increased in SAT and SUC following 4 and 7 days of dietary treatment (Figure 2.7).

Discussion

This study examined the short-term effects of diets enriched in fat or sucrose on protein synthesis in rats. The results demonstrate that diets enriched in fat or sucrose do not result in significant changes in hepatic, muscle or heart protein synthesis over a time course of 7 days.

Diets high in fat or sucrose are linked to obesity, insulin resistance, and NAFLD in humans (*61, 72, 73*). In rodent models, these same diets can induce insulin resistance and steatosis in the liver rapidly and prior to significant changes in body composition, and have been linked to disturbances in proteostasis (*11, 59, 60, 74-76*). Results from the present study suggest that diet-mediated changes in hepatic protein synthesis do not play a significant role in the early development of insulin resistance, steatosis or impaired proteostasis in the liver. It is important to note that energy intake, body weight and fat pad weight were not significantly different among dietary groups. The lack of "excess" nutrient intake and positive energy balance, both of which are important stimuli for protein synthesis, may minimize the need for an anabolic response.

Protein synthesis involves the cytosolic, ER, and mitochondrial compartments (*77, 78*). A lack of change in total protein synthesis does not preclude the possibility that diet composition might change the distribution of proteins synthesized among cellular compartments. Therefore, we monitored both total cellular protein synthesis (total lysate) and ER-associated protein synthesis (microsomal fraction) in the liver. Diet composition had no effect on total cellular or ER-associated protein synthesis.

The short term nature of this study led us to also investigate the effects of diet composition on genes associated with protein anabolic pathways. We measured the expression of genes involved in amino acid transport (Snat2, Snat3, Slc7a1, and Slc7a5), protein translation (Eprs and Sars), ER import and translocation (Sec23a, Sec31a, Sec61a1, Srpr, Copa, and Kdelr1), and ER quality control and degradation (Sil1, Hyou1, Serp1, Stt3a, Calr, Canx, Edem2, and Derl3). None

of the experimental diets elicited consistent or significant changes in any of the genes measured at 2, 4, or 7 days. These data suggest that diets high in sucrose, polyunsaturated fat, or saturated fat do not provoke changes to the transcriptional machinery associated with protein anabolism and are consistent with direct measurement of protein synthesis.

In mammals, the UPR consists of three proximal transmembrane sensors: inositol-requiring ER-to-nucleus signaling protein (IRE1α), RNA-dependent protein kinase-like ER eIF-2α kinase (PERK), and activating transcription factor 6 (ATF6) (*36*). In the present study, the high saturated fat and high sucrose diets resulted in increased XBP1 splicing (splXBP-1; mediated by IRE1α) and upregulation of genes associated with the UPR in the liver. A recent study demonstrated that splXBP-1 is important to the remodeling of the ER proteostasis network in HEK293 cells (*70*). Selective activation of splXBP-1 resulted in the upregulation of genes involved in amino acid transport, trafficking, protein folding and quality control. We did not detect changes in genes involved in amino acid transport and trafficking following dietary treatments at 2, 4, or 7 days. These data suggest that the regulation of genes associated with the proteostasis network by splXBP-1 is cell/tissue specific.

Although the high sucrose and high saturated fat diets resulted in increased splXBP-1 and upregulation of genes associated with the UPR, we did not observe significant differences in the phosphorylation of eukaryotic initiation factor 2α (mediated by PERK) among the dietary groups (data not shown). Therefore, whether short-term exposure to diets enriched in saturated fat or sucrose provokes ER stress or selectively activates only the IRE1 branch of the UPR is presently unclear.

In summary, the present study examined protein synthesis in total liver lysates and microsomes in response to diets enriched in polyunsaturated fat, saturated fat, and sucrose at

multiple time points over a 7-day period. All three diets resulted in hepatic steatosis and elevated fasting insulin levels. Diets enriched in saturated fat and sucrose also increased splXBP-1 and several UPR target genes. However, none of these diets increased protein synthesis in the liver.

Table 2.1: Gene primer sequences

Common Name (symbol)	Name	Primer Sequence
Snat2 (Slc38a2)	Solute carrier family 38 member 2	s: CTCCTGAGTGGCGTAGTCG as: GGTGAAGTCTGAGCGAGTTG
Snat3 (Slc38a3)	Solute carrier family 38 member 3	s: ACTCACAGACGGCATACACC as: GACAGCAATGGACAGGTTG
Slc7a1	Solute carrier family 7 member 1	s: CCTGCCGTGCTACTGGTAAG as: AGAGTAAGTGAAGAGGTGTAG
Slc7a5	Solute carrier family 7 member 5	s: GCTGGCTCTACACATTCAAG as: GGAATTATGGAGGTGGACAG
Eprs	Glyamyl-prolyl-tRNA synthetase	s: CGATGTGAGTGGCTGCTATAT as: CAATGTGGTTCTTCTCCTTCTC
Sars	Seryl-tRNA synthetase	s: AGCAGGCACTTATCCAGTATG as: CACTTCCTGCATGACCTCTTT
Sec23a	Sec23 homolog A, coat complex II component	s: GCAACCACCTCCTTCCAATAG as: GTCTCTTTCCTTGTGGTACAG
Sec31a	SEC31 homolog A, COPII complex component	s: CCGAGAAGATGAGTCAGTATG as: ATATCTGGCTGGTTGGTGTTG
Sec61a1	Sec 61 translocon alpha 1 subunit	s: CATCTATTTCCAGGGCTTCC as: GAATGTTGGAGGTGTAGAAGAG
Srpr (Srpra)	SRP receptor alpha subunit	s: TACAGTGCCTGGTAGACAAGTG as: CAGACAGCCTTCACCTTATTGC
Copa	Coatomer protein complex subunit alpha	s: GAGACATTTGACCCTGAGAAG as: CCTTTGGACACAGTCAGTAAG
Kdelr1	KDEL endoplasmic reticulum protein retention receptor 1	s: GAGACCATCACCAGCCATTAC as: TGGCGATGAGGTCAAAGAAGC
Sil1	SIL1 nucleotide exchange factor	s: CTGGAGTAAACGAGGTGAAAC as: GACGTGTAGGTGTTGGTATTG
Hyou1	Hypoxia up-regulated 1	s: AAATGGTGGAGGAGATAGGTG as: AGGGTCAAGTCCTCAAGTTTC
Serp1	Stress-associated endoplasmic reticulum protein 1	s: GGGAAACTTGCTACCTGTTCT as: CCTGTGCATCCCTAACTATTC
Stt3a	STT3A, catalytic subunit of the oligosaccharyltransferase complex	s: AGAAGTGAACGGATGGAAGAC as: CAGAGCTAGTCCTTGAGTTTG
Calr	Calreticulin	s: CTGACCCTGATGCTAAGAAG as: CTTCCATTCGCCCTTGTATTC
Canx	Calnexin	s: GTGATCCTCTTCTGCTGTTCT as: CCTTCTTCGTCCTTCACATCT
Edem2	ER degradation enhancing alpha-mannosidase like protein 2	s: CAGGATGGCGGAGGAAGC as: CCACAATGAAGGTCCCAATCC
Derl3	Derlin 3	s: TCTTCGGTGGTGTTCTTATGAC as: CGCCTGGAAGTTGAGTAAGC
CHOP (Ddit3)	DNA-damage inducible transcript 3 (C/EBP homologous protein)	s: CCAGCAGAGGTCACAAGCAC as: CGCACTGACCACTCTGTTTC
GADD34 (Ppp1r15a)	Protein phosphatase1, regulatory subunit 15A (Growth arrest and damage inducible protein 34)	s: CTTCCTCTGTCGTCCTCGTCTC as: CCCGCCTTCCTCCCAAGTC
GRP78 (Hspa5)	Heat shock protein family A member 5 (78 KDa glucose-regulated protein)	s: AACCCAGATGAGGCTGTAGCA as: ACATCAAGCAGAACCAGGTCAC
splXBP-1	Spliced X-box binding protein 1	s: GTCTGCTGAGTCCGCAGCAGG as: GATTAGCAGACTCTGGGGAAG

Table. 2.2: Animal Characteristics

Epididymal (Epi), Retroperitoneal (Retro), Non-esterified fatty acids (NEFA), Triglyceride (TG), control (CON), high saturated fat (SAT), high polyunsaturated fat (PUFA), and high sucrose (SUC) diets. Values are reported as mean ± SD, n = 6. * denotes significant difference from CON ($P < 0.05$).

Diet	Terminal Body Weight (g)	Total Energy Intake (Kcal)	Epi Fat Pad Weight (g)	Retro Fat Pad Weight (g)	Plasma Glucose (mM)	NEFA (µM)	Insulin (ng/mL)	Liver TG (mg/g)
2 days on diet								
CON	223.2 ± 9.1	135.8 ± 14.7	2.7 ± 0.9	2.1 ± 0.9	12.1 ± 1.7	244.0 ± 101.5	0.5 ± 0.0	10.7 ± 1.5
SAT	223.9 ± 15.8	149.5 ± 23.9	2.9 ± 0.7	2.2 ± 0.7	10.9 ± 3.0	* 365.0 ± 107.2	0.8 ± 0.1	14.4 ± 2.3
PUFA	235.2 ± 11.7	152.1 ± 9.3	2.6 ± 0.6	2.1 ± 0.6	10.5 ± 2.3	288.2 ± 34.9	0.7 ± 0.1	16.0 ± 4.0
SUC	222.97 ± 6.4	135.4 ± 18.5	2.7 ± 0.5	2.0 ± 0.6	10.6 ± 1.4	293.5 ± 60.1	0.8 ± 0.2	* 16.4 ± 2.5
4 days on diet								
CON	244.1 ± 11.3	296.0 ± 36.6	3.2 ± 0.9	2.9 ± 1.0	11.0 ± 2.1	359.1 ± 122.9	0.7 ± 0.1	11.2 ± 1.0
SAT	236.3 ± 16.9	310.4 ± 30.4	2.7 ± 0.4	* 2.0 ± 0.9	10.3 ± 1.5	379.1 ± 75.2	* 1.2 ± 0.2	14.7 ± 3.4
PUFA	240.0 ± 6.7	307.4 ± 26.7	2.9 ± 0.4	2.2 ± 0.2	10.8 ± 2.5	370.6 ± 65.4	* 1.0 ± 0.2	* 19.4 ± 5.3
SUC	246.8 ± 14.9	286.3 ± 33.2	3.2 ± 0.6	2.3 ± 0.6	11.9 ± 2.4	379.9 ± 94.1	* 1.0 ± 0.2	* 17.0 ± 2.7
7 days on diet								
CON	264.7 ± 9.4	500.7 ± 19.3	3.6 ± 0.5	3.2 ± 0.8	12.5 ± 3.0	281.6 ± 56.5	0.6 ± 0.1	11.6 ± 2.6
SAT	272.2 ±17.9	* 575.7 ± 83.7	3.3 ± 0.5	2.9 ± 0.6	10.7 ± 1.8	348.7 ± 67.4	* 1.3 ± 0.4	16.9 ± 1.2
PUFA	260.6 ± 8.0	536.1 ± 62.4	3.4 ± 0.5	2.9 ± 0.5	11.2 ± 2.3	316.1 ± 72.8	* 1.1 ± 0.2	* 22.2 ± 4.7
SUC	267.1 ± 16.4	504.9 ± 49.6	3.3 ± 0.5	3.1 ± 0.8	12.2 ± 2.1	361.0 ± 56.6	* 1.2 ± 0.2	* 21.1 ± 7.5

Figures

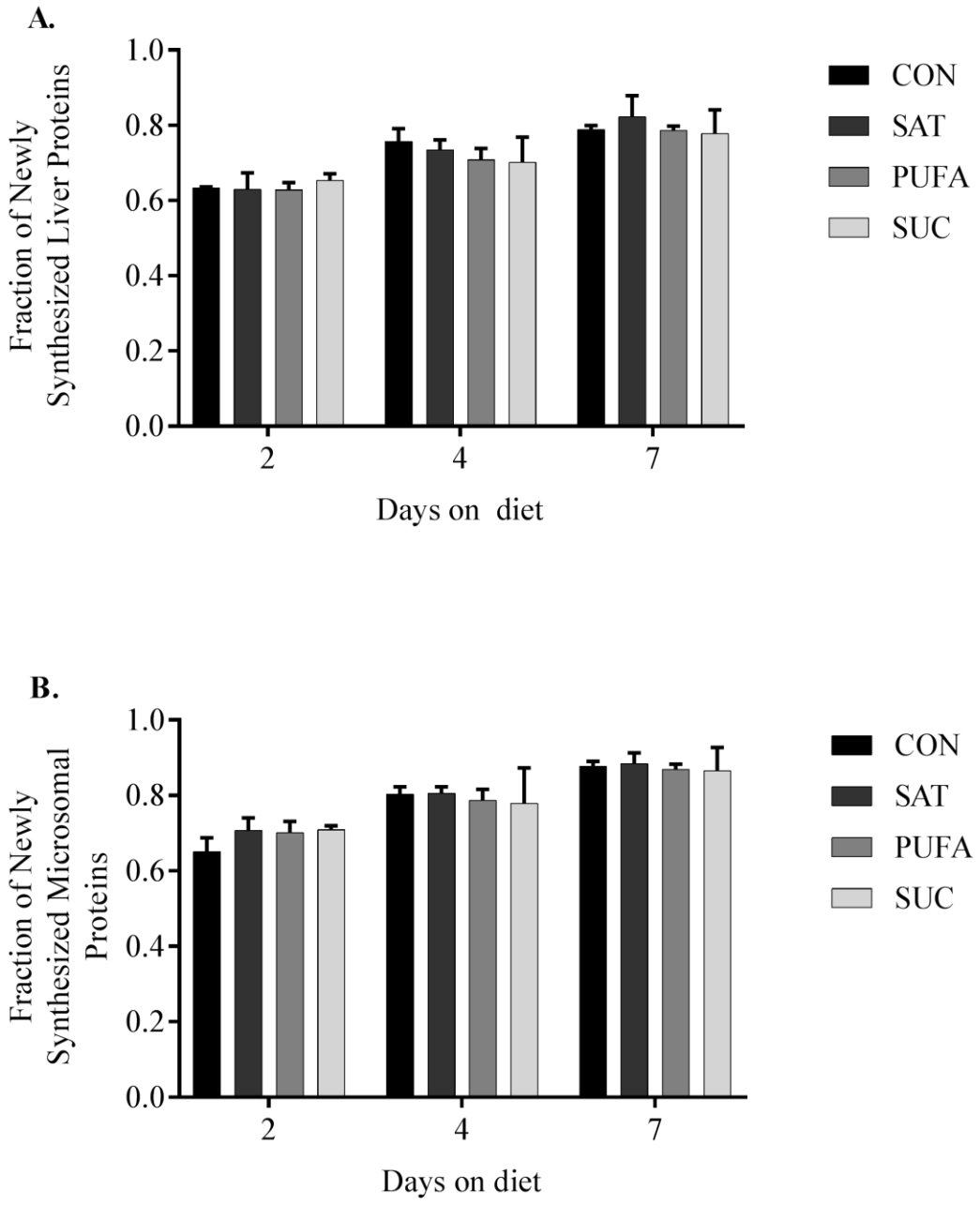

Figure 2.1: Effect of diet on protein synthesis in total liver lysates and microsomes

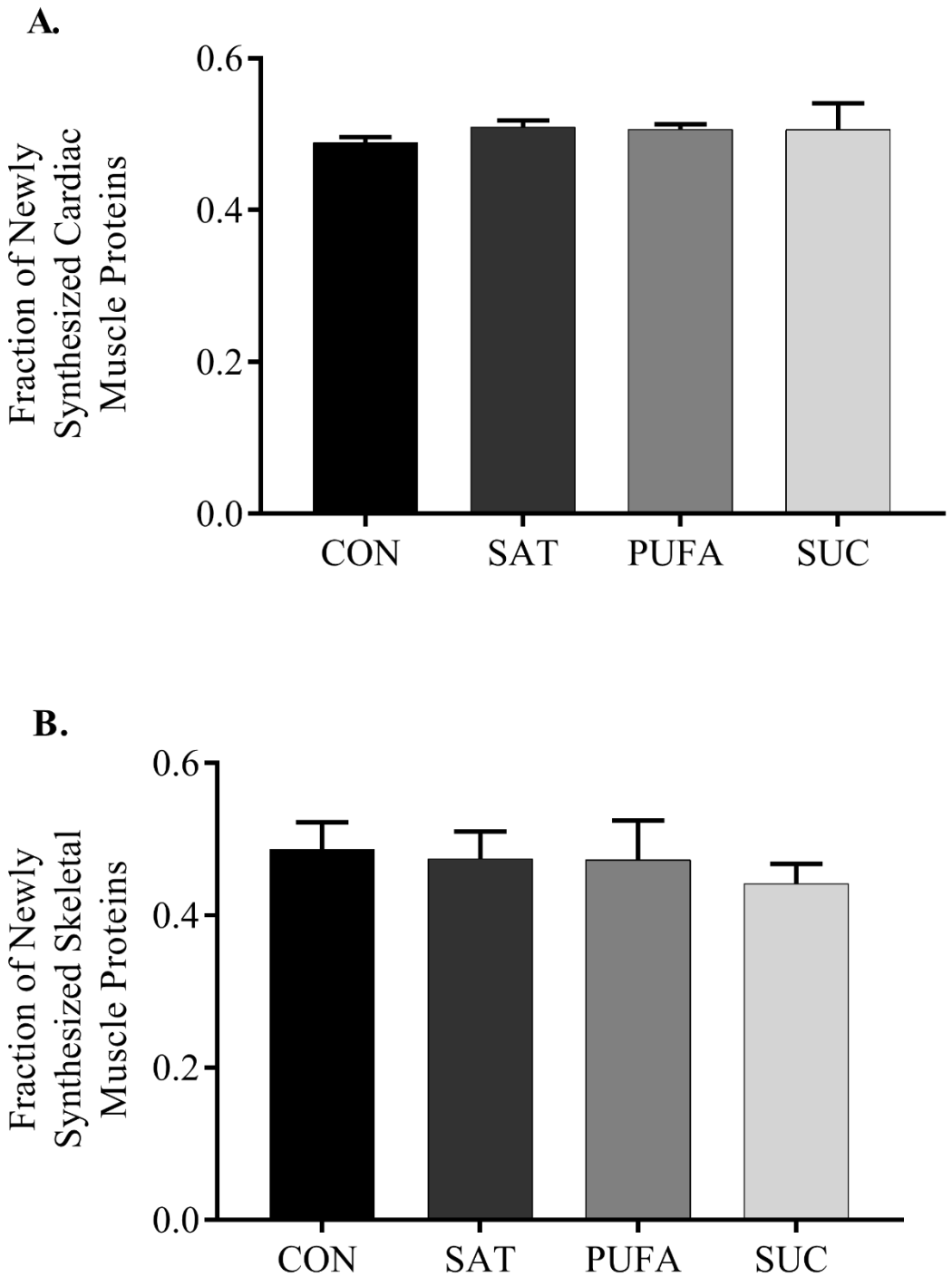

Figure 2.2: Effect on diet on protein synthesis in cardiac and skeletal muscle

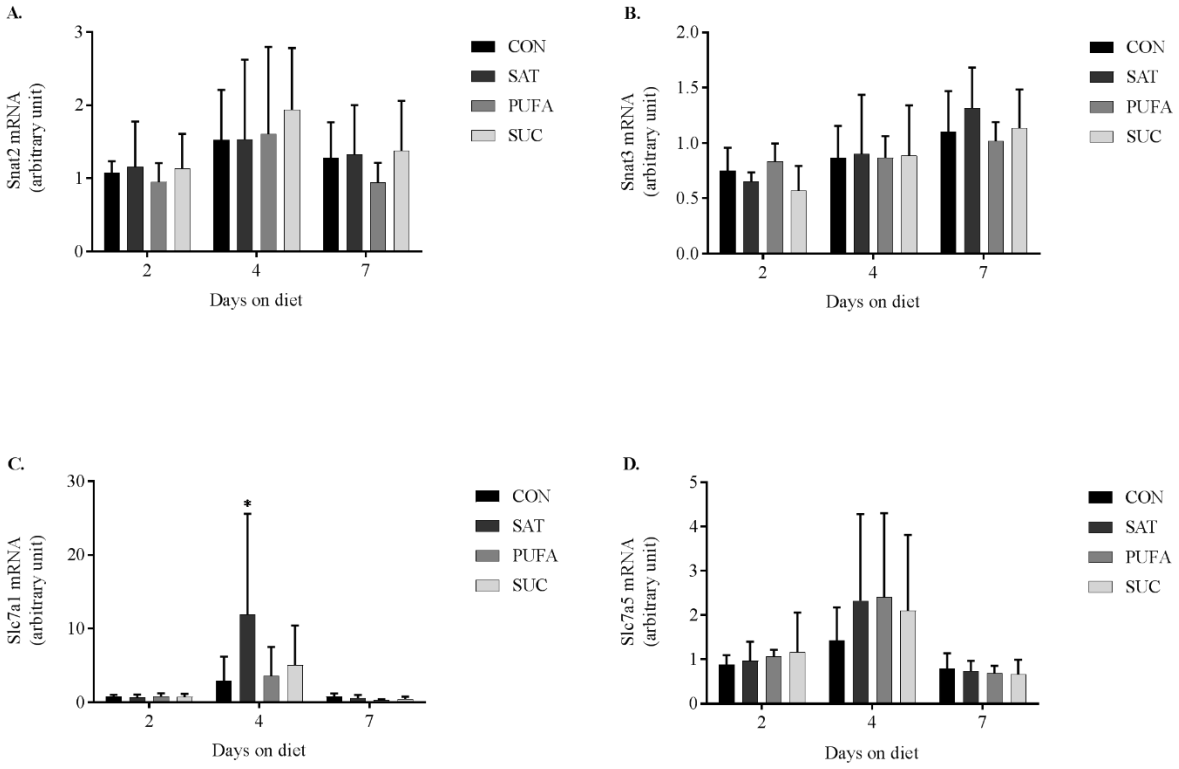

Figure 2.3: Effect on diet on genes involved in amino acid transport in the liver

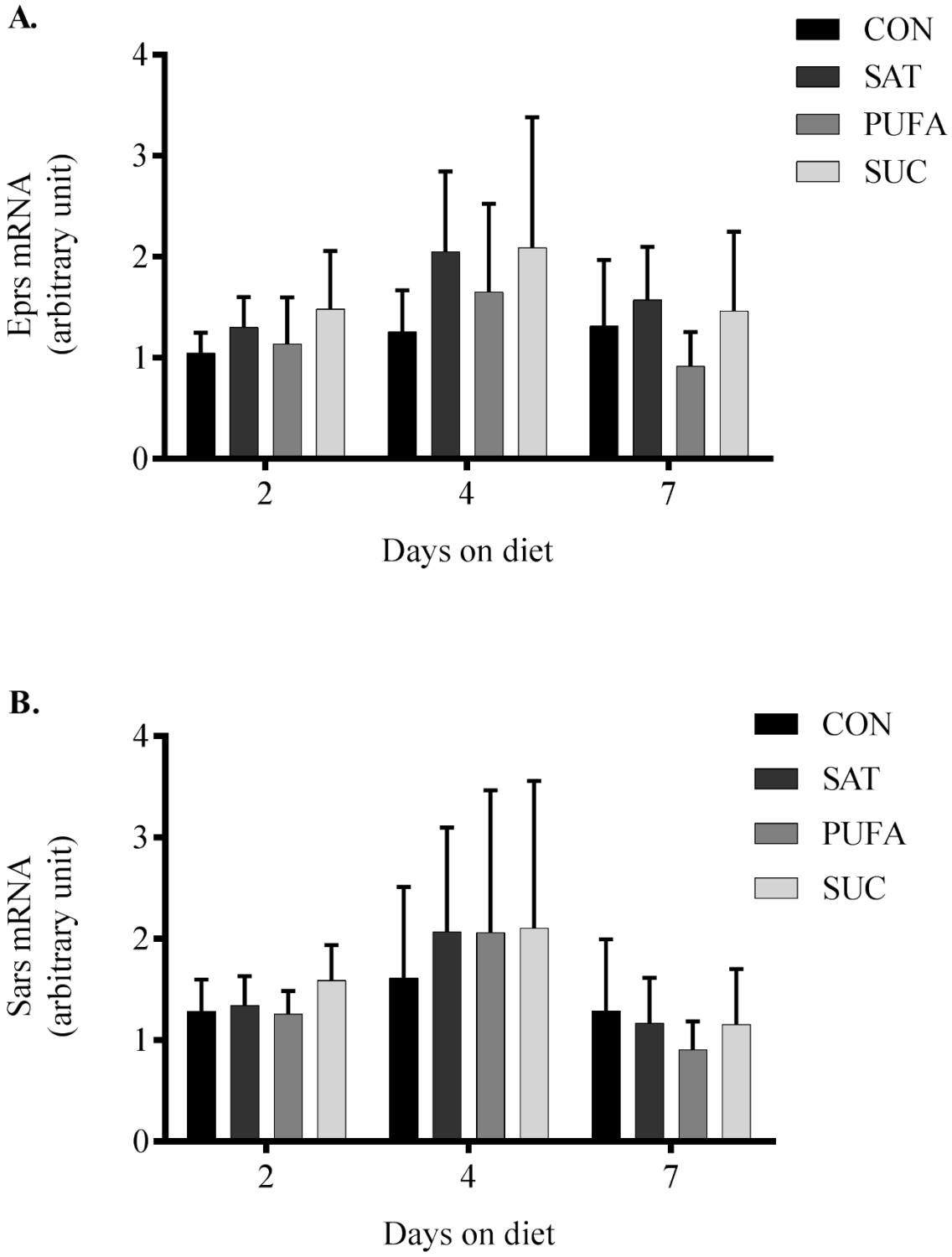

Figure 2.4: Effect of diet on genes involved in protein translation in the liver

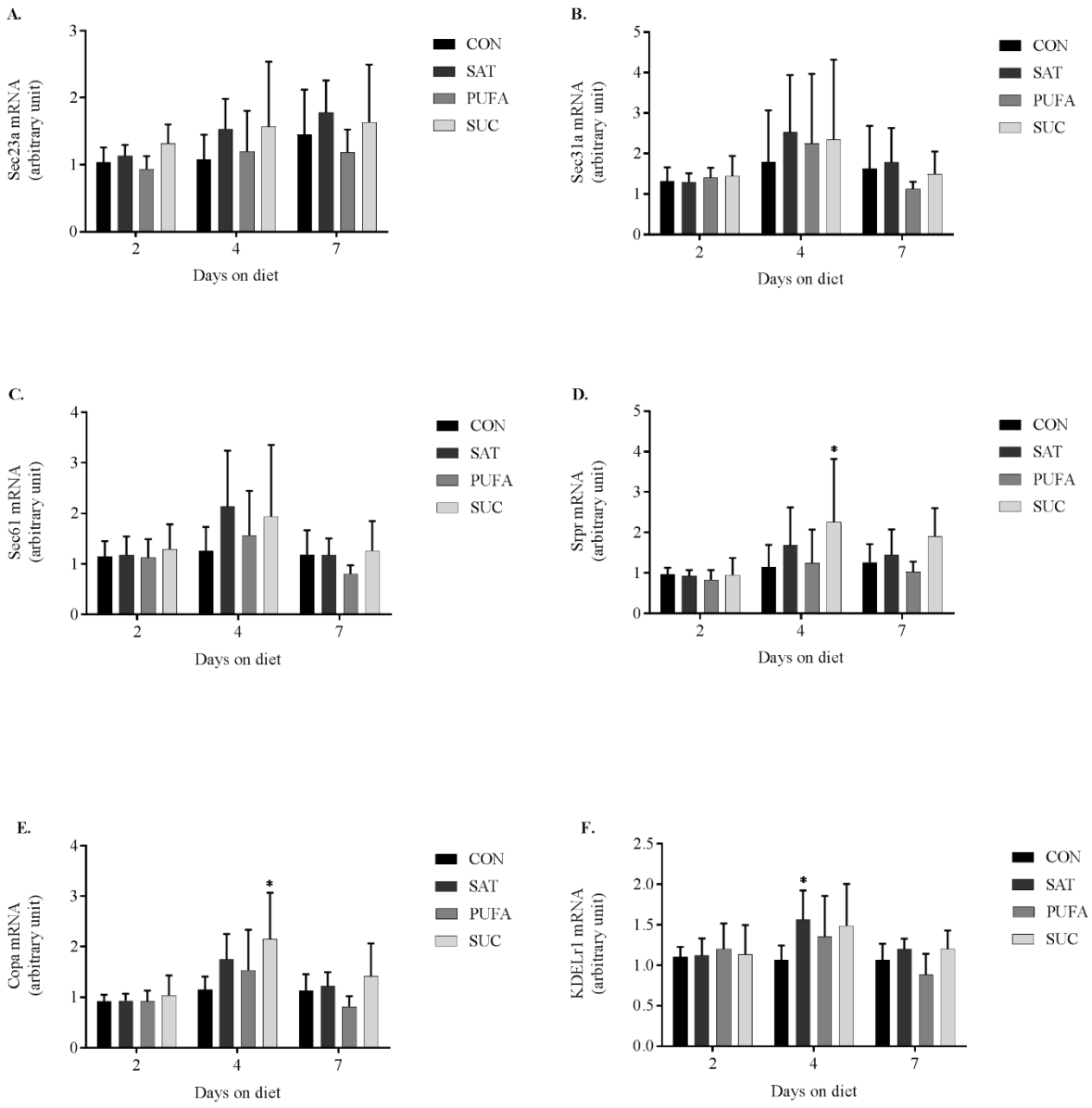

Figure 2.5: Effect of diet on genes involved in ER import and translocation in the liver

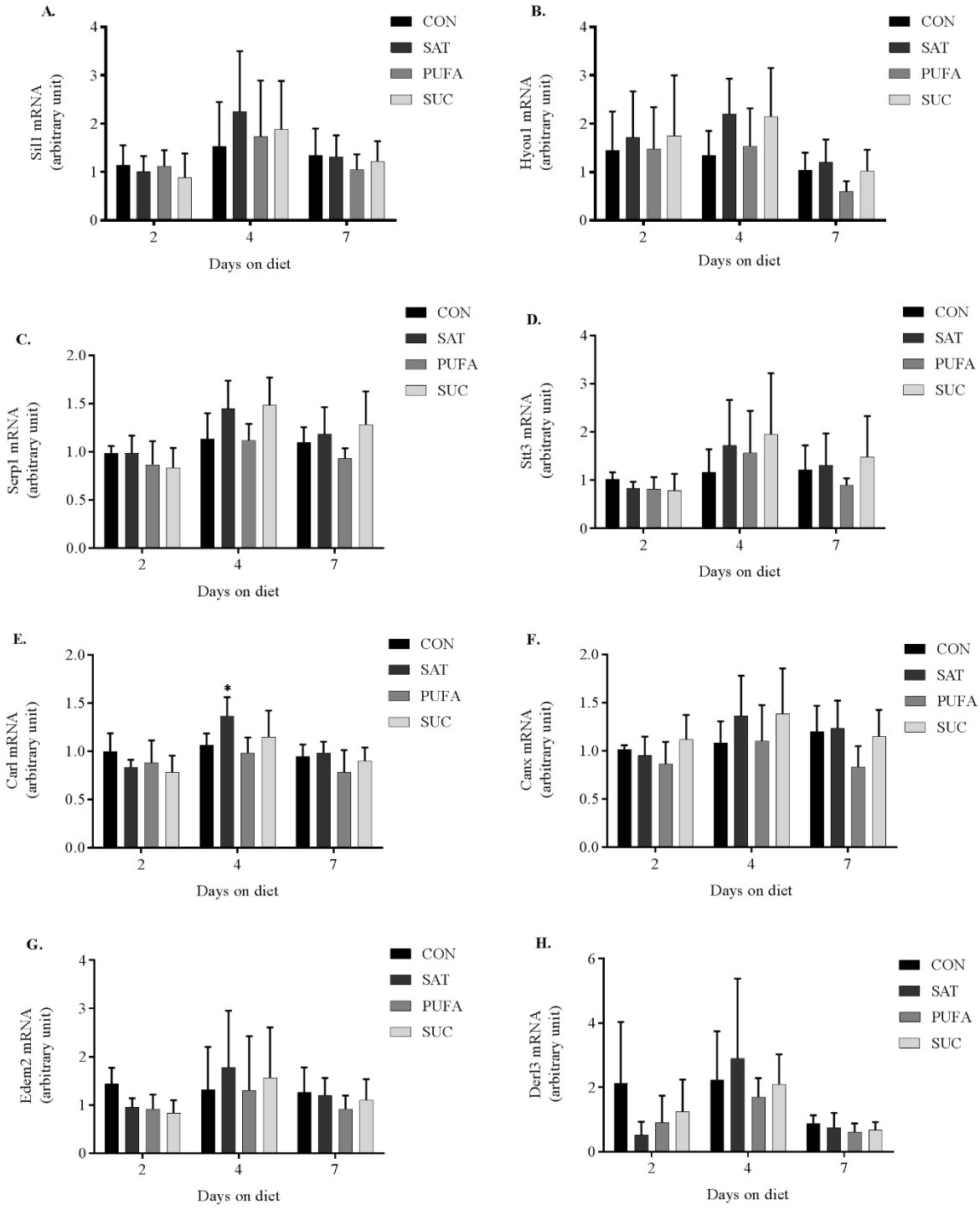

Figure 2.6: Effect of diet on genes involved in ER quality control and degradation in the liver

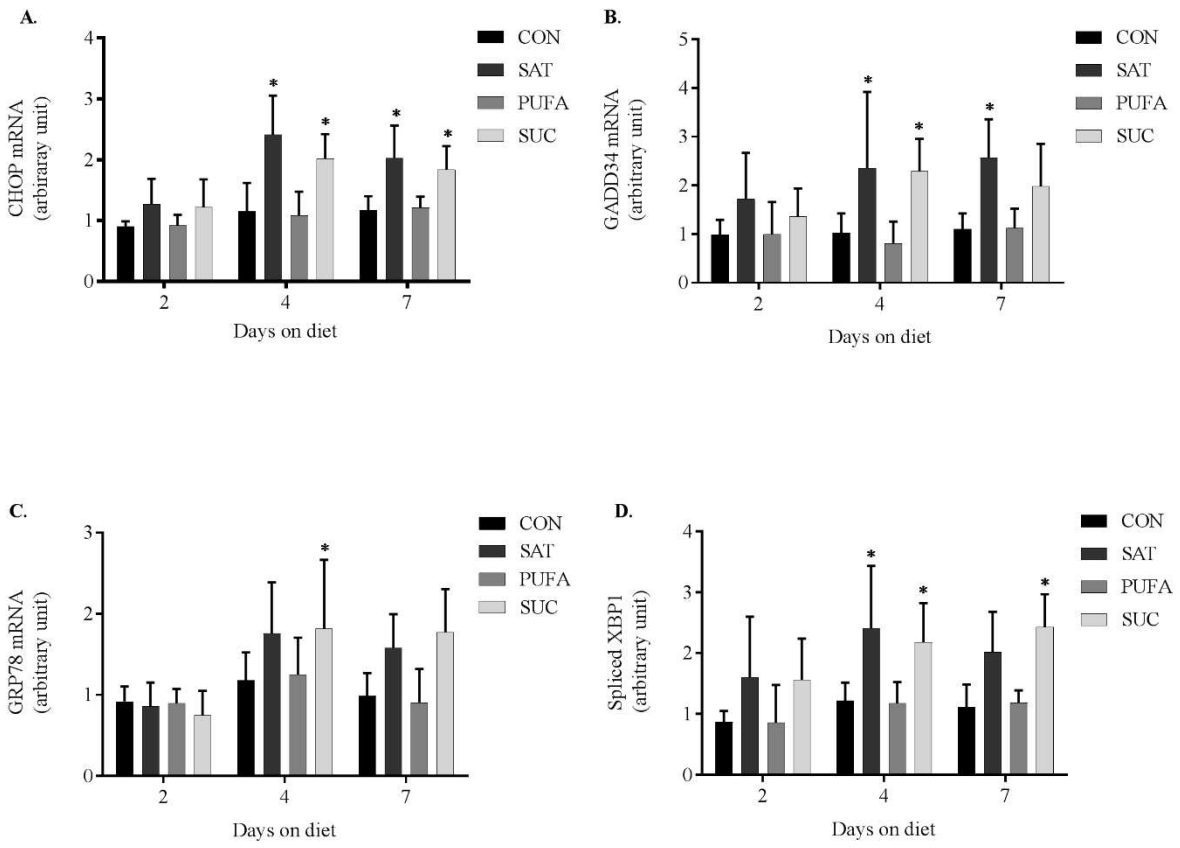

Figure 2.7: Effect of diet on ER UPR genes

Figure Legends

Figure 2.1. Effect of diet on protein synthesis in total liver lysates and microsomes. The fraction of newly synthesized proteins in total liver (A) and liver microsomes (B) following 2, 4, or 7 days on control (CON), high saturated fat (SAT), high polyunsaturated fat (PUFA) or high sucrose (SUC) diets. Values are reported as mean ± SD for n=3 per group per day.

Figure 2.2. Effect of diet on protein synthesis in cardiac and skeletal muscle. The fraction of newly synthesized proteins in cardiac (A) and skeletal (B) muscle following 7 days on control (CON), high saturated fat (SAT), high polyunsaturated fat (PUFA) or high sucrose (SUC) diets. Values are reported as mean ± SD for n=3 per group per day.

Figure 2.3. Effect on diet on genes involved in amino acid transport in the liver. Solute carrier family 38, member 2 (Snat2) (A), Solute carrier family 38, member 3 (Snat3) (B), solute carrier family 7 member 1 (Slc7a1) (C), solute carrier family 7 member 5 (Slc7a5) (D) mRNA following 2, 4, or 7 days on control (CON), high saturated fat (SAT), high polyunsaturated fat (PUFA) or high sucrose (SUC) diets. Values are reported as mean ± SD for n = 6 per group per day. * denotes significant difference from CON ($P < 0.05$).

Figure 2.4. Effect of diet on genes involved in protein translation in the liver. Glutamyl-prolyl-tRNA synthetase (Eprs) (A) and seryl-tRNA synthetase (Sars) (B) mRNA following 2, 4, or 7 days on control (CON), high saturated fat (SAT), high polyunsaturated fat (PUFA) or high sucrose (SUC) diets. Values are reported as mean ± SD for n = 6 per group per day.

Figure 2.5. Effect of diet on genes involved in ER import and translocation in the liver. Sec23 homolog A, coat complex II component (Sec23a) (A), SEC31 homolog A, COPII complex component (Sec31a) (B), Sec 61 translocon alpha 1 subunit (Sec61a1) (C), SRP receptor alpha subunit (Srpr) (D), Coatomer protein complex subunit alpha (Copa) (E), KDEL endoplasmic reticulum protein retention receptor 1 (Kdelr1) (F) mRNA following 2, 4, or 7 days on control (CON), high saturated fat (SAT), high polyunsaturated fat (PUFA) or high sucrose (SUC) diets. Values are reported as mean ± SD for n = 6 per group per day. * denotes significant difference from CON ($P < 0.05$).

Figure 2.6. Effect of diet on genes involved in ER quality control and degradation in the liver. SIL1 nucleotide exchange factor (Sil1) (A), hypoxia up-regulated 1 (Hyou1) (B), stress-associated endoplasmic reticulum protein 1 (Serp1) (C), STT3A, catalytic subunit of the oligosaccharyltransferase complex (Stt3a) (D), calreticulin (Calr) (E), calnexin (Canx) (F), ER degradation enhancing alpha-mannosidase like protein 2 (Edem2) (G), derlin 3 (Derl3) (H) in the liver following 2, 4, or 7 days on control (CON), high saturated fat (SAT), high polyunsaturated fat (PUFA) or high sucrose (SUC) diets. Values are reported as mean ± SD for n = 6 per group per day. * denotes significant difference from CON ($P < 0.05$).

Figure 2.7. Effect of diet on ER UPR genes. DNA-damage inducible transcript 3 (CHOP) (A), protein phosphatase1, regulatory subunit 15A (GADD34) (B), heat shock protein family A member 5 (GRP78) (C), spliced X-box binding protein 1 (splXBP-1) (D) mRNA in the liver following 2, 4, or 7 days on control (CON), high saturated fat (SAT), high polyunsaturated fat

(PUFA) or high sucrose (SUC) diets. Values are reported as mean ± SD for n = 6 per group per day. * denotes significant difference from CON ($P < 0.05$).

CHAPTER 3: Palmitate-induced ER stress is characterized by increased protein ubiquitination but not increased protein turnover in H4IIE cells

Summary

It is well established that saturated fatty acids disrupt endoplasmic reticulum (ER) homeostasis, a phenomenon commonly referred to as ER stress, in numerous cell types. ER homeostasis is regulated at multiple levels including protein synthesis, folding and degradation. The aims of the present study were to examine whether palmitate-mediated ER stress involved stimulation of protein synthesis and/or inhibition of protein degradation in H4IIE liver cells. To assess protein synthesis, deuterium oxide was added to the medium and H4IIE cells were cultured under control conditions or in the presence of 250 μM palmitate, 250 μM oleate, or 780 nM thapsigargin (chemical-inducer of ER stress) for 0.5, 1, 2, 4, or 6 hours (n=3-6 per condition/time point). These time points were chosen because they both precede and follow the induction palmitate-induced ER stress. Protein degradation was assessed by pre-labeling the protein pool with deuterium oxide and following the decay of enrichment in response to incubations under control, palmitate, oleate, or thapsigargin. Protein degradation was also assessed by measuring protein ubiquitination and proteasome activity. Palmitate increased markers of ER stress between 2 and 4 hours but did not stimulate protein synthesis or increase the expression of genes involved in the protein synthetic apparatus at any of the time points. Palmitate treatment for 6 hours increased protein ubiquitination by ~26%. Increased protein ubiquitination was observed independent of reductions in proteasome activity and protein degradation. In contrast, thapsigargin

treatment resulted in a reduction of protein synthesis (~1 hour) and upregulation of multiple genes involved in the protein synthetic apparatus (~2 – 4 hours). Thapsigargin treatment also reduced protein ubiquitination and protein degradation. The results from this study suggest that palmitate disrupts protein handling in H4IIE cells. In addition, we have identified critical differences in the proteostatic responses to chemical- versus palmitate-mediated ER stress.

Introduction

Protein homeostasis, or proteostasis is imperative for organ and tissue health, and is therefore tightly regulated at multiple levels including protein synthesis, protein folding, and protein degradation. Chronic impairments in proteostasis are characterized by irreversible protein damage, accumulation of cytotoxic protein aggregates, and cellular dysfunction (*37, 42, 47*). These impairments have been linked to age-associated and metabolic diseases such as dementia-associated neurological diseases, obesity, and non-alcoholic fatty liver disease (NAFLD) (*39-42*). Identifying the factors that target and disrupt proteostasis remains critical to understanding the pathogenesis of these diseases.

NAFLD is a significant health concern in both adults and children (*1-3*). Steatosis, the beginning stage of NAFLD, is characterized by fat accumulation in the liver in the absence of chronic alcohol consumption. In some individuals, steatosis progresses to non-alcoholic steatohepatitis (NASH), which is characterized by steatosis, inflammation, apoptosis and fibrosis, and can ultimately lead to end-stage liver disease (*4, 5*). Up to 80% of individuals with NAFLD are obese and have sera characterized by elevated circulating fatty acids (*4, 14*). Elevated fatty acids, in particular saturated fatty acids, can lead to impairments in a number of cellular organelles, including the endoplasmic reticulum (ER), a key organelle in maintaining cellular proteostasis. The ER folds and processes approximately one-third of all cellular proteins, specifically,

membrane and secretory proteins. Multiple studies have demonstrated that saturated fatty acids provoke ER stress, classically defined as accumulation of unfolded proteins in the ER lumen in various cell types including hepatocytes (*16-18, 29*). In order to combat this insult and restore ER proteostasis, an adaptive signaling pathway exists, termed the unfolded protein response (UPR). The fundamental goal of this response is to re-balance the protein load presented to the ER with the capacity of the ER to process or degrade incoming proteins (5). Activation of the UPR has been observed in the liver and adipose tissue of obese humans with NAFLD (*10-13*). The presence of UPR activation in the liver of humans with NAFLD, coupled with the ability of saturated fatty acids to provoke activation of the UPR suggests that ER proteostasis is impaired in NAFLD, in part, due to elevated fatty acids. However, whether saturated fatty acid-mediated impairments of ER proteostasis involve protein synthesis, folding and/or degradation in hepatocytes is presently unknown.

Several studies have demonstrated that fatty acid surplus, prevalent in both obesity and NAFLD, can influence protein dynamics. For example, incubation of hepatocytes with palmitate resulted in hyper-activation of the mTOR pathway, an important regulator of protein synthesis (*79*). Incubation of pancreatic β-cells with palmitate increased mRNA-polyribosome occupancy and amplified expression of translation machinery, both indicative of increased translation (*58*). Likewise, mice fed a high fat diet for 7 days had increased mRNA-polysome association and increased markers of translation machinery in pancreatic β-cells. Collectively, these data highlight a selective capacity for palmitate and high fat diets to influence protein translation. However, we are not aware of any studies that have examined the effects of palmitate on protein synthesis and degradation, and whether these effects can be linked to the induction of ER stress.

The intent of this study was to examine the roles of protein synthesis and degradation in palmitate-induced ER stress using controlled palmitate delivery to H4IIE liver cells. Our results demonstrate that palmitate does not selectively increase protein synthesis. However, palmitate does increase protein ubiquination in the absence of effects on proteasome activity or protein degradation.

Methods

Cell culture:

H4IIE rat hepatoma cells (American Type Culture Collection, Manassas, VA) were cultured in Eagle's Modified Essential Medium (EMEM), supplemented with 10% fetal bovine serum (FBS) and 50 U/mL penicillin-streptomycin sulfate. All experiments were performed at ~80% cell confluence using EMEM supplemented with 50 U/ml penicillin-streptomycin sulfate and 8 mM glucose (control condition).

Fatty acid treatment:

Three treatment groups were used: control (Con), 250 µM palmitate (Pal), or 250 µM oleate (Ole) (Sigma-Aldrich, St. Louis, MO). Briefly, fatty acid free bovine serum albumin was solubilized in control media. Fatty acids were then complexed to albumin by gentle vortexing and incubation at 37° C in a water bath for 1 hour in order to achieve a 2:1 fatty acid-to-albumin molar ratio (*18*).

Chemical ER stress induction:

Thapsigargin (Tg) (Sigma-Aldrich) a tumor-promoting sesquiterpene lactone that induces ER stress via inhibition of the ER-associated calcium ATPase (*80, 81*), was added to control media at a concentration of 780 nM, this dose was selected based on preliminary studies in which we

observe Tg induction of UPR activation over a similar time course to that of palmitate without excessive cell death (*81*).

Experimental Design

Protein synthesis:

Cells were exposed to control media enriched to either 4% or 10% with ^2H_2O (Initial studies were performed with 10% enrichment. In subsequent studies we found that 4% enrichment provided an adequate signal to assess protein synthesis.) (*67*). Media was enriched two hours prior to, and during administration of treatments (Con, Pal, Ole, or Tg). Treatment durations were 0.5, 1, 2, 4, or 6 hours (Con, Pal, Ole), or 0.5, 1, 2, and 4 hours (Con, Tg). These time points were chosen so that protein synthesis could be assessed prior to and following the induction of ER stress by palmitate and thapsigargin (*18*). In contrast, oleate does not induce ER stress in H4IIE cells (*16, 18, 30, 82*).

Protein degradation:

Cells were exposed to control media enriched to 15% with ^2H_2O for 5 passage cycles. Following this, ^2H_2O was removed and cells were treated with Con, Pal, Ole, or Tg for 0.5, 1, 2, 4, 6, or 10 hours.

Ubiquitination:

Cells were treated with Con, Pal, Ole, Mg132 (a proteasome inhibitor, Cayman Chemical, Ann Arbor, MI), or Tg for 6 hours. Cells were harvested and processed in the presence N-ethylmaleimide.

Proteasome activity:

Cells were transfected with the ZsProSensor-1 proteasome fluorescent reporter (Takara, Mountain View, CA), which fluoresces when proteasome activity is inhibited. Transfection was

accomplished using Lipofectamine in combination with the PLUS reagent (Invitrogen, Carlsbad, CA) according to the manufacturer's protocol. After 5 hours, cells were subcultured to poly-L-Lysine coated cover slips overnight. Cells were then treated with Con, Pal, Ole, Mg132 or Tg for 3 or 6 hours.

Cell proliferation:

Cells were plated in 96 well plates containing EMEM, 10% FBS, and 50 U/ml of penicillin-streptomycin sulfate overnight. Cells were then provided bromodeoxyuridine (BrdU, Roche Applied Science, Penzberg, Germany) and treated with Con, Pal, Ole, or Tg for 0.5, 1, 2, 4, or 6 hours.

Analytical Methods

Preparation of whole cell lysates for gas chromatography - mass spectrometric (GC-MS) analysis:

Whole cell lysates or ER microsomes (see below) were solubilized in 1M sodium hydroxide and agitated at 56°C for 15 minutes. Cellular proteins were hydrolyzed with 6 M hydrochloric acid at 120°C for 24 hours. Cation exchange was accomplished using a Dowex column (Ag50W – X8 resin, Bio-Rad Laboratories, Hercules, CA). Cation charged samples were eluted using 4 N ammonium hydroxide. Following vacuum drying, samples were reconstituted in molecular grade water, and derivatized using 50% acetonitrile (Mallinkrodt, Hazelwood, MO), 50 µL of 1 M potassium phosphate monobasic (ThermoFisher Scientific, Hampton, MA), and 20 µL of pentafluorobenzyl bromide (Sigma-Aldrich), and heating at 100°C for 1-hour. Derivatives were extracted using ethyl acetate (ThermoFisher Scientific); the organic layer was collected and dried under nitrogen and vacuum centrifugation for subsequent GC-MS analysis (*52, 66, 67*).

Subcellular fractionation:

Briefly, treated cells were washed in ice cold PBS three times and collected by centrifugation at 600 × g for 5 minutes (*67*). Whole cells were lysed in 30mM Tris-HCl pH 7.4 with 225mM mannitol, 75 mM sucrose, then sonicated 10 times for 1 second pulses. Lysates were centrifuged at 560 × g for 5 minutes to remove unbroken cells and debris. Purified lysates were centrifuged at 2800 × g for 10 minutes. The supernatant was centrifuged at 19,900g for 30 minutes. The final supernatant was centrifuged at 100,000g for 1 hour to yield the purified ER microsome. (All centrifugation steps were at 4° C) (*63*).

GC-MS analysis of derivatized amino acids:

Using negative chemical ionization (NCI), derivatized amino acids were analyzed on a DB5MS gas chromatograph column (Agilent, Santa Clara, CA). The starting temperature was 100°C, increasing 15°C per minute to reach a maximum of 220°C. For mass spectrometry, NCI with helium was used as the gas carrier and methane as the reagent gas. Mass-to-charge ratios of 448, 449, and 450 were monitored for the pentafluorobenzyl-*N*-*N*-di(pentafluorobenzyl) alanine derivative. Alanine standards (Fluka Analytical, St. Louis, MO) ranging from 7.8125 – 2000 µg/ml were used. All samples were run in duplicate. Run time was ~25 minutes, and peak elution occurred at ~17.8 minutes (*52, 67*).

Preparation of media for analysis of deuterated water enrichment - mass spectrometric analysis:

Deuterated water was extracted from media and plasma samples using heat evaporation overnight. Acetone proton exchange was accomplished by adding 20 µL acetone (Sigma-Aldrich) and allowed to sit overnight at room temperature. Acetone extraction was accomplished by the addition of 200 µL hexane (Sigma-Aldrich), and collection of the organic phase using anhydrous sodium sulfate for GC-MS analysis (*52, 67*).

GC-MS analysis of deuterated water enrichment:

Using electron ionization (EI), deuterium labeled acetone was analyzed on a DB17MS gas chromatograph column (Agilent). The starting temperature was 60° C, increasing 20° C per minute to reach 100° C, following a second temperature ramp increasing 50° C per minute to reach a maximum of 220° C. For mass spectrometry, helium was used as the carrier gas. Mass-to-charge ratios of 58 and 60 were monitored for 2-pentanone, 4-hydroxy-4-methyl; 4-hydroxy-2-keto-4-methylpentane (diacetone alcohol). Deuterated water standards ranging from 0-20% enrichment were used. All samples were run in duplicate. Run time was ~5.4 minutes and peak elution occurred at ~2.9 minutes (*52, 67*).

GC-MS-based data analysis:

Protein synthesis was measured via deuterium incorporation into alanine. The fraction of newly synthesized proteins was calculated by dividing protein bound alanine enrichment by the true precursor enrichment. The true precursor enrichment was determined using plasma deuterium enrichment adjusted to free alanine using mass isotopomer distribution analysis (MIDA) (*52, 66*). Protein degradation was determined by measuring the loss of alanine enrichment over time.

RNA isolation and analysis:

Total RNA was extracted from cells using TRIzol reagent as per the manufacturer's protocol (Invitrogen, Carlsbad, CA). For Real Time PCR, reverse transcription was performed using 0.5 μg of DNase-treated RNA, Superscript II RnaseH- and random hexamers. PCR reactions were performed in 96-well plates using transcribed cDNA and IQ-SYBR green master mix (Bio Rad Laboratories). Primer sets are provided in Table 3.1. PCR efficiency was between 90% and 105% for all primer and probe sets and linear over 5 orders of magnitude. The specificity of products generated for each set of primers was examined for each fragment using a melting curve

and gel electrophoresis. Reactions were run in triplicate and data calculated as the change in cycle threshold (ΔCT) for the target gene relative to the ΔCT for β_2-microglobulin (control gene) according to the procedures of Muller et al. (*65*).

Western blot:

Equivalent amounts of protein from cell lysates were subjected to SDS-PAGE and transferred to PVDF membranes (EMD Millipore, Billerica, MA). Membranes were incubated with anti-ubiquitin (SC-8017, Santa Cruz Biotechnology, Santa Cruz, CA), anti-CHOP (DDIT3 ab11418, Abcam Cambridge, United Kingdom), or anti-β-Actin (13E5, Cell Signaling, Danvers, MA). Membranes were rinsed in TBST, incubated for 1 hour with secondary detection antibodies (IRDye 800CW-conjugated anti-mouse, or IRDye 680RD-conjugated anti-rabbit) (LI-COR Biosciences, Lincoln, NE), washed in TBST, and scanned for infrared signal using the Odyssey CLx Imaging System (LI-COR Biosciences). Density was quantified using Image Studio Lite (LI-COR Biosciences).

***Fluorescence microscopy*:**

Briefly, cells were fixed with 4% paraformaldehyde in PBS for 10 minutes at room temperature and mounted using Vectashield mounting medium with DAPI (Vector Laboratories, Inc. Burlingame, CA). Images of fixed cells were acquired using the Olympus BX63F microscope (Olympus, Tokyo, Japan) equipped with the Olympus DP73 digital camera (Olympus) under BrightLine single-band filter set optimized for FITC (FITC-2024B, Semrock Inc; Rochester, NY). Fluorescent images were acquired using an UPlanSApo 20x/0.75 air objective (Olympus) at 1.6 seconds using CellSens (version 1.15, Olympus).

ELISA:

Analysis of BrdU was performed according the manufacturer's instructions (Roche Applied Science).

Statistics:

Statistical comparisons were made using 2-way ANOVA. Post-hoc comparisons among means were performed using Tukey's multiple comparisons test. Statistical significance was set at $p < 0.05$. All values are reported as mean ± SD.

Results

Palmitate induces ER stress in H4IIE cells

ER stress-mediated activation of the unfolded protein response (UPR) involves three ER membrane-bound proteins, double stranded RNA-dependent protein kinase-like ER kinase (PERK), inositol-requiring ER-to-nucleus signaling protein 1α (IRE1α), and activating transcription factor-6α (ATF6α). Activation of PERK, IRE1α and ATF6 results in post-translational protein modification (e.g. phosphorylation of the α-subunit of eukaryotic translation initiation factor-2 (eIF2α)), mRNA decay and splicing (e.g. splicing of the X-box-binding protein 1 (XBP1s)), and upregulation of transcription (e.g. glucose regulated protein78 (GRP78)), C/EBP Homologous Protein (CHOP), and growth arrest and DNA damage-inducible protein 34 (GADD34) (*36*). We have previously demonstrated that phosphorylation of eIF2α, splicing of XBP1, and expression of CHOP, GRP78, and GADD34 mRNA and protein were increased following 2-3 hour exposure of H4IIE liver cells to 250 µM palmitate, but not 250 µM oleate (*35*).

In the present study we monitored the expression of CHOP, GRP78 and GADD34 mRNA, spliced XBP1 mRNA, and the protein expression of CHOP as markers of ER stress and UPR activation. GADD34 mRNA and XBP1s were significantly increased following 2 hours of

palmitate exposure, whereas CHOP and GRP78 mRNA were significantly increased by palmitate treatment at 4 and 6 hours, respectively (Figure 3.1). Likewise, protein expression of CHOP was significantly increased following 4 and 6 hours of palmitate treatment (Figure 3.2). Treatment with oleate had no effect on any of these UPR markers. Induction of ER stress and activation of these UPR components occurred earlier and to a greater extent when H4IIE liver cells were treated with thapsigargin (Figure 3.1, 3.2).

Palmitate does not selectively increase protein synthesis or genes involved in the protein synthetic apparatus in H4IIE cells

The UPR senses and responds to an accumulation of unfolded proteins within the ER lumen, suggesting that palmitate-mediated ER stress involves direct effects to the ER client protein load. To examine whether palmitate-mediated ER stress involved an increase in the protein client load presented to the ER we measured protein synthesis. Protein synthesis was not increased following treatment with Pal over a time course that preceded, and occurred concomitantly with observed ER stress (Figure 3.3A). In order to assess whether palmitate stimulates synthesis of proteins directed to the ER, we also measured protein synthesis in ER microsomes following 1 and 2 hours of Pal treatment. Protein synthesis in ER microsomes was not selectively increased following treatment with Pal (Supplemental Figure 3.1). In contrast to palmitate, Tg treatment resulted in a significant reduction of protein synthesis at 1, 2 and 4 hours (Figure 3.3B). Cell proliferation, based on BrdU incorporation, was not significantly different among any of the treatment groups (Figure 3.3C).

In order to assess the impact of palmitate on the cellular capacity for protein synthesis, we examined a panel of genes involved in amino acid uptake (Snat2, Slc7a1 and Slc7a5), protein translation (Eprs and Sars), ER transport and translocation (Sec23a, Sec31a, and Copa), and ER

folding and processing (Hyou1 and Calr) that have previously been shown to increase rapidly upon chemical-induction of ER stress (*70, 71*). Pal increased the expression of only one gene, Sars, at one time point, 6 hours (Figures 3.4 - 3.7). In contrast, Tg increased the expression of Snat2, Slc7a1, Slc7a5, Eprs, Hyou1, and Calr at 2 and 4 hours, Sars at 4 hours, and Sec23a, Sec31a, and Copa at 2 hours (Figures 3.4 – 3.7).

Palmitate increases protein ubiquitination but does not reduce proteasome activity in H4IIE cells

Endoplasmic reticulum-associated degradation (ERAD) designates mis-folded proteins in the ER for degradation via the ubiquitin-proteasome system (*83, 84*). Therefore, to examine whether palmitate-mediated ER stress involved protein handling and/or degradation we measured protein ubiquitination and proteasome activity. Protein ubiquitination was increased by ~26% following 6 hours of palmitate treatment (Figure 3.8A). In contrast, protein ubiquitination was reduced by a 6-hour Tg treatment (Figure 3.8B). Proteasome activity was not reduced by either Pal or Tg (Figure 3.9).

Palmitate does not reduce protein degradation in H4IIE cells.

To further examine whether palmitate-mediated ER stress and increased ubiquitination involved effects on degradation we assessed total cellular protein degradation using deuterium oxide. Palmitate treatment did not significantly affect protein degradation (Figure 3.10A). In contrast, protein degradation was significantly reduced following thapsigargin treatment (Figure 3.10B).

Discussion

Recent evidence has implicated ER stress in the development of steatosis and progression of NAFLD (*6-9*). Both NAFLD, and its major risk factor obesity, are characterized by elevated

levels of free fatty acids, in particular saturated fatty acids. The ability of saturated fatty acids to provoke ER stress in different cell types including hepatocytes may be one mechanistic link between obesity and NAFLD (*16-19*). Given that classic ER stress results from the accumulation of unfolded proteins in the ER lumen, this study examined the regulation of proteostasis by palmitate. We tested the hypothesis that palmitate provokes ER stress by stimulating protein synthesis or inhibiting protein degradation. Our results demonstrate that palmitate does not stimulate protein synthesis in H4IIE cells. Palmitate does however increase protein ubiquitination independent of reductions in proteasome activity or protein degradation.

Palmitate increased gene and protein markers of UPR activation in H4IIE cells following 2-4 hours of incubation. Therefore, we hypothesized that if activation of the UPR was due to an increase in the protein load delivered to the ER, that protein synthesis would be increased over a time course similar to UPR activation. However, palmitate did not increase protein synthesis prior to, or during palmitate-mediated ER stress in total cell lysates or ER microsomes. These data are consistent with recent work from our laboratory in which we demonstrated that high saturated-fat diets, which provoke ER stress in the liver, do not stimulate hepatic protein synthesis (*85*). In contrast, previous work in β-cells demonstrated that 1-hour incubation with palmitate increased polysome-associated RNA, a marker of increased protein translation (*58*). Comparison of these studies suggests that the mechanisms involved in palmitate-mediated ER stress are likely cell type specific.

Previous studies have demonstrated that ER stress-independent activation of XBP1s and/or ATF6 upregulated anabolic transcriptional programs linked to amino acid uptake, ER folding and processing, and ERAD (*70*). Likewise, chemical induction of ER stress in pancreatic β-cells resulted in the upregulation of genes involved in amino acid uptake and tRNA synthesis (*71*).

Therefore, we measured a panel of genes associated with amino acid transport, protein translation, ER protein import and translocation, and ER folding and processing following incubation of H4IIE cells with palmitate. Palmitate, over a 6-hour incubation period, did not induce any significant changes in expression of these genes. These results are consistent with our direct measurement of protein synthesis, and support the notion that palmitate-mediated ER stress does not involve stimulation of protein synthesis in H4IIE cells.

We next considered an alternative mechanism whereby palmitate-mediated ER stress involved reduced protein degradation. ERAD involves recognition, cytosolic dislocation (or retrotranslocation), and ubiquitin-dependent proteasomal degradation, and is vital to proteostasis (*86*). Failure of this system is associated with an array of deleterious diseases including Parkinson's disease (*87*). The initial, enzyme-mediated attachment of ubiquitin to mis-folded or mutated substrates is a critical event in both cytosolic dislocation and degradation of proteins (*86*). Hence, we first examined protein ubiquitination in response to palmitate and oleate in H4IIE cells. Protein ubiquitination was increased by 26% in response to a 6-hour palmitate exposure. In contrast, treatment with oleate had no effect on protein ubiquitination. These data are consistent with a previous study that demonstrated a significant increase in protein ubiquitination in HepG2 cells exposed to 250 μM palmitate for 24 hours (*88*).

In order to assess the downstream efficiency for protein disposal, we evaluated the primary pathway for ubiquitin-associated protein degradation, the ubiquitin/proteasome system, using a fluorescent reporter protein. We reasoned that a decrease in proteasome activity might account for the observed increase of protein ubiquitination following palmitate exposure. However, proteasome activity was not decreased following 3 or 6 hours of palmitate treatment. Protein disposal of mis-folded and/or aggregated proteins in the cytosol can also occur through lysosomal-

mediated degradation. Therefore, we also assessed total cellular protein degradation by pre-labeling the protein pool with deuterium oxide and measuring the reduction of enrichment over time following palmitate exposure. In agreement with our proteasome activity findings, palmitate did not reduce protein degradation. Our data suggest that palmitate-mediated ER stress is not due to stimulation of protein synthesis or inhibition of protein degradation. The increase in protein ubiquitination also does not appear to be the result of reduced proteasome activity or total cellular protein degradation. We have not identified the specific lysine residues that undergo ubiquitination in response to palmitate. In mammalian cells, Lys-11, Lys-29, and Lys-48 increase upon inhibition of the proteasome (*89*). Future studies that attempt to identify the specific lysine residues and to identify target proteins are necessary to understand the role of palmitate-mediated ubiquitination in ER proteostasis.

Much of our understanding of ER stress and the UPR has been derived from studies in which chemical ER stress inducers, such as thapsigargin, have been used (*36, 71*). The present study identified important differences in the regulation of processes involved in ER proteostasis during palmitate- versus thapsigargin-mediated ER stress and activation of the UPR. Transient inhibition of protein synthesis in response to ER stress is a central mechanism used to restore ER proteostasis (*36*). Thapsigargin treatment resulted in a rapid reduction in protein synthesis (beginning at 1 hour), accompanied by an induction of multiple genes involved in the protein synthetic apparatus (beginning ~2 – 4 hours). In contrast, no changes in any of these processes were observed in response to palmitate. Certainly the presence of ER stress, due to accumulation of unfolded proteins, would be predicted to activate several degradative processes including ERAD, autophagy and proteasome-mediated degradation (*38, 89, 90*). Indeed, whereas palmitate increased protein ubiquitination, thapsigargin treatment reduced protein ubiquitination. Finally,

while palmitate treatment had no effect on protein degradation, thapsigargin treatment reduced protein degradation (beginning at 2 hours).

The simplest explanation for these differences may be related to differences in the magnitude of stress imposed on the cell by palmitate as compared to thapsigargin (Figures 3.1 and 3.2). In addition, several recent studies suggest that lipid-mediated ER stress may involve membrane events that can directly activate the UPR independently of unfolded protein accumulation in the ER (*91-93*). Results from the present study cannot determine whether palmitate-mediated changes in protein ubiquitination involve direct effects on protein processing or indirect effects mediated by changes in membrane composition.

The present study examined the hypothesis that the initial activation of the UPR by palmitate involved stimulation of protein synthesis and/or inhibition of protein degradation. Our data do not support this hypothesis, as palmitate did not stimulate protein synthesis, increase the expression of genes involved in the protein synthetic apparatus, reduce proteasome activity, or reduce protein degradation. Palmitate did increase protein ubiquitination. Therefore, palmitate appears to disturb protein handling in H4IIE cells. Finally, the present study has identified important differences in the processes involved in chemical induction of ER stress vs. palmitate-mediated ER stress, which should be considered when comparing nutrient-induced ER stress to chemically-induced ER stress.

Table 3.1: Gene primer sequences

Common Name (Symbol)	Name	Primer sequence
CHOP (Ddit3)	DNA-damage inducible transcript 3 (C/EBP homologous protein)	s: CCAGCAGAGGTCACAAGCAC as: CGCACTGACCACTCTGTTTC
GADD34 (Ppp1r15a)	Protein phosphatase1, regulatory subunit 15A (Growth arrest and damage inducible protein 34)	s: CTTCCTCTGTCGTCCTCGTCTC as: CCCGCCTTCCTCCCAAGTC
GRP78 (Hspa5)	Heat shock protein family A member 5 (78 kDa glucose-regulated protein)	s: AACCCAGATGAGGCTGTAGCA as: ACATCAAGCAGAACCAGGTCAC
splXBP-1	Spliced X-box binding protein 1	s: GTCTGCTGAGTCCGCAGCAGG as: GATTAGCAGACTCTGGGGAAG
Snat2 (Slc38a2)	Solute carrier family 38 member 2	s: CTCCTGAGTGGCGTAGTCG as: GGTGAAGTCTGAGCGAGTTG
Slc7a5	Solute carrier family 7 member 5	s: GCTGGCTCTACACATTCAAG as: GGAATTATGGAGGTGGACAG
Slc7a1	Solute carrier family 7 member 1	s: CCTGCCGTGCTACTGGTAAG as: CAGAGTAAGTGAAGAGGTGTAG
Eprs	Glutamatyl-prolyl-tRNA synthetase	s: CGATGTGAGTGGCTGCTATAT as: CAATGTGGTTCTTCTCCTTCTC
Sars	Seryl-tRNA synthetase	s: AGCAGGCACTTATCCAGTATG as: CACTTCCTGCATGACCTCTTT
Sec23a	Sec23 homolog A, coat complex II component	s: GCAACCACCTCCTTCCAATAG as: GTCTCTTTCCTTGTGGTACAG
Sec31a	Sec31 homolog A, COPII complex component	s: CCGAGAAGATGAGTCAGTATG as: ATATCTGGCTGGTTGGTGTTG
Copa	Coatomer protein complex subunit alpha	s: GAGACATTTGACCCTGAGAAG as: CCTTTGGACACAGTCAGTAAG
Hyou1	Hypoxia up-regulated 1	s: AAATGGTGGAGGAGATAGGTG as: AGGGTCAAGTCCTCAAGTTTC
Calr	Calreticulin	s: CTGACCCTGATGCTAAGAAG as: CTTCCATTCGCCCTTGTATTC

Figures

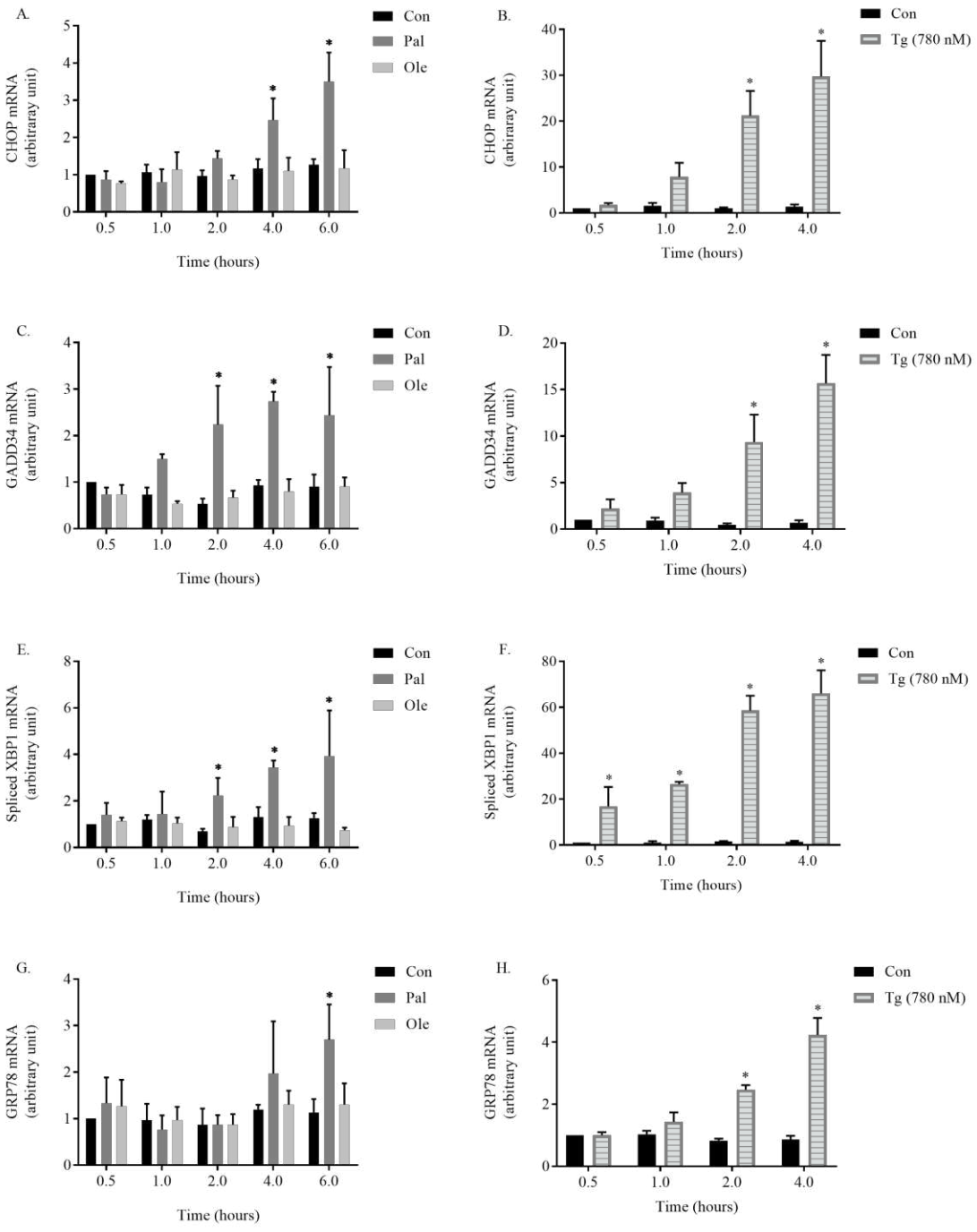

Figure 3.1: Effect of fatty acids or thapsigargin on gene markers of ER stress in H4IIE cells

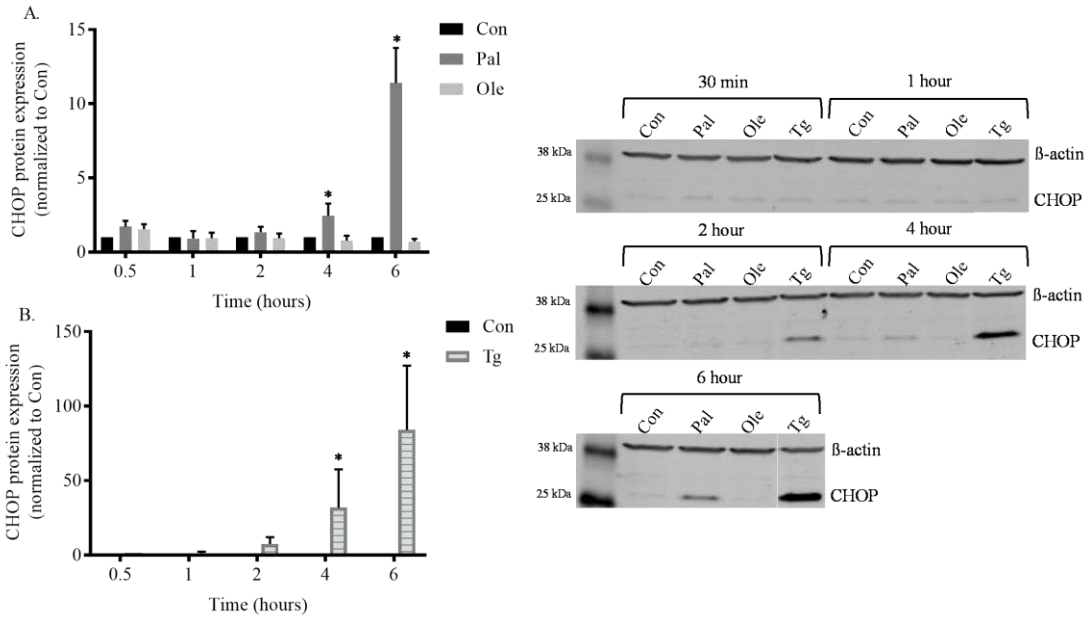

Figure 3.2: Effect of fatty acids or thapsigargin on protein expression of CHOP in H4IIE cells

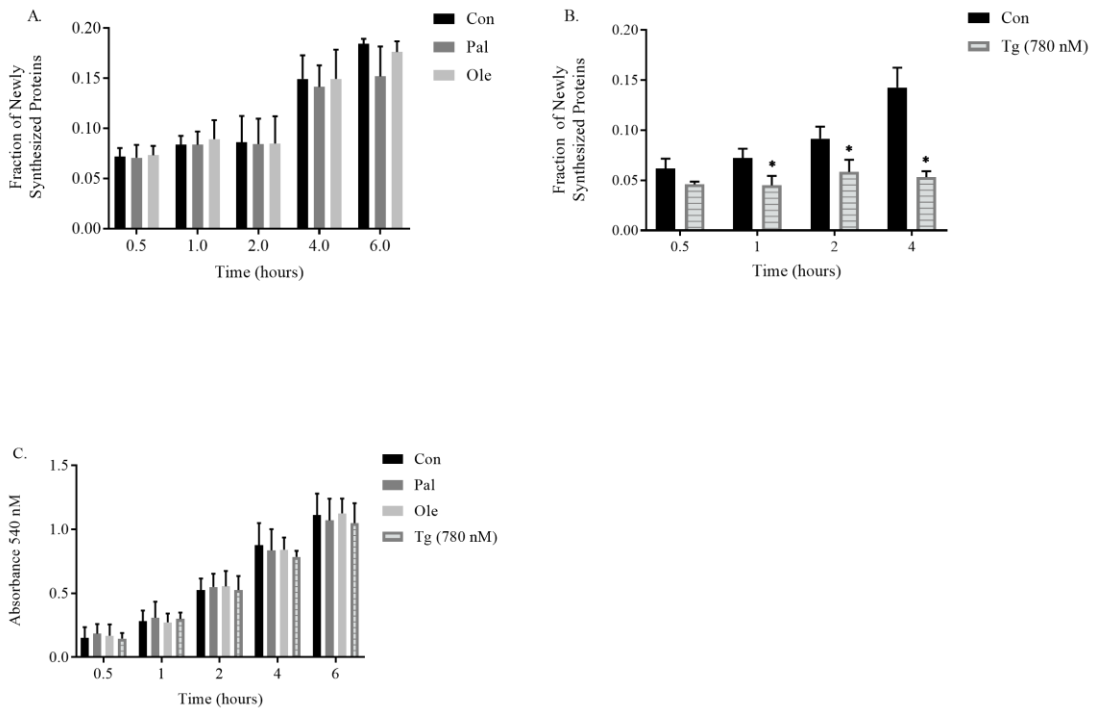

Figure 3.3: Effect of fatty acids or thapsigargin on protein synthesis (fraction of newly synthesized proteins) (A. B.), or cellular proliferation (bromodeoxyuridine incorporation) (C.) in H4IIE total lysates.

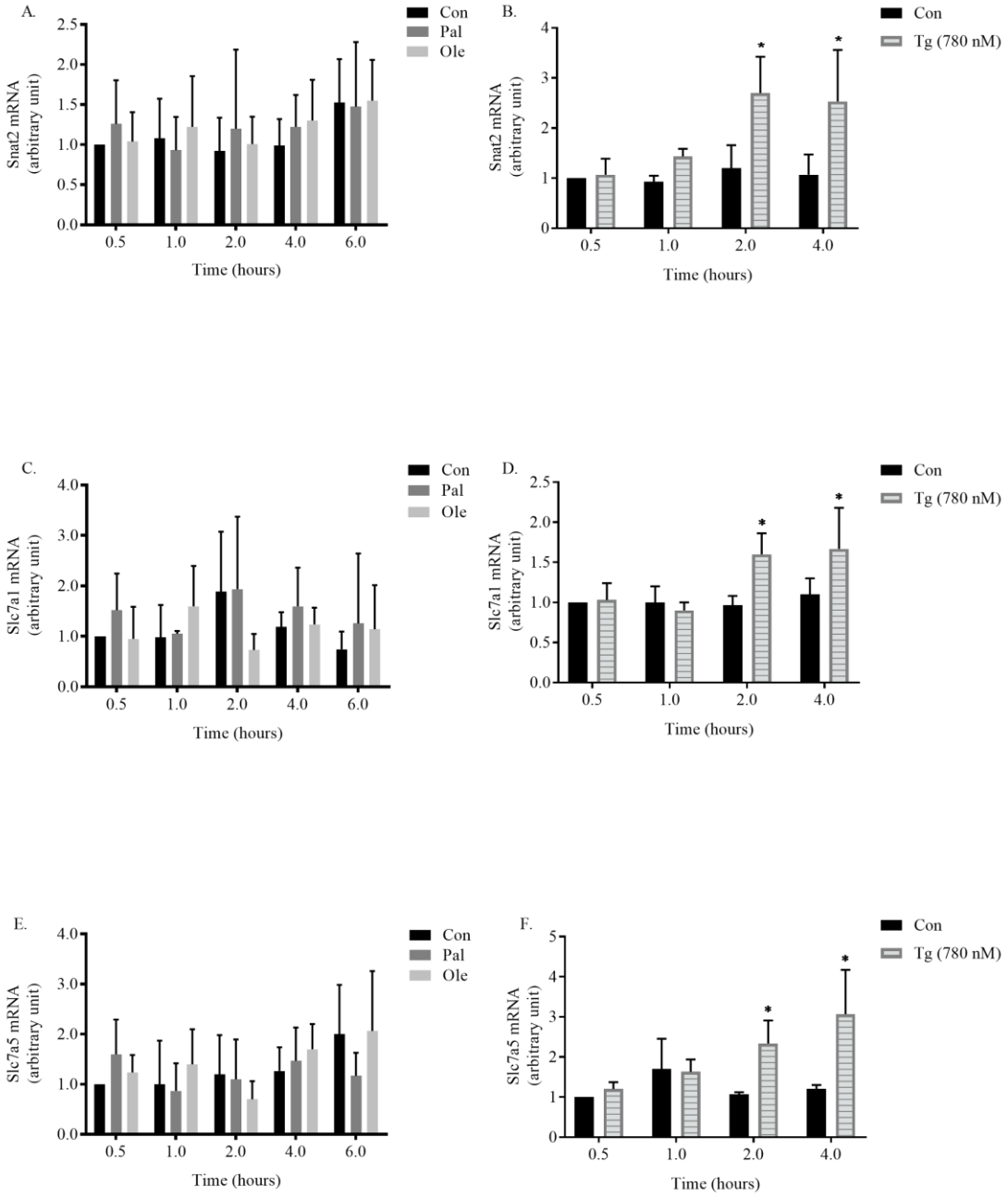

Figure 3.4: Effect of fatty acids or thapsigargin on genes involved in amino acid transport in H4IIE cells

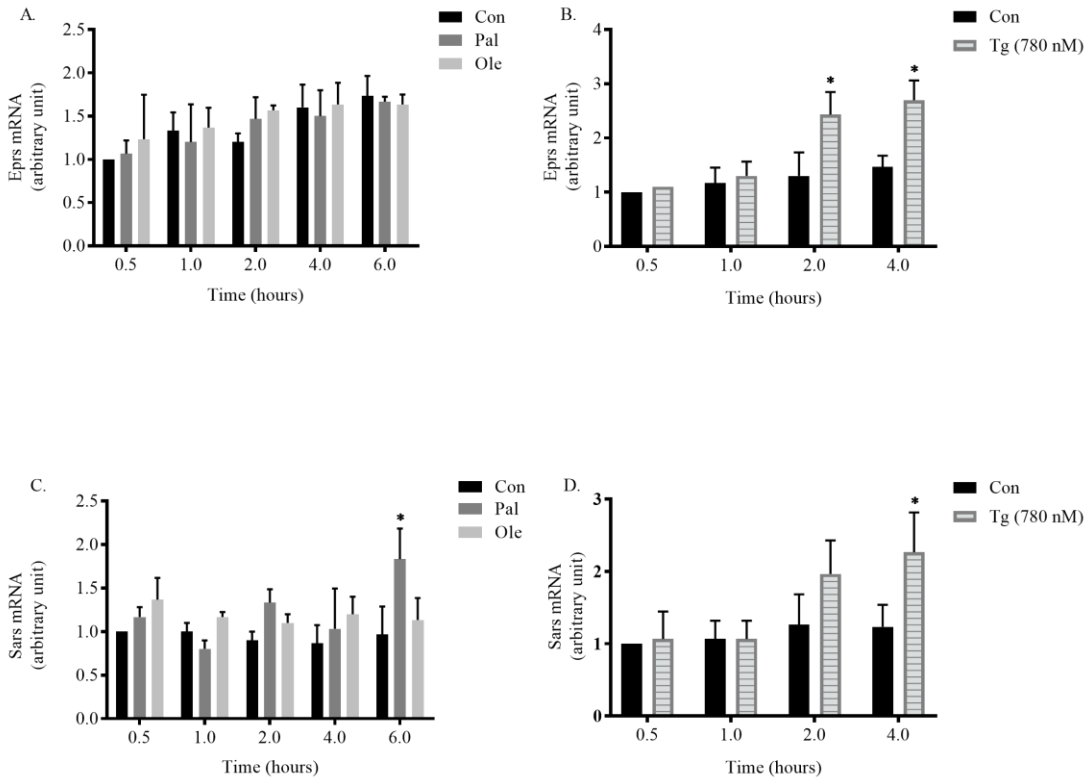

Figure 3.5: Effect of fatty acids or thapsigargin on genes involved in protein translation in H4IIE cells

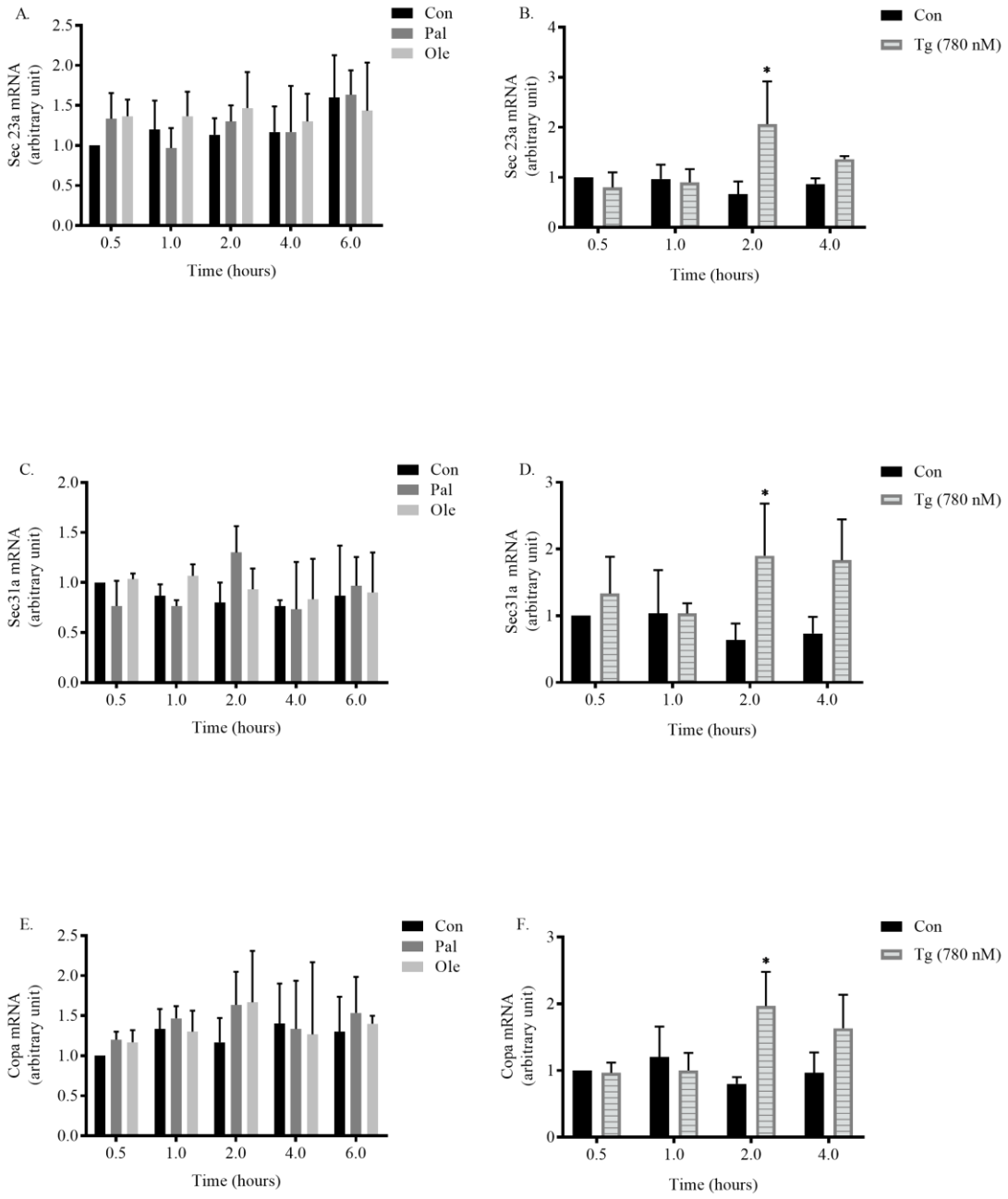

Figure 3.6: Effect of fatty acids or thapsigargin on genes involved in ER import and translocation in H4IIE cells

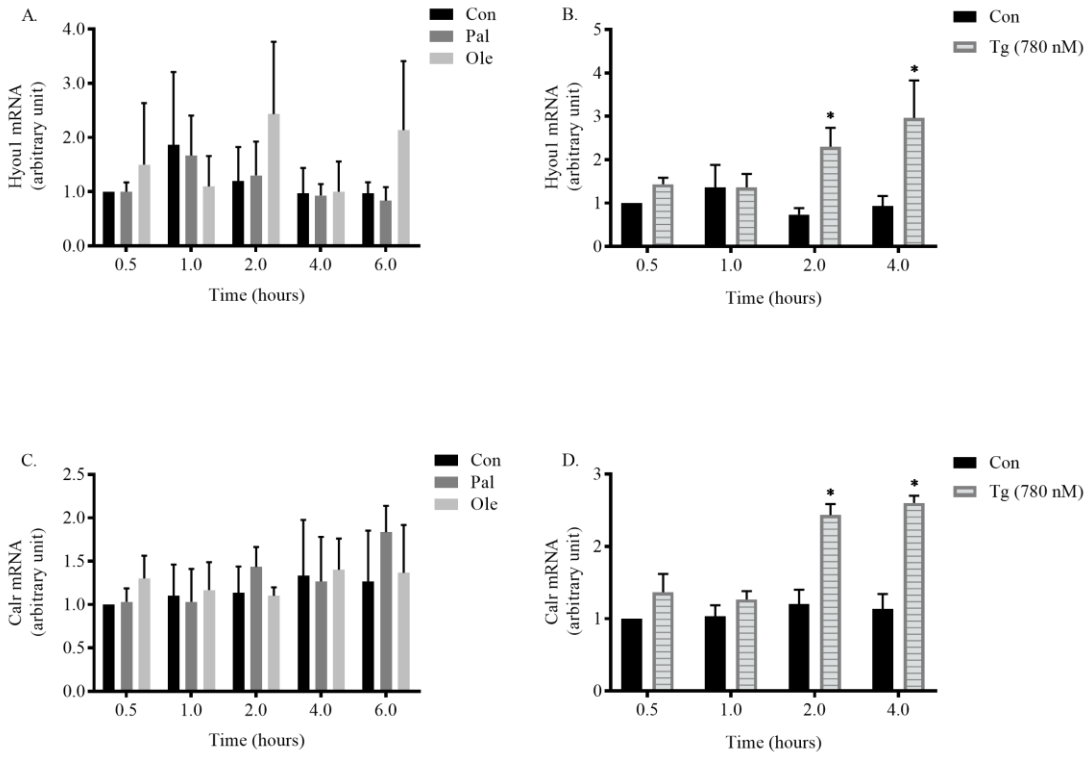

Figure 3.7: Effect of fatty acids or thapsigargin on genes involved in ER folding and processing in H4IIE cells

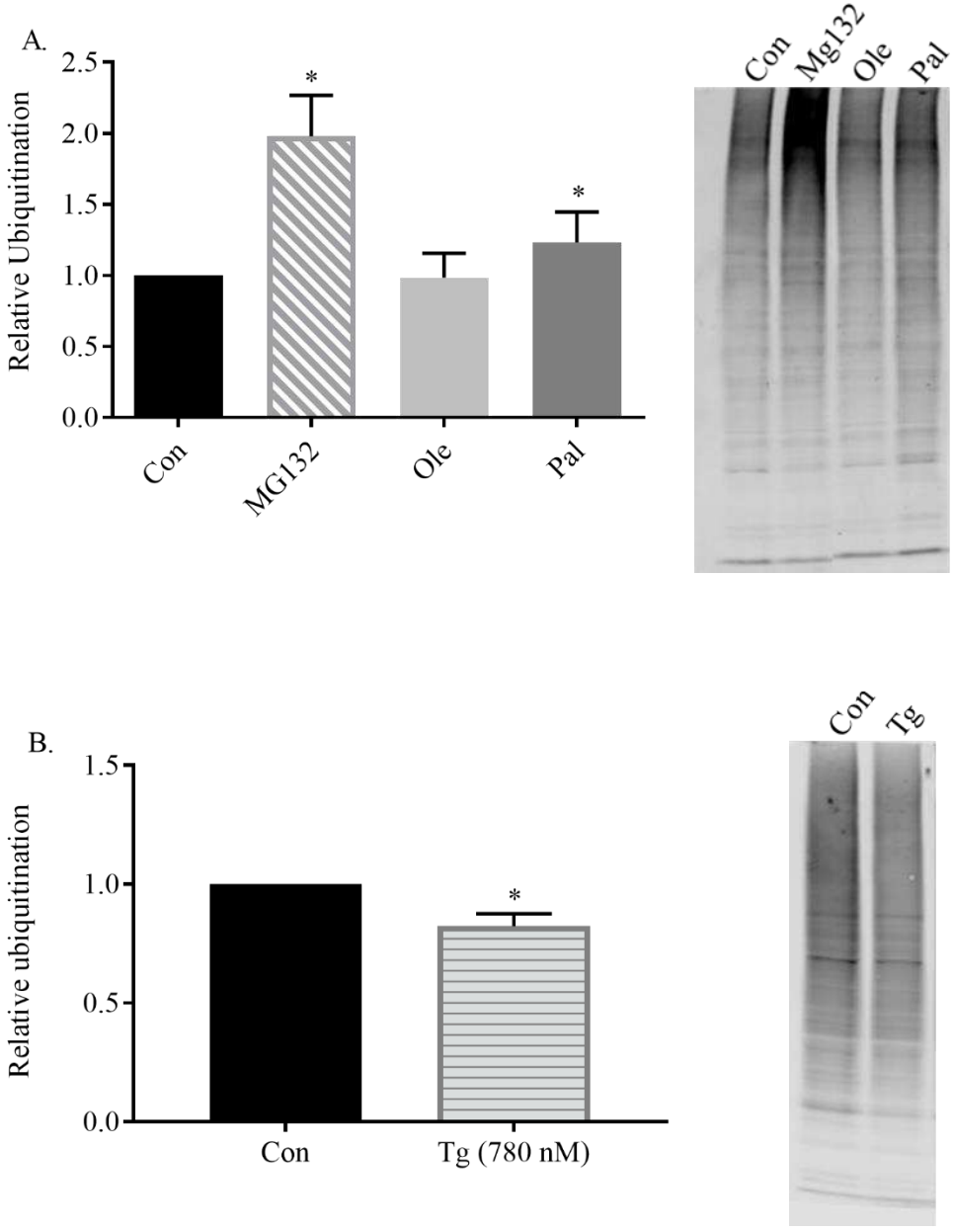

Figure 3.8: Effect of fatty acids or thapsigargin on ubiquitination in H4IIE cells

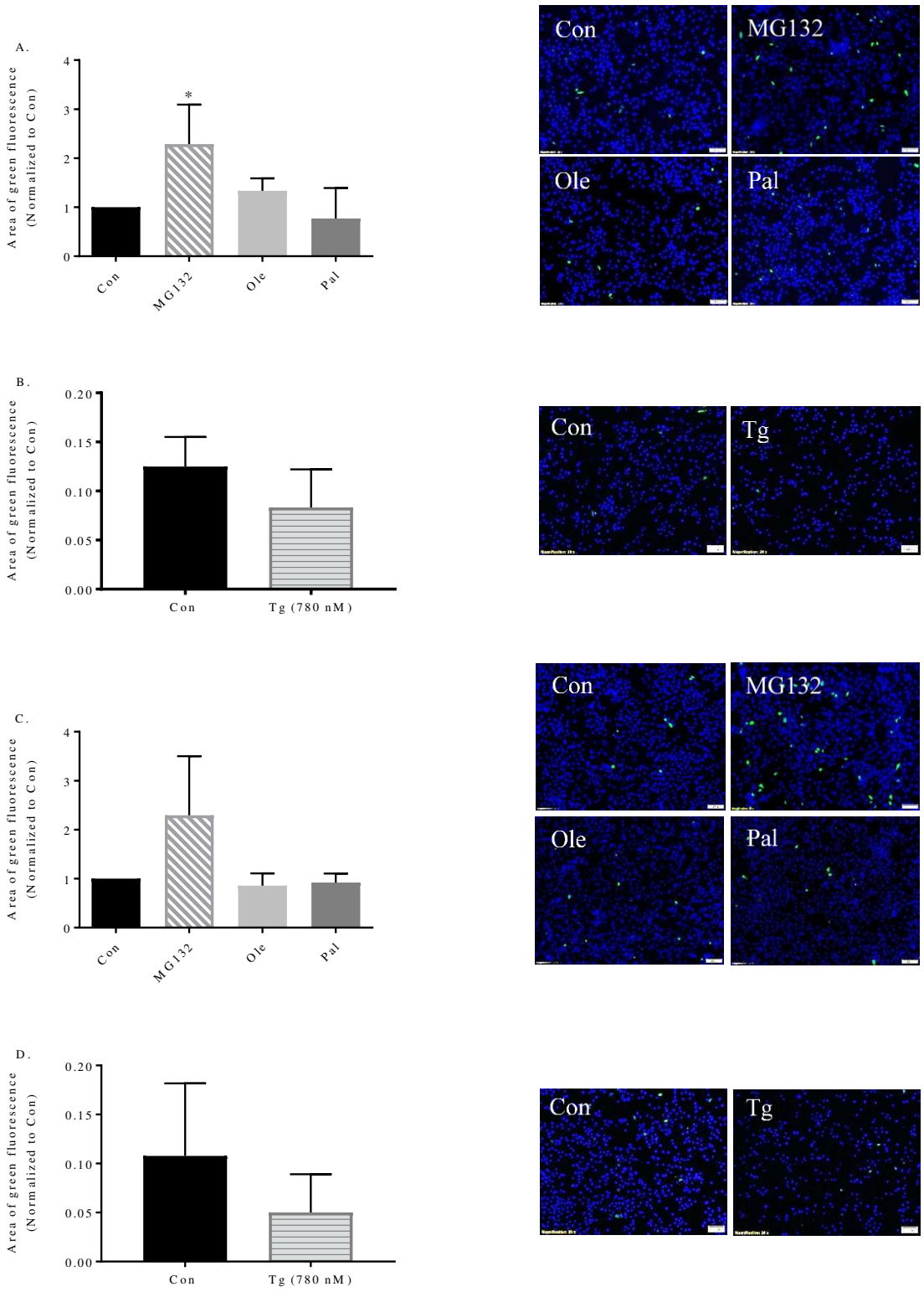

Figure 3.9: Effect of fatty acids or thapsigargin on proteasome activity after 3 (A. B.) or 6 hours (C. D.) in H4IIE cells

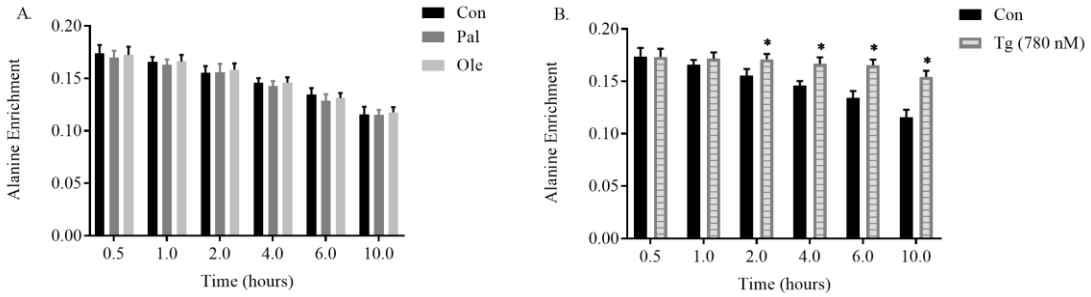

Figure 3.10: Effect of fatty acids, or thapsigargin on protein degradation (loss of alanine enrichment over time) in H4IIE total lysates

Figure Legends

Figure 3.1: Effect of fatty acids or thapsigargin on gene markers of ER stress in H4IIE cells. H4IIE cells were treated for 0.5, 1, 2, 4, or 6 hours under control conditions (Con) or with the following treatments, palmitate 250 µM (Pal), oleate 250 µM (Ole), or thapsigargin 780 nM (Tg). Real-time PCR analysis was performed to assess the relative mRNA expression of UPR markers, DNA-damage inducible transcript 3 (CHOP) (*A.B.*), Growth arrest and damage inducible protein 34 (GADD34) (*C. D.*), 78 kDa glucose-regulated protein (GRP78) (*E.F.*), and spliced X-box binding protein 1 (spliced XBP1) (*G.H.*). Data are expressed as a fold change from Con. Values are reported as mean ± SD for n = 3 per time point. * denotes significant difference from Con ($P < 0.05$).

Figure 3.2: Effect of fatty acids or thapsigargin on protein expression of DNA-damage inducible transcript 3 (CHOP). H4IIE cells were treated for 0.5, 1, 2, 4, or 6 hours under control conditions (Con) or with the following treatments, palmitate 250 µM (Pal), oleate 250 µM (Ole), or thapsigargin 780 nM (Tg). CHOP expression is reported as a ratio to β-actin and normalized to Con at each time point. Representative western blots indicate proteins detected with antibodies against CHOP or β-actin. Values are reported as mean ± SD for n = 3 per time point. * denotes significant difference from Con ($P < 0.05$).

Figure 3.3: Effect of fatty acids or thapsigargin on protein synthesis. H4IIE cells were treated for 0.5, 1, 2, 4, or 6 hours under control conditions (Con) or with the following treatments, palmitate 250 µM (Pal), oleate 250 µM (Ole), or thapsigargin 780 nM (Tg). The fraction of newly synthesized proteins was determined by enriching cell medium 4 or 10% with $^{2}H_2O$ and subsequent analysis via GC-MS/MS (*A. B.*). For cell proliferation, the percent incorporation of bromodeoxyuridine (BrdU) into DNA was measured (*C.*). Values are reported as mean ± SD for n = 3 - 6 per time point. * denotes significant difference from Con ($P < 0.05$).

Figure 3.4. Effect on fatty acids or thapsigargin on genes involved in amino acid transport. H4IIE cells were treated for 0.5, 1, 2, 4, or 6 hours under control conditions (Con) or with the following treatments, palmitate 250 µM (Pal), oleate 250 µM (Ole), or thapsigargin 780 nM (Tg). Real-time PCR analysis was performed to assess the relative mRNA expression of Solute carrier family 38, member 2 (Snat2) (*A. B.*), Solute carrier family 7 member 1 (Slc7a1) (*C. D.*), and Solute carrier family 7 member 5 (Slc7a5) (*E. F.*). Data are reported as a fold change from Con. Values are reported as mean ± SD for n = 3 per time point. * denotes significant difference from Con ($P < 0.05$).

Figure 3.5. Effect on fatty acids or thapsigargin on genes involved in protein translation. H4IIE cells were treated for 0.5, 1, 2, 4, or 6 hours under control conditions (Con) or with the following treatments, palmitate 250 µM (Pal), oleate 250 µM (Ole), or thapsigargin 780 nM (Tg). Real-time PCR analysis was performed to assess the relative mRNA expression of Glutamyl-prolyl-tRNA synthetase (Eprs) (*A. B.*) and Seryl-tRNA synthetase (Sars) (*C. D.*) as a fold change from Con. Values are reported as mean ± SD for n = 3 per time point. * denotes significant difference from Con ($P < 0.05$).

Figure 3.6. Effect on fatty acids or thapsigargin on genes involved in ER import and translocation. H4IIE cells were treated for 0.5, 1, 2, 4, or 6 hours under control conditions (Con) or with the

following treatments, palmitate 250 µM (Pal), oleate 250 µM (Ole), or thapsigargin 780 nM (Tg). Real-time PCR analysis was performed to assess the relative mRNA expression of Sec23 homolog A, coat complex II component (Sec23a) (*A. B.*), Sec31 homolog A, COPII complex component (Sec31a) (*C. D.*), and Coatomer protein complex subunit alpha (Copa) (*E. F.*). Data are reported as a fold change from Con. Values are reported as mean ± SD for n = 3 per time point. * denotes significant difference from Con ($P < 0.05$).

Figure 3.7. Effect on fatty acids or thapsigargin on genes involved in ER quality control and degradation. H4IIE cells were treated for 0.5, 1, 2, 4, or 6 hours under control conditions (Con) or with the following treatments, palmitate 250 µM (Pal), oleate 250 µM (Ole), or thapsigargin 780 nM (Tg). Real-time PCR analysis was performed to assess the relative mRNA expression of Hypoxia up-regulated 1 (Hyou1) (*A. B.*), and Calreticulin (Calr) (*C. D.*). Data are reported as a fold change from Con. Values are reported as mean ± SD for n = 3 per time point. * denotes significant difference from Con ($P < 0.05$).

Figure 3.8. Effect of fatty acids or thapsigargin on protein ubiquitination. H4IIE cells were treated for 6 hours under control conditions (Con) or with the following treatments, a proteasome inhibitor (Mg132), palmitate 250 µM (Pal), oleate 250 µM (Ole), or thapsigargin 780 nM (Tg). Ubiquitin protein expression was normalized to Con. Representative western blots indicate ubiquitinated proteins detected with an anti-Pan-ubiquitin antibody. Values are reported as mean ± SD for n = 3 per time point. * denotes significant difference from Con ($P < 0.05$).

Figure 3.9. Effect of fatty acids or thapsigargin on proteasome activity. H4IIE cells were transfected with the ZsProSensor-1 proteasome reporter, and treated for 3 (*A.B.),* or 6 hours (*C.D.*) under control conditions (Con) or with the following treatments, a proteasome inhibitor (Mg132), palmitate 250 µM (Pal), oleate 250 µM (Ole), or thapsigargin 780 nM (Tg). Proteasome activity was assessed by fluorescent accumulation of the reporter protein (higher fluorescence indicative of reduced proteasome activity). Values are reported as mean ± SD for n = 3 - 6 per time point. * denotes significant difference from Con ($P < 0.05$).

Figure 3.10. Effect of fatty acids or thapsigargin on protein degradation. H4IIE cells were grown in media enriched 15% with ^2H_2O for 5 passage cycles. ^2H_2O was removed and cells were treated under control conditions (Con) or with the following treatments, palmitate 250 µM (Pal), oleate 250 µM (Ole), or thapsigargin 780 nM (Tg). Protein degradation was measured as loss of alanine enrichment over time via GC-MS/MS. Values are reported as mean ± SD for n = 3 - 6 per time point. * denotes significant difference from Con ($P < 0.05$).

CHAPTER 4: Roles of palmitoylation and calcium in palmitate-induced endoplasmic reticulum stress in H4IIE liver cells

Summary

Elevated fatty acids, in particular saturated fatty acids, have been shown to induce endoplasmic reticulum (ER) stress in numerous cell types including hepatocytes. However, the specific mechanisms that link saturated fatty acids to ER stress are poorly understood. The present study sought to examine whether palmitate-induced ER stress involved alterations in the sarco-endoplasmic reticulum calcium ATPase (SERCA), the inositol triphosphate receptor (IP3R), or palmitoylation. H4IIE liver cells (n = 3 - 7) were treated with control media or control media supplemented with palmitate (250μM), a saturated fatty acid that induces ER stress, or oleate (250μM), an unsaturated fatty acid that does not induce ER stress. Only palmitate treated cells were characterized by ER stress. Addition of CDN1163, a SERCA activator, reduced cytosolic calcium and ER stress in palmitate-treated cells. In contrast, xestospongin, and IP3R inhibitor, had no effect on palmitate-mediated increased in cytosolic calcium or ER stress. Palmitate increased palmitoylation by approximately 25% compared to control and oleate-treated cells. Bromopalmitate reduced protein palmitoylation in palmitate treated cells to levels observed in control, but did not mitigate palmitate-induction of ER stress. These data suggest that palmitate-mediated ER stress is characterized by a reduction in SERCA activity. Although palmitate increases protein palmitoylation, this does not appear to play a significant role in palmitate-mediated ER stress over the time course studied.

Introduction

The endoplasmic reticulum (ER) has been implicated in the development and progression of non-alcoholic fatty liver disease (NAFLD), a disease characterized by steatosis of the liver in the absence of chronic alcohol consumption (*44, 45*). The ER is a multifunctional organelle that serves as the main site for lipid biosynthesis, protein processing and cellular calcium storage (*94, 95*). Approximately one-third of all new cellular proteins are directed to the ER for protein folding, processing and/or modification. The unique environment within the ER lumen includes a redox environment to drive disulfide bond formation, chaperones and foldases, and a high concentration of calcium, all of which serve to promote protein folding. Additionally, post-translational machinery for glycosylation, acetylation, and palmitoylation within the ER promote protein modifications necessary for protein folding, function, and trafficking (*34, 96-99*).

ER sequestered calcium plays a critical role in chaperone-mediated protein folding (*100-102*). Calcium concentrations within the ER lumen are estimated to be ~1000-fold higher than the cytosol (*102*). Depletion and mobilization of free intra-luminal calcium to the cytosol disrupts protein synthesis, chaperone mediated folding, ER client protein secretion, and induces proclivity for apoptosis (*103-105*). Obesity and elevated circulating saturated fatty acids, both characteristic features of NAFLD, can disrupt ER protein homeostasis (proteostasis) and induce ER stress (*10, 12, 13, 15, 106-108*). Recent studies have suggested that saturated fatty acid- and obesity-induced ER stress may involve a reduction in ER luminal calcium (*109-111*). The ER-cytosolic calcium gradient is maintained by three ER membrane-bound receptors: the sarco-endoplasmic reticulum calcium ATPase (SERCA), inositol triphosphate receptor (IP3R) and ryanodine receptor (RyR) (*100, 112, 113*). A reduction in SERCA activity has been observed in the liver of obese mice and this reduction was directly linked to obesity-mediated ER stress (*114, 115*). One purpose of the present study was to examine the independent roles of SERCA and IP3R in saturated fatty acid-

induced ER stress using a pharmacological activator of SERCA, CDN1163, or an inhibitor of the IP3R, xestospongin (*116, 117*).

One of the most common post-translational modifications within the ER is S-acylation, or palmitoylation. It involves the attachment of palmitate, a 16-carbon saturated fatty acid, onto sulfhydryl groups of cysteine residues via a thioester linkage. Palmitoylation has been shown to play a role in protein function, subcellular localization, stability and aggregation (*99, 118*). The initial phase of palmitoylation involves autoacylation of the palmitoyl acyltransfease (PAT) enzyme, a process that is mediated, in part, by the cellular concentration of fatty acids, in particular palmitate (*14, 15*). In the case of nutrient overload, such as that encountered in NAFLD, elevated saturated fatty acids could drastically influence protein palmitoylation on a chronic basis. Palmitoylation also appears to be linked to the disruption of ER homeostasis. 2-Bromopalmitate (Brp), a chemical inhibitor of palmitoylation, attenuated palmitate-induced ER stress and cell death in pancreatic β-cells (*82*). Likewise, provision of Brp to neuronal cells reversed saturated fatty acid-induced ER stress and apoptosis (*119*). Recent evidence has also demonstrated that the palmitoylation status of the ER chaperone calnexin, determined its role in protein folding versus calcium regulation (*120*). The second aim of the present study was to determine if palmitate increased protein palmitoylation in H4IIE liver cells, and if so, whether inhibition of palmitoylation reduced palmitate-mediated ER stress.

Methods

Experimental Designs

Cell culture:

H4IIE rat hepatoma cells (American Type Culture Collection, Manassas, VI) were cultured in Eagle's Modified Essential Medium (EMEM), supplemented with 10% fetal bovine serum

(FBS) and 50 U/mL penicillin- streptomycin sulfate. All experiments were performed at ~80% cell confluence using EMEM supplemented with 50 U/ml penicillin-streptomycin sulfate and 8 mM glucose (control condition).

Fatty acid treatment:

Three treatment groups were used: control (Con), 250 µM palmitate (Pal) – which induces ER stress (*18, 121*), or 250 µM oleate (Ole) – which does not induce ER stress (*16, 18, 30, 82*) (Sigma-Aldrich, St. Louis, MO). Briefly, fatty acid free bovine serum albumin was solubilized in control media. Fatty acids were then complexed to albumin by gentle vortexing and incubation at 37° C in a water bath for 1 hour in order to achieve a 2:1 fatty acid-to-albumin molar ratio (*18*).

Calcium experimental designs:

The SERCA agonist, CDN1163 at 10 µM (CDN), or the IP3R antagonist, Xestospongin at 1 µM (Xest) were added to Con media (all CDN treatment groups were pre-treated with CDN for 30 minutes). For cytosolic calcium concentration measurements Con or Pal treatments were administered in the absence or presence of CDN or Xest for 6 hours (n = 4). For measurements of UPR gene markers Con, Pal, or Ole treatments were administered in the absence or presence of CDN or Xest for 6 hours (CDN treatments, n = 7, Xest treatments, n = 5). For DNA laddering assessment, Con, Pal, or Ole treatments were administered in the absence or presence of CDN or Xest for 16 hours (n = 3).

Palmitoylation experimental designs:

The potent palmitoylation inhibitor, 2-bromopalmitate at 200 µM (Brp) was added to Con media (all Brp treatment groups were pre-treated for 1 hour). For protein palmitoylation measurements, Con or Pal treatments were administered in the absence or presence of Brp for 6 hours (Con, Pal, Brp n = 6, Pal / Brp n = 3). For PAT gene expression, Con, Pal, or Ole treatments

were administered for 1, 4, or 6 hours (n = 3). For measurements of UPR gene markers Con, Pal, treatments were administered in the absence or presence of Brp for 6 hours (n = 5). For DNA laddering assessment, Con or Pal treatments were administered in the absence or presence of Brp for 16 hours (n = 3).

Experimental Methods

Cytosolic calcium:

Cytosolic calcium was measured using the Fluo-4 NW Calcium Assay Kit (Molecular Probes Inc., Eugene, OR). Briefly, H4IIE cells were plated at 30,000 to 50,000 cells/well in a 96-well culture plate and grown overnight. As per the manufacture's protocol, cells were washed with 2.5 mM probenecid, a chemical used to inhibit anion-transporters in the cell membrane. The dye loading solution (100 µL) was added to each well and the plate was incubated at 37°C for 30 minutes, then at room temperature for an additional 30 minutes. Fluorescent emission was measured every minute for five minutes using Biotek Synergy 2 (Biotek Instruments Inc., Winooski, VT) with excitation at 488/20 nm and emission at 528/20 nm.

DNA laddering:

DNA laddering was evaluated using a modification of the protocols of Blialik et al. (2), and Listenberger et al. (22).

Protein palmitoylation:

In order to characterize the palmitoylated proteome, we utilized an acyl-biotin exchange (ABE) technique described by Davis et al. (*122*) to capture palmitoylated proteins. Briefly, free thiol groups were blocked using N-ethylmaleimide. Existing Cys-palmitoyl thioester bonds were cleaved via hydroxylamine. Freed thiol groups were labeled via incubation with 10 µM Biotin-HPDP-N-[6-(Biotinamido)hexyl]-3-(2'-pyridyldithio)propionamide (Biotin-HPDP). Equivalent

amounts of Biotin-HPDP labeled proteins were separated via SDS-PAGE, and transferred to PVDF membranes (EMD Millipore, Billerica, MA). Membranes were incubated with a fluorophore-conjugated streptavidin antibody (C40403-01, IRDye 800CW Streptavidin, LI-COR Biosciences, Lincoln, NE). Density was quantified using Image Studio Lite (LI-COR Biosciences).

RNA isolation and analysis:

Total RNA was extracted from cells using TRIzol reagent as per the manufacturer's protocol (Invitrogen, Carlsbad, CA). For Real Time PCR, reverse transcription was performed using 0.5 μg of DNase-treated RNA, Superscript II RnaseH- and random hexamers. PCR reactions were performed in 96-well plates using transcribed cDNA and IQ-SYBR green master mix (Bio-Rad Laboratories, Hercules, CA). Primer sets are provided in Table 4.1. PCR efficiency was between 90% and 105% for all primer and probe sets and linear over 5 orders of magnitude. The specificity of products generated for each set of primers was examined for each fragment using a melting curve and gel electrophoresis. Reactions were run in triplicate and data calculated as the change in cycle threshold (ΔCT) for the target gene relative to the ΔCT for β_2-microglobulin (control gene) according to the procedures of Muller et al. (*65*).

Statistics:

Statistical comparisons were made using 1-way ANOVA. Post-hoc comparisons among means were performed using Tukey's multiple comparisons test. Statistical significance was set at $p < 0.05$. All values are reported as mean ± SD.

Results

Palmitate increases palmitoylation, but not PAT gene expression, in H4IIE cells

Optimization experiments were performed to determine a concentration of biotin-HPDP analog that would adequately capture palmitoylated proteins and also result in minimal

background and/or non-specific binding. Based on a predicted abundance of palmitoylated proteins, we examined a concentration range of 3 μM – 30 μM biotin-HPDP (*123*). We chose a concentration of 10 μM, which appeared to result in adequate capture with a minimum of background (Figure 4.1). Hydroxylamine (HA) is a reducing agent used during acyl-biotin exchange chemistry to cleave palmitate from cysteine residues immediately prior to provision of biotin-HPDP. The presence of distinct bands in the –HA lanes (Figure 4.1) likely identifies proteins (e.g. carboxylases) that are endogenously biotinylated (*123*).

Protein palmitoylation was significantly increased by ~25% in Pal compared to Con (Figure 4.2A). The presence of bromopalmitate normalized protein palmitoylation in response to Pal to values observed in Con (Figure 4.2A). A family of at least 23 palmitoyl aclytranferases (PATs) are responsible for catalyzing the palmitoylation modification (*124*). We postulated that the palmitate-mediated increase in palmitoylation was via induction of PAT gene expression. Palmitate did not selectively increased the expression of DHHC2, DHHC5, and DHHC7 mRNA at 1, 4, or 6 hours (Figure 4.2B-D). In addition, we measured the same panel of genes at 16 hours and found there was no change in gene expression following long-term incubation with palmitate (Supplementary Figure 4.1).

Bromopalmitate does not reduce palmitate-induced ER stress

Our lab has previously demonstrated that treatment with palmitate at 250 μM induces ER stress in H4IIE liver cells beginning at ~2-3 hours (*35*). In order to evaluate whether the palmitate-mediated increase in protein palmitoylation contributed to palmitate-induced ER stress we measured a panel of UPR gene markers (C/EBP homologous protein (CHOP), spliced X-box binding-protein 1 (XBP1s), growth arrest and DNA damage-inducible protein-34 (GADD34), glucose regulated protein-78 (GRP78)). Pal increased the expression of GADD34, XBP1s, and

CHOP after 6 hours. However, the presence of bromopalmitate (Pal / Brp), which normalized the palmitate-mediated increase in palmitoylation (Figure 4.2A), did not reduce expression of this panel of gene ER stress markers (Figure 4.3A-D).

We, and others, have reported that long term (16-hour) incubation with palmitate results in DNA laddering and cell death (*18, 28, 35*). Therefore, we next assessed the effects of bromopalmitate on palmitate-induced DNA laddering. Bromopalmitate did not reduce DNA laddering in response to palmitate (Figure 4.3E).

A SERCA activator, CDN1163, reduces the palmitate-mediated increase in cytosolic calcium

We, and others, have previously reported that a redistribution of ER luminal calcium to the cytosol plays a role in palmitate-mediated ER stress and cell death (*109, 110, 125*). Therefore, we sought to further characterize which ER calcium receptor(s) was responsible for mediating this response. We employed CDN1163, a SERCA agonist, or xestospongin, an IP3R antagonist, in conjunction with palmitate treatment. Palmitate treatment alone resulted in a significant increase in cytosolic calcium (Figure 4.4). The co-incubation of palmitate with CDN1163 restored cytosolic calcium to levels observed in control treatment (Figure 4.4). In contrast, cytosolic calcium levels were not significantly different in palmitate-treated cells when compared to cells incubated in the presence of palmitate and xestospongin (Figure 4.4).

A SERCA activator, CDN1163, reduces palmitate-induced activation/upregulation of UPR gene markers and DNA laddering.

Palmitate treatment significantly increased UPR gene markers, GADD34, XBP1s, and CHOP after 6 hours, and significantly increased DNA laddering after 16 hours (Figure 4.5A-E). Co-incubation of palmitate with CDN1163 reduced expression of UPR gene markers and DNA

laddering (Figure 4.5A-E). In contrast, co-incubation of palmitate with xestospongin had no effect on UPR gene markers or DNA laddering (Figure 4.5A-E).

Discussion

An impaired ability to process proteins in the ER, or ER stress, has been observed in the liver of humans with NAFLD (*12, 106-108*). Elevated fatty acids, in particular saturated fatty acids, not only induce ER stress but also can induce inflammation, apoptosis and cell injury, all of which are characteristic features of NAFLD (*11, 15, 18, 25, 126*). However, the molecular mechanisms linking saturated fatty acids to ER stress in the liver are unknown. The present study sought to characterize the contributions of protein palmitoylation and calcium homeostasis in palmitate-induced ER stress in H4IIE liver cells. Palmitate increased protein palmitoylation, however inhibition of palmitoylation did not reduced palmitate-mediated ER stress or DNA laddering. Palmitate increased cytosolic calcium levels, and activation of SERCA reduced cytosolic calcium ER stress and DNA laddering in response to palmitate. These data suggest that palmitate-mediated ER stress involves selective effects on SERCA in liver cells.

Excessive or attenuated post-translational modification of proteins can induce ER stress (*36*). Protein palmitoylation, in particular, has been linked to palmitate-induced ER stress in SH-SY5Y human neuroblastoma cells and β-cells (*82, 119*). Therefore, we sought to investigate if provision of palmitate increased protein palmitoylation, and whether mitigation of this response using bromopalmitate attenuated palmitate-induced ER stress in H4IIE liver cells. Our results suggest that palmitate increased protein palmitoylation independent of changes in several PAT mRNAs. This increase in palmitoylation occurred over a time course similar to the induction of gene markers of ER stress. Although bromopalmitate prevented the palmitate-mediated increase in palmitoylation, its presence did not mitigate palmitate-induced ER stress in H4IIE liver cells.

Our results are consistent with a substrate (i.e. palmitate) driven induction of palmitoylation. This palmitate-driven induction of palmitoylation does not appear to be responsible for palmitate-mediated ER stress or DNA laddering in H4IIE liver cells. Our data suggest that the mechanisms involved in palmitate-mediated ER stress are cell specific. Bromopalmitate treatment alone increased gene markers of ER stress and DNA laddering, but did not appear to affect protein palmitoylation. Therefore, we cannot rule out the possibility that these presumed off-target effects of bromopalmitate mask our ability to identify the role of protein palmitoylation in palmitate-mediated ER stress (*127*).

The most dramatic effects of palmitate on protein palmitoylation occurred just above and below the 38 kDa marker and midway between the 38 and 70 kDa marker. Bromopalmitate also appeared to reduce palmitoylation most effectively at these sites. Therefore, future work will attempt to identify this group of palmitoylated proteins in order to further understand the link between palmitate-mediated ER stress and protein palmitoylation.

Intracellular calcium supports a wide variety of cellular processes, including proliferation, nutrient metabolism, gene transcription, and apoptosis. The ER lumen is characterized by a high concentration of calcium, which is required for protein folding and signal transduction (*112, 128*). The loss of ER luminal calcium has been linked to the induction of ER stress and activation of apoptotic pathways (*128, 129*). Several studies have demonstrated that palmitate-induced ER stress may be linked to the loss of ER luminal calcium (*109, 110, 130*). Obesity-associated ER stress in the liver has also been linked to aberrant regulation of the ER-localized SERCA pump (*114, 115*). However, calcium regulation involves at least three ER localized proteins, SERCA, IP3R and the ryanodine receptor (*128, 131*). Therefore, in the present study we examined the roles of SERCA and IP3R in palmitate-mediated ER stress. Our results demonstrate that the palmitate-mediated

increase in cytosolic calcium was prevented by activation of SERCA. In contrast, inhibition of IP3R had no effect on the increase in cytosolic calcium in cells treated with palmitate. Palmitate-mediated ER stress and DNA laddering were also reduced in the presence of the SERCA activator whereas the IP3R antagonist, xestopongin had no effect on these parameters. These data suggest that palmitate-mediated ER stress in liver cells involves a reduction in SERCA activity.

The present study does not identify the mechanism(s) linking palmitate to alterations in SERCA activity. The cholesterol concentration, as well as the phospholipid and fatty acid composition of ER membrane lipids have been linked to changes in membrane integrity, reductions in SERCA activity and/or activation of the unfolded protein response (UPR). In this context, we hypothesize that changes in the amount of saturated fatty acids within the ER membrane reduces SERCA activity. In turn, changes in the saturation state of the ER membrane induces ER stress via a reduction in ER luminal calcium. In addition, changes in the saturation state of the ER membrane may have effects on ER membrane proteins involved in the initiation of the UPR that are independent of folding events in the ER lumen.

The present study utilized gene markers of ER stress and activation of the UPR. We have demonstrated in multiple previous publications that these markers are valid readouts of UPR activation over the time course used in the present study (*18, 35*). We cannot rule out the possibility that the ryanodine receptor also plays a role in palmitate-mediated ER stress in liver cells.

The present study sought to characterize the contribution(s) protein palmitoylation and calcium homeostasis in palmitate-induced ER stress in H4IIE liver cells. Our data do not support a role for protein palmitoylation in palmitate-mediated ER stress. Palmitate-mediated ER stress in liver cells appears to involved reductions in SERCA activity. The results of this study provide new insight regarding the role of saturated fatty acids in cellular proteostasis.

Table 4.1: Gene primer sequences

Common Name (Symbol)	Name	Primer sequence
CHOP (Ddit3)	DNA-damage inducible transcript 3 (C/EBP homologous protein)	s: CCAGCAGAGGTCACAAGCAC as: CGCACTGACCACTCTGTTTC
GADD34 (Ppp1r15a)	Protein phosphatase1, regulatory subunit 15A (Growth arrest and damage inducible protein 34)	s: CTTCCTCTGTCGTCCTCGTCTC as: CCCGCCTTCCTCCCAAGTC
GRP78 (Hspa5)	Heat shock protein family A member 5 (78 kDa glucose-regulated protein)	s: AACCCAGATGAGGCTGTAGCA as: ACATCAAGCAGAACCAGGTCAC
splXBP-1	Spliced X-box binding protein 1	s: GTCTGCTGAGTCCGCAGCAGG as: GATTAGCAGACTCTGGGGAAG
Zdhhc2 (Srec)	Palmitoyltransferase ZDHHC2	s: CTGTATTTGGGAGCAGGTAAGA as: CCCAAGGACAGATAACCTTTAG
Zdhhc5	Palmitoyltransferase ZDHHC5	s: GGAGGTGTGAATCCCTTTAC as: GTCTTCTCTTTCTTTGGTCTC
Zdhhc7 (Serz)	Palmitoyltransferase ZDHHC7	s: GCCTCCTGTTCTTCACTTTC as: TTCTCACTCTTCAGCCTCTC

Figures

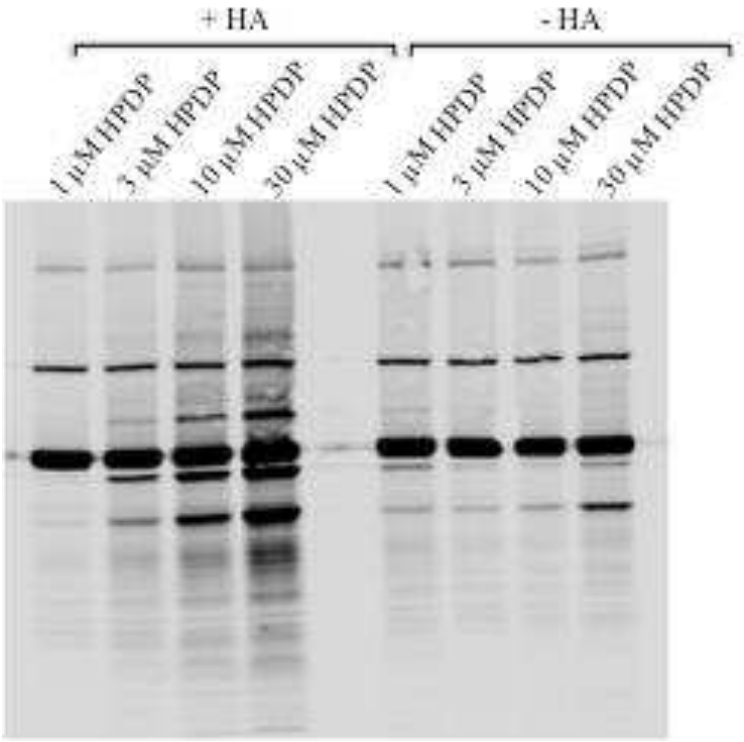

Figure 4.1: Acyl-biotin exchange optimization

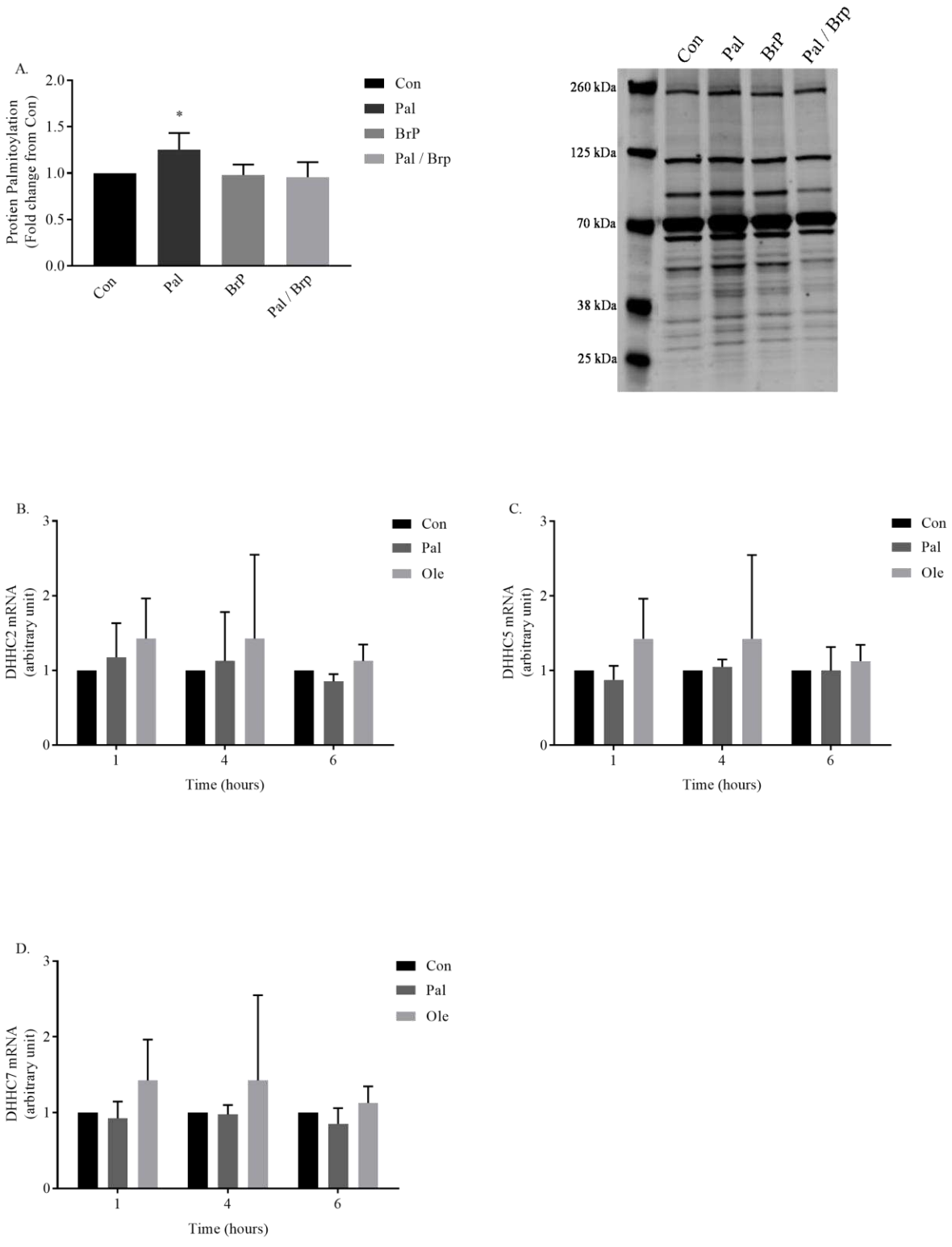

Figure 4.2: Palmitate increases palmitoylation in H4IIE cells (*A.*) but does not increase PAT gene expression (*B. - D.*).

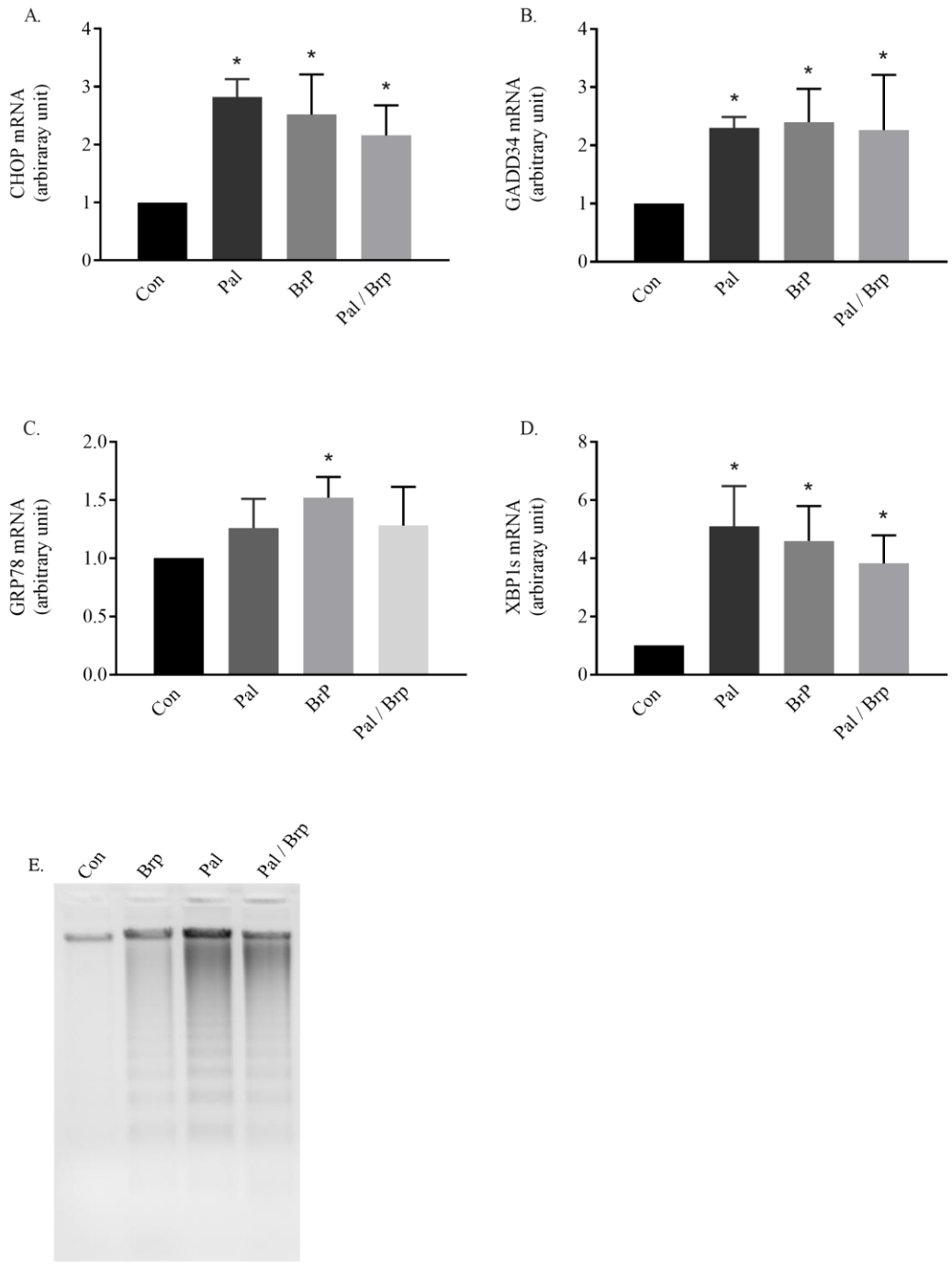

Figure 4.3: Bromopalmitate does not reduce palmitate-induced ER stress (*A.*-*D.*), or DNA laddering (*E.*)

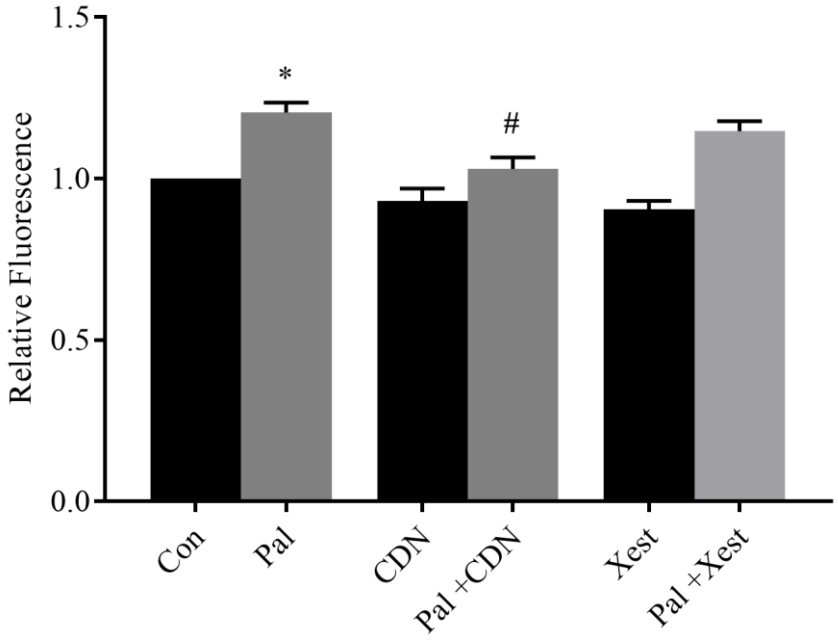

Figure 4.4: The presence of CDN1163 reduces palmitate-induced increase in cytosolic calcium

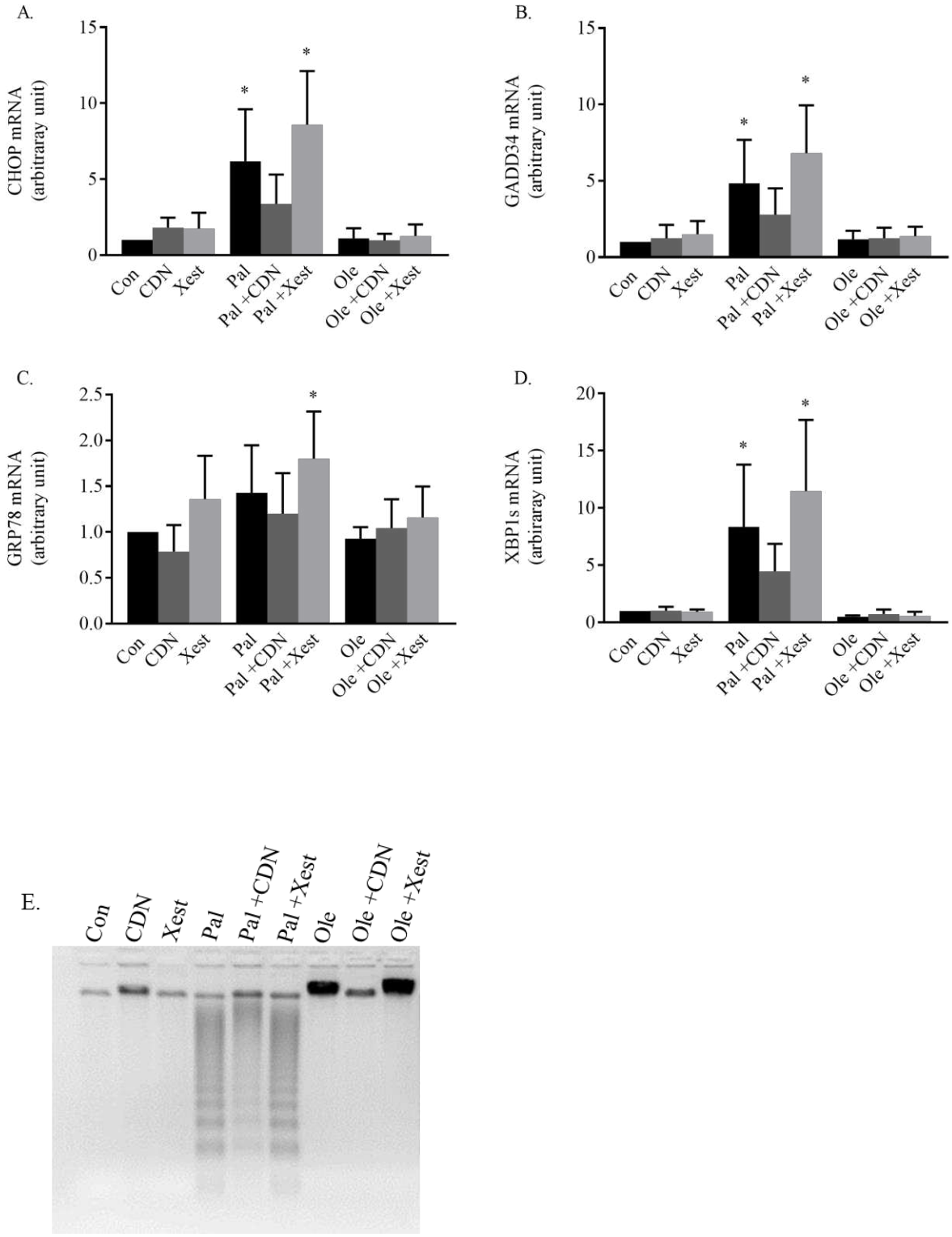

Figure 4.5: The presence of CDN1163 reduces palmitate-induced activation/upregulation of UPR gene markers (*A.*–*D.*), and DNA laddering (*E.*)

Figure Legends

Figure 4.1: To optimize the use of ABE chemistry, H4IIE liver hepatocytes were lysed and taken through the ABE method using 4 doses of biotin-HPDP, 1 µM, 3 µM, 10 µM, and 30 µM in the absence and presence of hydroxyl amine (HA), an experimental control. Proteins were separated via SDS-PAGE and probed using a streptavidin-conjugated antibody. Representative western blots indicate proteins detected with anti-streptavidin antibody.

Figure 4.2: To assess the effect of palmitate on protein palmitoylation in H4IIE liver hepatocytes were treated under control conditions (Con) or with the following treatments, palmitate 250 µM (Pal), bromopalmitate 200 µM (Brp), or a combination of palmitate 250 µM / bromopalmitate 200 µM (Pal / Brp) for 6 hours (n = 6 for Con vs. Pal, and Brp, n = 3 for Con vs. Pal / Brp). All Brp treatments were pre-treated for 1 hour. Detection of protein palmitoylation was accomplished using the acyl-biotin exchange method. Proteins were separated via SDS-PAGE and probed for using a streptavidin-conjugated antibody. Representative western blots indicate proteins detected with anti-streptavidin antibody (*A.*). Effect of fatty acids or bromopalmitate on PAT gene expression where H4IIE cells treated under control conditions (Con) or with the following treatments, palmitate 250 µM (Pal), bromopalmitate 200 µM (Brp), or a combination of palmitate 250 µM / bromopalmitate 200 µM (Pal / Brp) for 1, 4, or 6 hours (n = 3). Real-time PCR analysis was performed to assess the relative mRNA expression the following palmitoylacyltransferases, Palmitoyltransferase ZDHHC2 (Zdhhc2) (*B.*), Palmitoyltransferase ZDHHC5 (Zdhhc5) (*C*), and Palmitoyltransferase ZDHHC7 (Zdhhc7) (*D.*). Data are expressed as a fold change from Con. Values are reported as mean ± SD. * denotes significant difference from Con ($P < 0.05$).

Figure 4.3: To assess the effect of inhibiting palmitoylation on palmitate-induced on gene markers of ER stress. H4IIE cells were treated under control conditions (Con) or with the following treatments, palmitate 250 µM (Pal), bromopalmitate 200 µM (Brp), or a combination of palmitate 250 µM / bromopalmitate 200 µM (Pal / Brp) for 6 hours (n = 5). Real-time PCR analysis was performed to assess the relative mRNA expression of UPR markers, DNA-damage inducible transcript 3 (CHOP) (*A.*), Growth arrest and damage inducible protein 34 (GADD34) (*B.*), 78 kDa glucose-regulated protein (GRP78) (*C.*), and spliced X-box binding protein 1 (spliced XBP1) (*D.*). To assess the effect of inhibiting palmitoylation on palmitate-induced DNA laddering (*E.*), H4IIE cells were treated under control conditions (Con) or with the following treatments, palmitate 250 µM (Pal), bromopalmitate 200 µM (Brp), or a combination of palmitate 250 µM / bromopalmitate 200 µM (Pal / Brp) for 16 hours (n = 3). Data are expressed as a fold change from Con. Values are reported as mean ± SD. * denotes significant difference from Con ($P < 0.05$).

Figure 4.4: H4IIE cells were treated in the presence or absence of CDN1163 (10µM) or Xestospongin (1µM) under control conditions (Con) or with palmitate 250 µM (Pal) for 6 hours (n=4). Calcium was measured using the Fluo-4 AM NW calcium indicator kit. Fluorescence (Excitation: 488, Emission: 528) was measured over a 5 minute period. Data are reported as mean +/- SD. * = $P < 0.05$ from Con. # = $P < 0.05$ from Pal.

Figure 4.5: H4IIE cells were treated for in the absence or presence of CDN1163 (10µM) or Xestospongin (1µM) under control conditions (Con) or with the following treatments palmitate 250 µM (Pal), oleate 250 µM (Ole) for 6 hours (n=5). Real-time PCR analysis was performed to assess the relative mRNA expression of UPR markers, DNA-damage inducible transcript 3

(CHOP) (*A.*), Growth arrest and damage inducible protein 34 (GADD34) (*B.*), 78 kDa glucose-regulated protein (GRP78) (*C.*), and spliced X-box binding protein 1 (spliced XBP1) (*D.*). To assess DNA laddering (*E.*), H4IIE cells were treated in the absence or presence of CDN1163 (10μM) or Xestospongin (1μM) under control conditions (Con) or with the following treatments palmitate 250 μM (Pal), oleate 250 μM (Ole) for 16 hours (n = 3). Data are expressed as a fold change from Con. Values are reported as mean ± SD. * denotes significant difference from Con ($P < 0.05$).

CHAPTER 5: Summary and future directions

A significant body of research has identified deranged proteostasis as a hallmark feature of an array of deleterious diseases. We, and others, have identified a fundamental role of saturated fat-induced ER stress in NAFLD development and progression, however the molecular mechanisms by which saturated fat disrupts ER proteostasis is unknown. Understanding whether and how determinants of ER proteostasis change in response to saturated fatty acids will improve our understanding of ER stress in the context of chronic diseases.

The work in this dissertation examined the mechanism(s) of saturated fat-induced ER stress using a model that targeted the following components: protein synthesis, protein folding and post-translational modifications, and protein degradation. We first hypothesized that saturated fat-induced ER stress was due to increased protein synthesis and therefore an increased protein load to the ER. We found that diets high in saturated fat, which have been linked to impaired proteostasis, and which promote hepatic steatosis and insulin resistance, did not affect hepatic protein synthesis in rats. In agreement with this observation, in vitro treatment with palmitate did not result in a selective stimulation of protein synthesis. We next hypothesized that saturated fatty acid-induced ER stress was due to impairments in protein handling and/or protein degradation. Provision of palmitate to H4IIE liver hepatocytes increased protein ubiquitination independently of reductions in proteasome activity or total cellular protein degradation. Finally, we hypothesized that changes in protein handling involved saturated fatty acid-mediated effects on calcium homeostasis. Our data suggest that palmitate-mediated ER stress involves a reduction of SERCA activity. Therefore, we speculate that saturated fatty acid-mediated ER stress involves changes in

protein handling within the ER that result from reduced SERCA activity and reduced calcium levels in the ER lumen.

Lipid accumulation and elevated free fatty acids, including saturated fatty acids, are a central component of NAFLD. Several studies have demonstrated that the UPR is activated in the liver of humans with NAFLD. The data in this dissertation identify a link between saturated fatty acids and ER stress (or activation of the UPR) that involves the ER membrane associated SERCA protein. Therefore, changes to the SERCA protein may be an important component of human NAFLD.

Most of what we know about the regulation and downstream consequences of ER stress involve studies that have used chemicals such as tunicamycin and thapsigargin to induce ER stress. Our data highlight a vast difference between palmitate- vs. chemical-mediated ER stress. For example, palmitate had no effect on the protein synthetic machinery or protein degradation. In contrast, thapsigargin resulted in increased expression of multiple genes involved in the protein synthetic machinery and reduced protein degradation. This may be due to the magnitude of stress imposed by thapsigargin compared to palmitate and/or to a difference in the mechanisms by which ER stress is induced.

Future studies will be directed at identifying the lysine residues that are ubiquitinated in response to palmitate. We are particularly interested in lysine residues 11, 48 and 63, as ubiquitination of residues 11 and 48 typically targets protein for degradation, whereas, ubiquitination of lysine 63 is most commonly linked to cell signaling events. Future studies will also examine whether changes in membrane saturation are responsible for saturated fatty acid-mediated reductions in SERCA activity. Since we have previously demonstrated that the loss of ER luminal calcium can lead to mitochondrial-mediated apoptosis, future studies will also examine

the role of the mitochondrial-associated membrane (MAM) in saturated fatty acid-mediated ER stress. The MAM is a pseudo-organelle that mediates the transfer of calcium from the ER to mitochondria, and the transfer of ATP from mitochondria to the ER. It is currently unknown whether saturated fatty acids influence the composition or formation of the MAM.

REFERENCES

1. S. Caldwell, C. Argo, The natural history of non-alcoholic fatty liver disease. *Digestive diseases (Basel, Switzerland)* **28**, 162-168 (2010).
2. D. Papandreou, I. Rousso, I. Mavromichalis, Update on non-alcoholic fatty liver disease in children. *Clinical nutrition (Edinburgh, Scotland)* **26**, 409-415 (2007).
3. J. Y. Yap, C. O'Connor, D. R. Mager, G. Taylor, E. A. Roberts, Diagnostic challenges of nonalcoholic fatty liver disease (NAFLD) in children of normal weight. *Clinics and research in hepatology and gastroenterology* **35**, 500-505 (2011).
4. D. Festi *et al.*, Hepatic steatosis in obese patients: clinical aspects and prognostic significance. *Obesity reviews : an official journal of the International Association for the Study of Obesity* **5**, 27-42 (2004).
5. F. Diraison, P. Moulin, M. Beylot, Contribution of hepatic de novo lipogenesis and reesterification of plasma non esterified fatty acids to plasma triglyceride synthesis during non-alcoholic fatty liver disease. *Diabetes & metabolism* **29**, 478-485 (2003).
6. H. Jo *et al.*, ER stress induces hepatic steatosis via increased expression of the hepatic VLDL receptor. *Hepatology (Baltimore, Md.)*, (2012).
7. A. H. Lee, E. F. Scapa, D. E. Cohen, L. H. Glimcher, Regulation of hepatic lipogenesis by the transcription factor XBP1. *Science (New York, N.Y.)* **320**, 1492-1496 (2008).
8. S. Oyadomari, H. P. Harding, Y. Zhang, M. Oyadomari, D. Ron, Dephosphorylation of translation initiation factor 2alpha enhances glucose tolerance and attenuates hepatosteatosis in mice. *Cell Metab* **7**, 520-532 (2008).

9. D. T. Rutkowski *et al.*, UPR pathways combine to prevent hepatic steatosis caused by ER stress-mediated suppression of transcriptional master regulators. *Developmental cell* **15**, 829-840 (2008).

10. U. Ozcan *et al.*, Endoplasmic reticulum stress links obesity, insulin action, and type 2 diabetes. *Science (New York, N.Y.)* **306**, 457-461 (2004).

11. D. Wang, Y. Wei, M. J. Pagliassotti, Saturated fatty acids promote endoplasmic reticulum stress and liver injury in rats with hepatic steatosis. *Endocrinology* **147**, 943-951 (2006).

12. P. Puri *et al.*, Activation and dysregulation of the unfolded protein response in nonalcoholic fatty liver disease. *Gastroenterology* **134**, 568-576 (2008).

13. G. Boden *et al.*, Increase in endoplasmic reticulum stress-related proteins and genes in adipose tissue of obese, insulin-resistant individuals. *Diabetes* **57**, 2438-2444 (2008).

14. V. Nehra, P. Angulo, A. L. Buchman, K. D. Lindor, Nutritional and metabolic considerations in the etiology of nonalcoholic steatohepatitis. *Digestive diseases and sciences* **46**, 2347-2352 (2001).

15. A. M. Nivala, L. Reese, M. Frye, C. L. Gentile, M. J. Pagliassotti, Fatty acid-mediated endoplasmic reticulum stress in vivo: differential response to the infusion of Soybean and Lard Oil in rats. *Metabolism* **62**, 753-760 (2013).

16. N. M. Borradaile *et al.*, Disruption of endoplasmic reticulum structure and integrity in lipotoxic cell death. *Journal of lipid research* **47**, 2726-2737 (2006).

17. J. H. Moffitt *et al.*, Adverse physicochemical properties of tripalmitin in beta cells lead to morphological changes and lipotoxicity in vitro. *Diabetologia* **48**, 1819-1829 (2005).

18. Y. Wei, D. Wang, F. Topczewski, M. J. Pagliassotti, Saturated fatty acids induce endoplasmic reticulum stress and apoptosis independently of ceramide in liver cells. *American journal of physiology. Endocrinology and metabolism* **291**, E275-281 (2006).

19. L. Salvado *et al.*, Oleate prevents saturated-fatty-acid-induced ER stress, inflammation and insulin resistance in skeletal muscle cells through an AMPK-dependent mechanism. *Diabetologia* **56**, 1372-1382 (2013).

20. L. Miele *et al.*, The natural history and risk factors for progression of non-alcoholic fatty liver disease and steatohepatitis. *Eur Rev Med Pharmacol Sci* **9**, 273-277 (2005).

21. C. K. Argo, S. H. Caldwell, Epidemiology and natural history of non-alcoholic steatohepatitis. *Clin Liver Dis* **13**, 511-531 (2009).

22. F. Marra, A. Gastaldelli, G. Svegliati Baroni, G. Tell, C. Tiribelli, Molecular basis and mechanisms of progression of non-alcoholic steatohepatitis. *Trends Mol Med* **14**, 72-81 (2008).

23. W. K. Chan, N. H. Ida, P. L. Cheah, K. L. Goh, Progression of liver disease in non-alcoholic fatty liver disease: a prospective clinicopathological follow-up study. *J Dig Dis* **15**, 545-552 (2014).

24. C. K. Argo, P. G. Northup, A. M. Al-Osaimi, S. H. Caldwell, Systematic review of risk factors for fibrosis progression in non-alcoholic steatohepatitis. *J Hepatol* **51**, 371-379 (2009).

25. K. L. Donnelly *et al.*, Sources of fatty acids stored in liver and secreted via lipoproteins in patients with nonalcoholic fatty liver disease. *J Clin Invest* **115**, 1343-1351 (2005).

26. S. Rigazio *et al.*, The lowering of hepatic fatty acid uptake improves liver function and insulin sensitivity without affecting hepatic fat content in humans. *Am J Physiol Endocrinol Metab* **295**, E413-419 (2008).

27. P. Puri *et al.*, A lipidomic analysis of nonalcoholic fatty liver disease. *Hepatology* **46**, 1081-1090 (2007).

28. H. Malhi, S. F. Bronk, N. W. Werneburg, G. J. Gores, Free fatty acids induce JNK-dependent hepatocyte lipoapoptosis. *J Biol Chem* **281**, 12093-12101 (2006).

29. C. M. Mayer, D. D. Belsham, Palmitate Attenuates Insulin Signaling and Induces Endoplasmic Reticulum Stress and Apoptosis in Hypothalamic Neurons: Rescue of Resistance and Apoptosis through Adenosine 5′ Monophosphate-Activated Protein Kinase Activation. *Endocrinology* **151**, 576-585 (2010).

30. J. E. de Vries *et al.*, Saturated but not mono-unsaturated fatty acids induce apoptotic cell death in neonatal rat ventricular myocytes. *Journal of lipid research* **38**, 1384-1394 (1997).

31. M. J. Pagliassotti, Endoplasmic reticulum stress in nonalcoholic fatty liver disease. *Annu Rev Nutr* **32**, 17-33 (2012).

32. N. Borgese, M. Francolini, E. Snapp, Endoplasmic reticulum architecture: structures in flux. *Curr Opin Cell Biol* **18**, 358-364 (2006).

33. R. J. Ellis, Macromolecular crowding: obvious but underappreciated. *Trends in biochemical sciences* **26**, 597-604 (2001).

34. J. D. Malhotra, R. J. Kaufman, The endoplasmic reticulum and the unfolded protein response. *Semin Cell Dev Biol* **18**, 716-731 (2007).

35. Y. Wei, D. Wang, M. J. Pagliassotti, Saturated fatty acid-mediated endoplasmic reticulum stress and apoptosis are augmented by trans-10, cis-12-conjugated linoleic acid in liver cells. *Mol Cell Biochem* **303**, 105-113 (2007).

36. R. J. Kaufman, Stress signaling from the lumen of the endoplasmic reticulum: coordination of gene transcriptional and translational controls. *Genes Dev* **13**, 1211-1233 (1999).

37. J. Labbadia, R. I. Morimoto, The biology of proteostasis in aging and disease. *Annu Rev Biochem* **84**, 435-464 (2015).

38. J. F. Diaz-Villanueva, R. Diaz-Molina, V. Garcia-Gonzalez, Protein Folding and Mechanisms of Proteostasis. *Int J Mol Sci* **16**, 17193-17230 (2015).

39. A. Baiceanu, P. Mesdom, M. Lagouge, F. Foufelle, Endoplasmic reticulum proteostasis in hepatic steatosis. *Nat Rev Endocrinol* **12**, 710-722 (2016).

40. S. Jaisson, P. Gillery, Impaired proteostasis: role in the pathogenesis of diabetes mellitus. *Diabetologia* **57**, 1517-1527 (2014).

41. S. Kaushik, A. M. Cuervo, Proteostasis and aging. *Nat Med* **21**, 1406-1415 (2015).

42. R. I. Morimoto, A. M. Cuervo, Proteostasis and the aging proteome in health and disease. *J Gerontol A Biol Sci Med Sci* **69 Suppl 1**, S33-38 (2014).

43. R. C. Taylor, A. Dillin, Aging as an event of proteostasis collapse. *Cold Spring Harb Perspect Biol* **3**, (2011).

44. G. S. Hotamisligil, Endoplasmic reticulum stress and the inflammatory basis of metabolic disease. *Cell* **140**, 900-917 (2010).

45. C. L. Gentile, M. Frye, M. J. Pagliassotti, Endoplasmic reticulum stress and the unfolded protein response in nonalcoholic fatty liver disease. *Antioxid Redox Signal* **15**, 505-521 (2011).

46. K. K. Steffen, A. Dillin, A Ribosomal Perspective on Proteostasis and Aging. *Cell Metab* **23**, 1004-1012 (2016).

47. M. S. Hipp, S. H. Park, F. U. Hartl, Proteostasis impairment in protein-misfolding and -aggregation diseases. *Trends Cell Biol* **24**, 506-514 (2014).

48. M. Ostankovitch, J. Buchner, The network of molecular chaperones: insights in the cellular proteostasis machinery. *J Mol Biol* **427**, 2899-2903 (2015).

49. D. E. Harrison *et al.*, Rapamycin fed late in life extends lifespan in genetically heterogeneous mice. *Nature* **460**, 392-395 (2009).

50. K. Z. Pan *et al.*, Inhibition of mRNA translation extends lifespan in Caenorhabditis elegans. *Aging Cell* **6**, 111-119 (2007).

51. M. Kaeberlein *et al.*, Regulation of yeast replicative life span by TOR and Sch9 in response to nutrients. *Science* **310**, 1193-1196 (2005).

52. J. C. Drake *et al.*, Long-lived Snell dwarf mice display increased proteostatic mechanisms that are not dependent on decreased mTORC1 activity. *Aging Cell* **14**, 474-482 (2015).

53. J. C. Drake *et al.*, Assessment of mitochondrial biogenesis and mTORC1 signaling during chronic rapamycin feeding in male and female mice. *J Gerontol A Biol Sci Med Sci* **68**, 1493-1501 (2013).

54. S. R. Anderson, D. A. Gilge, A. L. Steiber, S. F. Previs, Diet-induced obesity alters protein synthesis: tissue-specific effects in fasted versus fed mice. *Metabolism* **57**, 347-354 (2008).

55. A. Masgrau *et al.*, Time-course changes of muscle protein synthesis associated with obesity-induced lipotoxicity. *J Physiol* **590**, 5199-5210 (2012).

56. S. Fu *et al.*, Polysome profiling in liver identifies dynamic regulation of endoplasmic reticulum translatome by obesity and fasting. *PLoS Genet* **8**, e1002902 (2012).

57. K. L. Lipson *et al.*, Regulation of insulin biosynthesis in pancreatic beta cells by an endoplasmic reticulum-resident protein kinase IRE1. *Cell Metab* **4**, 245-254 (2006).

58. M. Hatanaka *et al.*, Palmitate induces mRNA translation and increases ER protein load in islet beta-cells via activation of the mammalian target of rapamycin pathway. *Diabetes* **63**, 3404-3415 (2014).

59. M. J. Pagliassotti, P. A. Prach, T. A. Koppenhafer, D. A. Pan, Changes in insulin action, triglycerides, and lipid composition during sucrose feeding in rats. *Am J Physiol* **271**, R1319-1326 (1996).

60. E. W. Kraegen *et al.*, Development of muscle insulin resistance after liver insulin resistance in high-fat-fed rats. *Diabetes* **40**, 1397-1403 (1991).

61. P. H. Bisschop *et al.*, Dietary fat content alters insulin-mediated glucose metabolism in healthy men. *Am J Clin Nutr* **73**, 554-559 (2001).

62. K. L. Stanhope *et al.*, Consuming fructose-sweetened, not glucose-sweetened, beverages increases visceral adiposity and lipids and decreases insulin sensitivity in overweight/obese humans. *J Clin Invest* **119**, 1322-1334 (2009).

63. M. R. Wieckowski, C. Giorgi, M. Lebiedzinska, J. Duszynski, P. Pinton, Isolation of mitochondria-associated membranes and mitochondria from animal tissues and cells. *Nat Protoc* **4**, 1582-1590 (2009).

64. E. G. Bligh, W. J. Dyer, A rapid method of total lipid extraction and purification. *Canadian journal of biochemistry and physiology* **37**, 911-917 (1959).

65. P. Y. Muller, H. Janovjak, A. R. Miserez, Z. Dobbie, Processing of gene expression data generated by quantitative real-time RT-PCR. *Biotechniques* **32**, 1372-1374, 1376, 1378-1379 (2002).

66. R. Busch *et al.*, Measurement of protein turnover rates by heavy water labeling of nonessential amino acids. *Biochimica et biophysica acta* **1760**, 730-744 (2006).

67. B. F. Miller, C. A. Wolff, F. F. Peelor, 3rd, P. D. Shipman, K. L. Hamilton, Modeling the contribution of individual proteins to mixed skeletal muscle protein synthetic rates over increasing periods of label incorporation. *J Appl Physiol (1985)* **118**, 655-661 (2015).

68. D. Yang *et al.*, Assay of low deuterium enrichment of water by isotopic exchange with [U-13C3]acetone and gas chromatography-mass spectrometry. *Anal Biochem* **258**, 315-321 (1998).

69. B. J. McCabe *et al.*, Reproducibility of gas chromatography-mass spectrometry measurements of 2H labeling of water: application for measuring body composition in mice. *Anal Biochem* **350**, 171-176 (2006).

70. M. D. Shoulders *et al.*, Stress-independent activation of XBP1s and/or ATF6 reveals three functionally diverse ER proteostasis environments. *Cell Rep* **3**, 1279-1292 (2013).

71. D. Krokowski *et al.*, A self-defeating anabolic program leads to beta-cell apoptosis in endoplasmic reticulum stress-induced diabetes via regulation of amino acid flux. *J Biol Chem* **288**, 17202-17213 (2013).

72. T. F. Chan *et al.*, Consumption of sugar-sweetened beverages is associated with components of the metabolic syndrome in adolescents. *Nutrients* **6**, 2088-2103 (2014).

73. C. Xiao, A. Giacca, A. Carpentier, G. F. Lewis, Differential effects of monounsaturated, polyunsaturated and saturated fat ingestion on glucose-stimulated insulin secretion, sensitivity and clearance in overweight and obese, non-diabetic humans. *Diabetologia* **49**, 1371-1379 (2006).

74. V. H. Fengler *et al.*, Susceptibility of Different Mouse Wild Type Strains to Develop Diet-Induced NAFLD/AFLD-Associated Liver Disease. *PLoS One* **11**, e0155163 (2016).

75. J. J. Maher, New insights from rodent models of fatty liver disease. *Antioxid Redox Signal* **15**, 535-550 (2011).

76. D. B. Savage *et al.*, Reversal of diet-induced hepatic steatosis and hepatic insulin resistance by antisense oligonucleotide inhibitors of acetyl-CoA carboxylases 1 and 2. *J Clin Invest* **116**, 817-824 (2006).

77. A. Roy, W. F. Wonderlin, The permeability of the endoplasmic reticulum is dynamically coupled to protein synthesis. *J Biol Chem* **278**, 4397-4403 (2003).

78. S. B. Stephens, C. V. Nicchitta, Divergent regulation of protein synthesis in the cytosol and endoplasmic reticulum compartments of mammalian cells. *Mol Biol Cell* **19**, 623-632 (2008).

79. S. Mordier, P. B. Iynedjian, Activation of mammalian target of rapamycin complex 1 and insulin resistance induced by palmitate in hepatocytes. *Biochemical and biophysical research communications* **362**, 206-211 (2007).

80. R. J. Kaufman, Orchestrating the unfolded protein response in health and disease. *J Clin Invest* **110**, 1389-1398 (2002).

81. O. Thastrup, P. J. Cullen, B. K. Drobak, M. R. Hanley, A. P. Dawson, Thapsigargin, a tumor promoter, discharges intracellular Ca2+ stores by specific inhibition of the endoplasmic reticulum Ca2(+)-ATPase. *Proc Natl Acad Sci U S A* **87**, 2466-2470 (1990).

82. A. C. Baldwin, C. D. Green, L. K. Olson, M. A. Moxley, J. A. Corbett, A role for aberrant protein palmitoylation in FFA-induced ER stress and beta-cell death. *Am J Physiol Endocrinol Metab* **302**, E1390-1398 (2012).

83. J. S. Bett, Proteostasis regulation by the ubiquitin system. *Essays Biochem* **60**, 143-151 (2016).

84. J. C. Christianson, Y. Ye, Cleaning up in the endoplasmic reticulum: ubiquitin in charge. *Nat Struct Mol Biol* **21**, 325-335 (2014).

85. A. L. Estrada *et al.*, Short-term changes in diet composition do not affect in vivo hepatic protein synthesis in rats. *American journal of physiology. Endocrinology and metabolism*, ajpendo.00209.02017 (2017).

86. J. Stevenson, E. Y. Huang, J. A. Olzmann, Endoplasmic Reticulum-Associated Degradation and Lipid Homeostasis. *Annu Rev Nutr* **36**, 511-542 (2016).

87. N. Gregersen, P. Bross, S. Vang, J. H. Christensen, Protein misfolding and human disease. *Annual review of genomics and human genetics* **7**, 103-124 (2006).

88. M. Ishii, A. Maeda, S. Tani, M. Akagawa, Palmitate induces insulin resistance in human HepG2 hepatocytes by enhancing ubiquitination and proteasomal degradation of key insulin signaling molecules. *Arch Biochem Biophys* **566**, 26-35 (2015).

89. G. M. Preston, J. L. Brodsky, The evolving role of ubiquitin modification in endoplasmic reticulum-associated degradation. *Biochem J* **474**, 445-469 (2017).

90. S. Doroudgar *et al.*, Hrd1 and ER-Associated Protein Degradation, ERAD, are Critical Elements of the Adaptive ER Stress Response in Cardiac Myocytes. *Circ Res* **117**, 536-546 (2015).

91. T. Promlek *et al.*, Membrane aberrancy and unfolded proteins activate the endoplasmic reticulum stress sensor Ire1 in different ways. *Mol Biol Cell* **22**, 3520-3532 (2011).

92. N. S. Hou *et al.*, Activation of the endoplasmic reticulum unfolded protein response by lipid disequilibrium without disturbed proteostasis in vivo. *Proc Natl Acad Sci U S A* **111**, E2271-2280 (2014).

93. R. Volmer, K. van der Ploeg, D. Ron, Membrane lipid saturation activates endoplasmic reticulum unfolded protein response transducers through their transmembrane domains. *Proc Natl Acad Sci U S A* **110**, 4628-4633 (2013).

94. D. Ron, P. Walter, Signal integration in the endoplasmic reticulum unfolded protein response. *Nature reviews. Molecular cell biology* **8**, 519-529 (2007).

95. M. Schroder, R. J. Kaufman, ER stress and the unfolded protein response. *Mutation research* **569**, 29-63 (2005).

96. F. U. Hartl, A. Bracher, M. Hayer-Hartl, Molecular chaperones in protein folding and proteostasis. *Nature* **475**, 324-332 (2011).

97. M. Okumura, H. Kadokura, K. Inaba, Structures and functions of protein disulfide isomerase family members involved in proteostasis in the endoplasmic reticulum. *Free Radic Biol Med* **83**, 314-322 (2015).

98. C. Duran-Aniotz, V. H. Cornejo, C. Hetz, Targeting endoplasmic reticulum acetylation to restore proteostasis in Alzheimer's disease. *Brain* **139**, 650-652 (2016).

99. M. E. Linder, R. J. Deschenes, Palmitoylation: policing protein stability and traffic. *Nat Rev Mol Cell Biol* **8**, 74-84 (2007).

100. G. L. Koch, The endoplasmic reticulum and calcium storage. *Bioessays* **12**, 527-531 (1990).

101. E. F. Corbett, M. Michalak, Calcium, a signaling molecule in the endoplasmic reticulum? *Trends in biochemical sciences* **25**, 307-311 (2000).

102. F. L. Bygrave, A. Benedetti, What is the concentration of calcium ions in the endoplasmic reticulum? *Cell calcium* **19**, 547-551 (1996).

103. J. F. Sambrook, The involvement of calcium in transport of secretory proteins from the endoplasmic reticulum. *Cell* **61**, 197-199 (1990).

104. E. F. Corbett *et al.*, Ca2+ regulation of interactions between endoplasmic reticulum chaperones. *J Biol Chem* **274**, 6203-6211 (1999).

105. H. F. Lodish, N. Kong, Perturbation of cellular calcium blocks exit of secretory proteins from the rough endoplasmic reticulum. *J Biol Chem* **265**, 10893-10899 (1990).

106. M. F. Gregor *et al.*, Endoplasmic reticulum stress is reduced in tissues of obese subjects after weight loss. *Diabetes* **58**, 693-700 (2009).

107. N. K. Sharma *et al.*, Endoplasmic reticulum stress markers are associated with obesity in nondiabetic subjects. *J Clin Endocrinol Metab* **93**, 4532-4541 (2008).

108. S. K. Das *et al.*, Effect of pioglitazone treatment on endoplasmic reticulum stress response in human adipose and in palmitate-induced stress in human liver and adipose cell lines. *Am J Physiol Endocrinol Metab* **295**, E393-400 (2008).

109. Y. Wei, D. Wang, C. L. Gentile, M. J. Pagliassotti, Reduced endoplasmic reticulum luminal calcium links saturated fatty acid-mediated endoplasmic reticulum stress and cell death in liver cells. *Mol Cell Biochem* **331**, 31-40 (2009).

110. K. S. Gwiazda, T. L. Yang, Y. Lin, J. D. Johnson, Effects of palmitate on ER and cytosolic Ca2+ homeostasis in beta-cells. *Am J Physiol Endocrinol Metab* **296**, E690-701 (2009).

111. S. Xu *et al.*, Palmitate induces ER calcium depletion and apoptosis in mouse podocytes subsequent to mitochondrial oxidative stress. *Cell Death Dis* **6**, e1976 (2015).

112. A. Raffaello, C. Mammucari, G. Gherardi, R. Rizzuto, Calcium at the Center of Cell Signaling: Interplay between Endoplasmic Reticulum, Mitochondria, and Lysosomes. *Trends Biochem Sci* **41**, 1035-1049 (2016).

113. D. Mekahli, G. Bultynck, J. B. Parys, H. De Smedt, L. Missiaen, Endoplasmic-reticulum calcium depletion and disease. *Cold Spring Harb Perspect Biol* **3**, (2011).

114. S. Fu *et al.*, Aberrant lipid metabolism disrupts calcium homeostasis causing liver endoplasmic reticulum stress in obesity. *Nature* **473**, 528-531 (2011).

115. S. W. Park, Y. Zhou, J. Lee, J. Lee, U. Ozcan, Sarco(endo)plasmic reticulum Ca2+-ATPase 2b is a major regulator of endoplasmic reticulum stress and glucose homeostasis in obesity. *Proc Natl Acad Sci U S A* **107**, 19320-19325 (2010).

116. N. A. Shirwany, J. Xie, Q. Guo, Regulation of intracellular calcium in cortical neurons transgenic for human Abeta40 and Abeta42 following nutritive challenge. *Int J Clin Exp Med* **2**, 149-158 (2009).

117. S. Kang *et al.*, Small Molecular Allosteric Activator of the Sarco/Endoplasmic Reticulum Ca2+-ATPase (SERCA) Attenuates Diabetes and Metabolic Disorders. *J Biol Chem* **291**, 5185-5198 (2016).

118. J. Greaves, L. H. Chamberlain, Palmitoylation-dependent protein sorting. *The Journal of cell biology* **176**, 249-254 (2007).

119. Y.-H. Hsiao, C.-I. Lin, H. Liao, Y.-H. Chen, S.-H. Lin, Palmitic acid-induced neuron cell cycle G2/M arrest and endoplasmic reticular stress through protein palmitoylation in SH-SY5Y human neuroblastoma cells.

120. E. M. Lynes *et al.*, Palmitoylation is the switch that assigns calnexin to quality control or ER Ca2+ signaling. *J Cell Sci* **126**, 3893-3903 (2013).

121. Y. Zhang, R. Xue, Z. Zhang, X. Yang, H. Shi, Palmitic and linoleic acids induce ER stress and apoptosis in hepatoma cells. *Lipids Health Dis* **11**, 1 (2012).

122. J. Wan, A. F. Roth, A. O. Bailey, N. G. Davis, Palmitoylated proteins: purification and identification. *Nat Protoc* **2**, 1573-1584 (2007).

123. G. S. Brigidi, S. X. Bamji, Detection of protein palmitoylation in cultured hippocampal neurons by immunoprecipitation and acyl-biotin exchange (ABE). *J Vis Exp*, (2013).

124. B. Chavda, J. A. Arnott, S. L. Planey, Targeting protein palmitoylation: selective inhibitors and implications in disease. *Expert Opin Drug Discov* **9**, 1005-1019 (2014).

125. L. L. Listenberger *et al.*, Triglyceride accumulation protects against fatty acid-induced lipotoxicity. *Proc Natl Acad Sci U S A* **100**, 3077-3082 (2003).

126. M. E. Ertunc, G. S. Hotamisligil, Lipid signaling and lipotoxicity in metaflammation: indications for metabolic disease pathogenesis and treatment. *J Lipid Res* **57**, 2099-2114 (2016).

127. K. Hellemans *et al.*, Peroxisome proliferator-activated receptor α–retinoid X receptor agonists induce beta-cell protection against palmitate toxicity. *FEBS Journal* **274**, 6094-6105 (2007).

128. A. Gorlach, P. Klappa, T. Kietzmann, The endoplasmic reticulum: folding, calcium homeostasis, signaling, and redox control. *Antioxid Redox Signal* **8**, 1391-1418 (2006).

129. S. Wang, W. S. El-Deiry, Cytochrome c: a crosslink between the mitochondria and the endoplasmic reticulum in calcium-dependent apoptosis. *Cancer Biol Ther* **3**, 44-46 (2004).

130. E. S. Wires *et al.*, High fat diet disrupts endoplasmic reticulum calcium homeostasis in the rat liver. *Journal of hepatology*, (2017).

131. D. S. Luciani *et al.*, Roles of IP3R and RyR Ca2+ channels in endoplasmic reticulum stress and beta-cell death. *Diabetes* **58**, 422-432 (2009).

132. Y. Li *et al.*, Enrichment of endoplasmic reticulum with cholesterol inhibits sarcoplasmic-endoplasmic reticulum calcium ATPase-2b activity in parallel with increased order of membrane lipids: implications for depletion of endoplasmic reticulum calcium stores and apoptosis in cholesterol-loaded macrophages. *J Biol Chem* **279**, 37030-37039 (2004).

133. Z. Li *et al.*, The ratio of phosphatidylcholine to phosphatidylethanolamine influences membrane integrity and steatohepatitis. *Cell Metab* **3**, 321-331 (2006).

134. H. Ariyama, N. Kono, S. Matsuda, T. Inoue, H. Arai, Decrease in membrane phospholipid unsaturation induces unfolded protein response. *J Biol Chem* **285**, 22027-22035 (2010).

APPENDIX

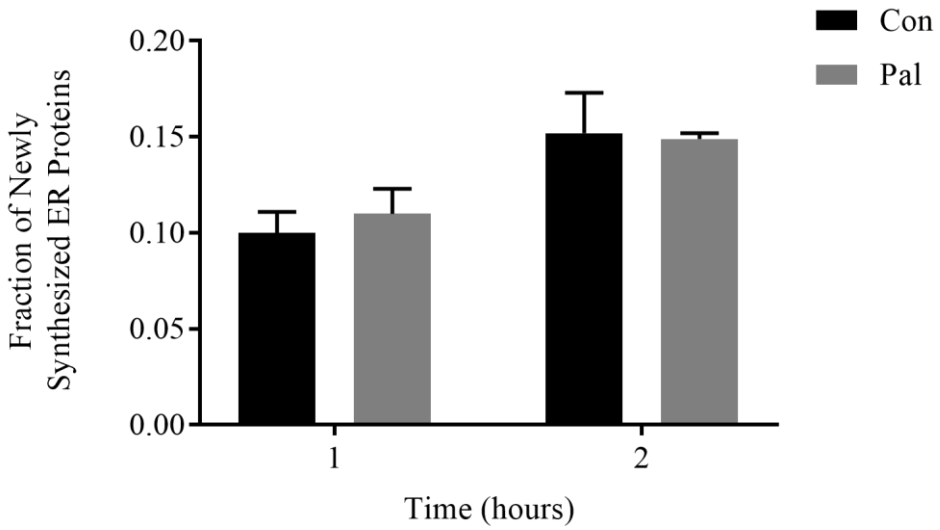

Supplemental Figure 3.1: Fraction of newly synthesized ER proteins

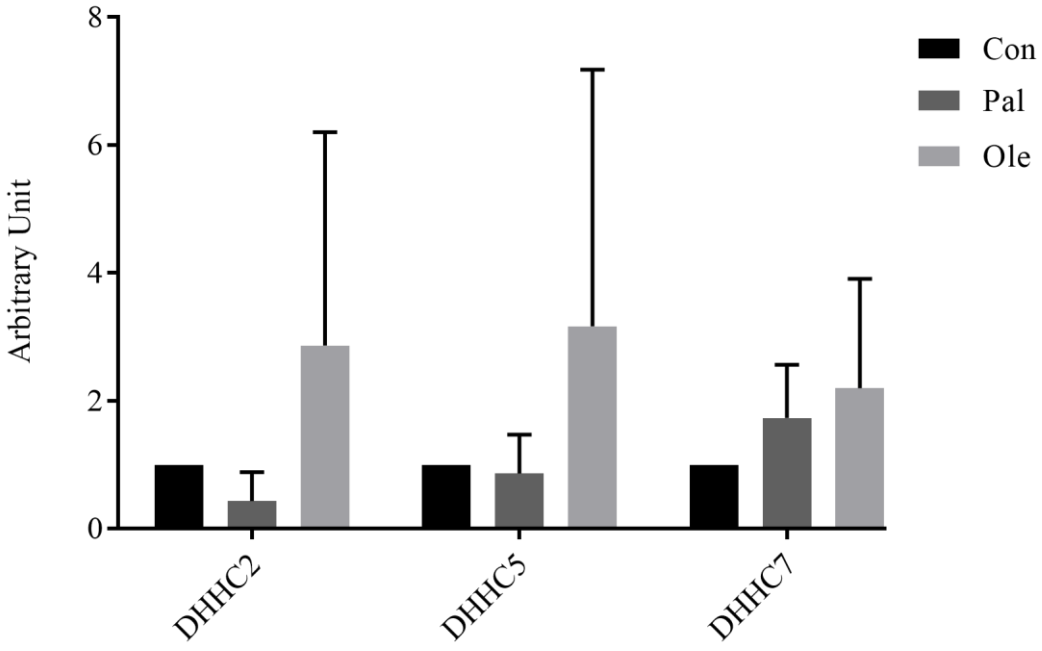

Supplemental figure 4.1: Palmitate does not increase PAT gene expression

Figure Legends

Supplementary Figure 3.1: Effect of fatty acids on ER protein synthesis. H4IIE cells were treated for 1, or 2 hours under control conditions (Con) or with palmitate 250 µM (Pal). The fraction of newly synthesized ER proteins was determined by enriching cell medium 4% with $^{2}H_{2}O$ followed by microsome fractionation and GC-MS/MS analysis.

Supplemental figure 4.1: To assess the effect of fatty acids or bromopalmitate on PAT gene expression in H4IIE cells were treated under control conditions (Con) or with the following treatments, palmitate 250 µM (Pal), bromopalmitate 200 µM (Brp), or a combination of palmitate 250 µM / bromopalmitate 200 µM (Pal / Brp) for 16 hours (n = 3). Real-time PCR analysis was performed to assess the relative mRNA expression the following palmitoylacyltransferases, Palmitoyltransferase ZDHHC2 (Zdhhc2), Palmitoyltransferase ZDHHC5 (Zdhhc5), and Palmitoyltransferase ZDHHC7 (Zdhhc7). Data are expressed as a fold change from Con. Values are reported as mean ± SD. * denotes significant difference from Con ($P < 0.05$).